

ABSTRACT

CHEMISTRY

BARR, JARVIS T.

B.S., CLARK COLLEGE, 1989

A DIFFUSE REFLECTANCE INFRARED FOURIER TRANSFORM
SPECTROSCOPY (DRIFTS) ANALYSIS OF IRON AND MOLYBDENUM
COMPLEXES IMPREGNATED ON PARTIALLY DEHYDROXYLATED
GAMMA ALUMINA

Advisor: Dr. Eric Mintz

Thesis dated December, 1994

A Diffuse Reflectance Infrared Fourier Transform Spectroscopy (DRIFTS) analysis using temperature programmed decomposition (TPDE) was carried out on iron and molybdenum complexes that were impregnated on partially dehydroxylated γ -alumina. Cyclopentadienyliron dicarbonyl dimer, di- μ -carbonyl-cis-(1-5- η :1'-5'- η' -dicyclopentadienyldimethylsilane)bis(carbonyl-diiron)(FeFe), a mixture of cyclopentadienyliron dicarbonyl dimer and di- μ -carbonyl-cis-(1-5- η :1'-5'- η' -dicyclopentadienyldimethylsilane)bis(carbonyl-diiron)(FeFe), cyclopentadienyldicarbonyliodoiron (II), cyclopentadienyldicarbonyl-2,4-cyclopentadienyliron, and [α,α' -m-xylenebis(η^5 -cyclopentadienyl)]bis[tricarbonylmolybdenum], were impregnated on partially dehydroxylated γ -alumina. Assuming four OH groups per binding site and 4.4×10^{20} of these sites /m², samples of approximately 1/20, 1/10, 2/10, 3/10, and 4/10 coverage were analyzed using DRIFTS and TPDE. The samples of 1/20 and 1/10 coverage were too dilute to obtain any useful information in the region of interest 1700-2200 cm⁻¹.

DRIFTS analysis indicated that the pure compounds of cyclopentadienyliron dicarbonyl dimer formed a trimer; an equilibrium reaction occurred between the bridged and unbridged species of di- μ -carbonyl-cis-(1-5- η :1'-5'- η' -dicyclopentadienyldimethylsilane)bis(carbonyldiiron)(FeFe); the mixture of cyclopentadienyliron dicarbonyl dimer and di- μ -carbonyl-cis-(1-5- η :1'-5'- η' -dicyclopentadienyldimethylsilane)bis(carbonyldiiron)(FeFe) formed a tetramer; cyclopentadienyldicarbonyliron (II) melted; and [α,α' -m-xylenebis(η^5 -cyclopentadienyl)]bis[tricarbonylmolybdenum] polymerized. When placed on alumina a reaction occurred with cyclopentadienyldicarbonyl-2,4-cyclopentadienyliron that resulted in the formation of a ferrocene compound. The data also indicated that on partially dehydroxylated γ -alumina Lewis acid binding occurred and was identified for each compound. In addition, when the compound was placed on alumina decarbonylation occurred more readily than for the pure compound.

**A DIFFUSE REFLECTANCE INFRARED FOURIER TRANSFORM
SPECTROSCOPY (DRIFTS) ANALYSIS OF IRON AND MOLYBDENUM
COMPLEXES IMPREGNATED ON PARTIALLY DEHYDROXYLATED
GAMMA ALUMINA**

**A THESIS
SUBMITTED TO THE FACULTY OF CLARK ATLANTA UNIVERSITY
IN PARTIAL FULFILLMENT OF THE REQUIREMENTS FOR THE
DEGREE OF MASTER OF SCIENCE**

**BY
JARVIS T. BARR**

DEPARTMENT OF CHEMISTRY

**ATLANTA, GEORGIA
DECEMBER 1994**

R. xiii T. 96

(c) 1994

JARVIS T. BARR

All Rights Reserved

ACKNOWLEDGMENTS

I would especially like to thank Dr. Eric Mintz for his guidance and patience throughout my research project.

My sincere thanks to my committee members, Dr. Alfred Spriggs, Dr. Roosevelt Thedford, and Dr. Cass Parker. I would also like to thank Dr. Mark Mitchell, Dr. Vasumathi Charkravathy, Nykarura Gatimu, Wallace Smith, and Gwen Callaway who also assisted me in my research project.

Finally, I wish to thank my labmates: Dr. James Bu, Dr. Jana Donovalova, Calandra Hopkins, Ollienia Holloway, Cynthia Bryant, Gayla Wilson, Andrea Bowens and Danny Hubbard for making coming to the laboratory enjoyable.

TABLE OF CONTENTS

ACKNOWLEDGMENTS	ii
LIST OF TABLES	v
LIST OF FIGURES	vi
LIST OF ABBREVIATIONS	xiii
CHAPTER	
1. HISTORICAL	1
Interaction of the Metal Oxide Support and Organometallic Complexes	4
2. EXPERIMENTAL	13
General	13
Impregnation of cyclopentadienyliron dicarbonyl dimer, 1 , on γ -alumina	17
Impregnation of di- μ -carbonyl-cis- μ -(1-5- η : 1'-5'- η '-dicyclopentadienyldimethylsilane)bis(carbonyl- diiron)(FeFe), 3 , on γ -alumina	18
Cyclopentadienyliron dicarbonyl dimer and di- μ - carbonyl-cis- μ -(1-5- η :1'-5'- η '-dicyclopentadienyl- dimethylsilane)bis(carbonyldiiron)(FeFe): (1 and 3)	19
Impregnation of cyclopentadienyldicarbonyliodoiron(II), 4 , on γ -alumina	19
Impregnation of cyclopentadienyl-dicarbonyl-2,4- cyclopentadienyliron, 5 , on γ -alumina	19

Impregnation of [α,α' -m-xylenebis(η^5 -cyclopentadienyl)]bis[tricarbonylmolybdenum], 9 , on γ -alumina	20
3. RESULTS AND DISCUSSION	22
Cyclopentadienyliron dicarbonyl dimer: 1	23
Di- μ -carbonyl-cis- μ -(1-5- η :1'-5'- η' -dicyclopentadienyldimethylsilane)bis(carbonyldiiron)(Fe:Fe), 3	35
Cyclopentadienyliron dicarbonyl dimer and di- μ -carbonyl-cis- μ -(1-5- η :1'-5'- η' -dicyclopentadienyldimethylsilane)bis(carbonyldiiron)(FeFe): (1 and 3)	50
Cyclopentadienyldicarbonyliodoiron (II): 4	58
Cyclopentadienyl-dicarbonyl-2,4-cyclopentadienyliron: 5	69
[α,α' -m-xylenebis(η^5 -cyclopentadienyl)]bis[tricarbonylmolybdenum]: 9	73
4. CONCLUSION	91
REFERENCES	93

LIST OF TABLES

Table	Page
I. Temperature Effect on Surface Activity of Alumina	3
II. Complex Characteristics of 1 for Specified Alumina Coverage	18
III. Complex Characteristics of 3 for Specified Alumina Coverage	18
IV. Complex Characteristics of 4 for Specified Alumina Coverage	19
V. Complex Characteristics of 9 for Specified Alumina Coverage	20
VI. DRIFTS data for (1) as a function of temperature and coverage (in wavenumbers)	35
VII. DRIFTS data for (3) as a function of temperature and coverage (in wavenumbers)	48
VIII. DRIFTS data for (1 and 3) as a function of temperature and coverage (in wavenumbers)	57
IX. DRIFTS data for (4) as a function of temperature and coverage (in wavenumbers)	69
X. DRIFTS data for (5) as a function of temperature and coverage (in wavenumbers)	73
XI. DRIFTS data for (9) as a function of temperature and coverage (in wavenumbers)	89

LIST OF FIGURES

Figure	Page
1. Illustration of aluminium binding to a hydroxyl group	2
2. Binding at a bridging carbonyl for the iron species $\text{Fe}_3(\text{CO})_{12}$	7
3. Diagram depicting the formation of the anionic hydride cluster $[\text{HFe}_3(\text{CO})_{11}]^-$	8
4. Diagram showing binding to the surface via a donor-acceptor interaction	11
5. Diagram illustrating binding to alumina at a bridging carbonyl site in 1	25
6. Diagram illustrating binding to alumina at metal site in 3	37
7. Diagram illustrating binding to alumina at terminal carbonyl site in 5	70
8. Ferrocene	71
9. Diagram illustrating binding to alumina at a metal in 9	75
10. FT-IR of cyclopentadienyliron dicarbonyl dimer, (1), in hexane	27
11. DRIFTS Spectrum of (1) at Room Temperature	28
12. DRIFTS Spectrum of (1) at 40 °C	28
13. DRIFTS Spectrum of (1) at 80 °C	29

Figure	Page
14. DRIFTS Spectrum of (1) at 100 °C	29
15. DRIFTS Spectrum of (1) on γ -Al ₂ O ₃ (4/10 coverage) at Room Temperature	30
16. DRIFTS Spectrum of (1) on γ -Al ₂ O ₃ (4/10 coverage) at 80 °C	30
17. DRIFTS Spectrum of (1) on γ -Al ₂ O ₃ (4/10 coverage) at 100 °C	31
18. DRIFTS Spectrum of (1) on γ -Al ₂ O ₃ (3/10 coverage) at Room Temperature	31
19. DRIFTS Spectrum of (1) on γ -Al ₂ O ₃ (3/10 coverage) at 60 °C	32
20. DRIFTS Spectrum of (1) on γ -Al ₂ O ₃ (3/10 coverage) at 100 °C	32
21. DRIFTS Spectrum of (1) on γ -Al ₂ O ₃ (2/10 coverage) at Room Temperature	33
22. DRIFTS Spectrum of (1) on γ -Al ₂ O ₃ (2/10 coverage) at 40 °C	33
23. DRIFTS Spectrum of (1) on γ -Al ₂ O ₃ (2/10 coverage) at 80 °C	34
24. FT-IR Spectrum of di- μ -carbonyl-cis- μ -(1-5- η :1'-5'- η '-dicyclopentadienyldimethyl- silane)bis(carbonyldiiron)(FeFe), (3), in nujol	39
25. DRIFTS Spectrum of (3) at Room Temperature	39
26. DRIFTS Spectrum of (3) at 60 °C	40

Figure	Page
27. DRIFTS Spectrum of (3) at 80 °C	40
28. DRIFTS Spectrum of (3) at 100 °C	41
29. DRIFTS Spectrum of (3) at 140 °C	41
30. DRIFTS Spectrum of (3) on γ -Al ₂ O ₃ (4/10 coverage) at Room Temperature	42
31. DRIFTS Spectrum of (3) on γ -Al ₂ O ₃ (4/10 coverage) at 150 °C	42
32. DRIFTS Spectrum of (3) on γ -Al ₂ O ₃ (4/10 coverage) at 200 °C	43
33. DRIFTS Spectrum of (3) on γ -Al ₂ O ₃ (3/10 coverage) at Room Temperature	44
34. DRIFTS Spectrum of (3) on γ -Al ₂ O ₃ (3/10 coverage) at 100 °C	45
35. DRIFTS Spectrum of (3) on γ -Al ₂ O ₃ (2/10 coverage) at Room Temperature	46
36. DRIFTS Spectrum of (3) on γ -Al ₂ O ₃ (2/10 coverage) at 40 °C	46
37. DRIFTS Spectrum of (3) on γ -Al ₂ O ₃ (2/10 coverage) at 100 °C	47
38. DRIFTS Spectrum of cyclopentadienylirondicarbonyldimer and di- μ - carbonyl-cis- μ -(1-5- η :1'-5'- η '-dicyclopentadienyldimethylsilane) bis(carbonyldiiron)(FeFe), (1 and 3), at Room Temperature	53
39. DRIFTS Spectrum of (1 and 3) at 60 °C	53
40. DRIFTS Spectrum of (1 and 3) at 80 °C	54

Figure	Page
41. DRIFTS Spectrum of (1 and 3) at 100 °C	54
42. DRIFTS Spectrum of (1 and 3) on γ -Al ₂ O ₃ (4/10 coverage) at Room Temperature	55
43. DRIFTS Spectrum of (1 and 3) on γ -Al ₂ O ₃ (4/10 coverage) at 80 °C	55
44. DRIFTS Spectrum of (1 and 3) on γ -Al ₂ O ₃ (4/10 coverage) at 120 °C	56
45. DRIFTS Spectrum of (1 and 3) on γ -Al ₂ O ₃ (4/10 coverage) at 140 °C	56
46. FT-IR Spectrum of cyclopentadienyldicarbonyl- iodoiron (II), (4), in chloroform	56
47. DRIFTS Spectrum of (4) at Room Temperature	56
48. DRIFTS Spectrum of (4) at 60 °C	61
49. DRIFTS Spectrum of (4) at 100 °C	61
50. DRIFTS Spectrum of (4) at 40 °C	62
51. DRIFTS Spectrum of (4) cooled to Room Temperature	62
52. DRIFTS Spectrum of (4) at 100 °C	63
53. DRIFTS Spectrum of (4) cooled to Room Temperature	63
54. DRIFTS Spectrum of (4) on γ -Alumina (4/10 coverage) at Room Temperature	64
55. DRIFTS Spectrum of (4) on γ -Alumina (4/10 coverage) at 80 °C	64

Figure	Page
56. DRIFTS Spectrum of (4) on γ -Alumina (4/10 coverage) at 100 °C	65
57. DRIFTS Spectrum of (4) on γ -Alumina (4/10 coverage) at Room Temperature after cooling	65
58. DRIFTS Spectrum of (4) on γ -Alumina (3/10 coverage) at Room Temperature	66
59. DRIFTS Spectrum of (4) on γ -Alumina (4/10 coverage) at 60 °C	66
60. DRIFTS Spectrum of (4) on γ -Alumina (4/10 coverage) at 80 °C	67
61. DRIFTS Spectrum of (4) on γ -Alumina (2/10 coverage) at Room Temperature	67
62. DRIFTS Spectrum of (4) on γ -Alumina (2/10 coverage) at 60 °C	68
63. DRIFTS Spectrum of (4) on γ -Alumina (2/10 coverage) at 80 °C	68
64. DRIFTS Spectrum of Cyclopentadienyl- dicarbonyl-2,4-cyclopentadienyliron, (5), on 101 mg of γ -Al ₂ O ₃ at Room Temperature	71
65. DRIFTS Spectrum (5) on 101 mg of γ -Al ₂ O ₃ at 40 °C	72
66. DRIFTS Spectrum (5) on 101 mg of γ -Al ₂ O ₃ at 60 °C	72
67. DRIFTS Spectrum of (5) on 101mg γ -Al ₂ O ₃ at 80 °C	73

Figure	Page
68. FT-IR Spectrum of [α,α' -m-xylenebis(η^5 -cyclopentadienyl)]bis[tricarbonylmolybdenum], (9), in hexane	77
69. DRIFTS Spectrum of (9) at Room Temperature	77
70. DRIFTS Spectrum of (9) at 150 °C	78
71. DRIFTS Spectrum of (9) at 350 °C	78
72. DRIFTS Spectrum of (9) at 400 °C	79
73. DRIFTS Spectrum of (9) at Room Temperature after cooling	79
74. DRIFTS Spectrum of (9) on γ -Alumina (4/10 coverage) at Room Temperature	80
75. DRIFTS Spectrum of (9) on γ -Alumina (4/10 coverage) at 80 °C	80
76. DRIFTS Spectrum of (9) (4/10 coverage) at 100 °C	81
77. DRIFTS Spectrum of (9) on γ -Alumina (4/10 coverage) at 150 °C	81
78. DRIFTS Spectrum of (9) on γ -Alumina (4/10 coverage) at 200 °C	82
79. DRIFTS Spectrum of (9) on γ -Alumina (4/10 coverage) at 250 °C	82
80. DRIFTS Spectrum of (9) on γ -Alumina (4/10 coverage) at 100 °C	83
81. DRIFTS Spectrum of (9) on γ -Alumina (3/10 coverage) at Room Temperature	83

Figure	Page
82. DRIFTS Spectrum of (9) on γ -Alumina (3/10 coverage) at 100 °C	84
83. DRIFTS Spectrum of (9) on γ -Alumina (3/10 coverage) at 150 °C	84
84. DRIFTS Spectrum of (9) on γ -Alumina (3/10 coverage) at 250 °C	85
85. DRIFTS Spectrum of (9) on γ -Alumina (3/10 coverage) at 300 °C	85
86. DRIFTS Spectrum of (9) on γ -Alumina (3/10 coverage) at 200 °C	86
87. DRIFTS Spectrum of (9) on γ -Alumina (3/10 coverage) at Room Temperature	86
88. DRIFTS Spectrum of (9) on γ -Alumina (2/10 coverage) at Room Temperature	87
89. DRIFTS Spectrum of (9) on γ -Alumina (2/10 coverage) at 200 °C	87
90. DRIFTS Spectrum of (9) on γ -Alumina (2/10 coverage) at 300 °C	88

LIST OF ABBREVIATIONS

m	=	medium
s	=	strong
v	=	very

CHAPTER 1

HISTORICAL

The interaction of an organometallic complex with a metal oxide support is a topic of interest in the field of catalysis. Catalysts containing supported complexes are of special concern as they provide certain advantages over non-supported catalysts. These advantages include thermal stability, specificity, and reproducibility. Another advantage is a decrease in the rate of sintering of the metal particles since they are not in close proximity to each other. In addition to this, such catalysts provide a high surface to volume ratio of the metal.

Alumina is a unmodified inorganic metal oxide that can be used as the support. Alumina is an amphoteric compound.¹ The structure of alumina is that of a crystal lattice resembling a spinel.² The texture of alumina resembles that of a loose cemented gravel bed where the main particles are crystalline and have a specific diameter and surface area. The crystals consist of a cubic close packed lattice of O^{2-} ions in which Al^{3+} ions are distributed among the tetrahedral and octahedral holes. The hydroxyl groups present are terminal, and each is coordinated to single tetrahedral and octahedral cations (Fig. 1).³

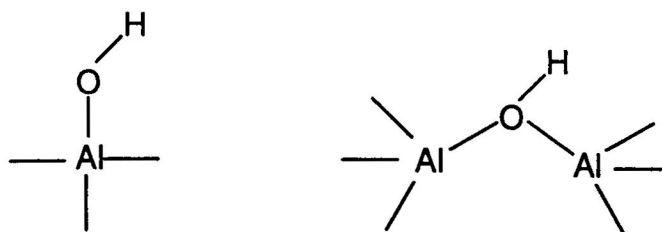
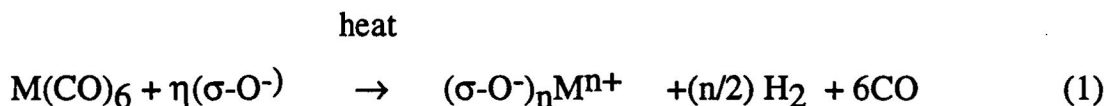


Fig. 1. Illustration of aluminium binding to a hydroxyl group.

The acidic and basic catalytic sites were first recognized by H. Pines.⁴ Further research conducted by Correa and associates illustrated that the basic and acidic sites could exist at immediate adjacent positions.⁵ The surface oxide ions ($\sigma\text{-O}^-$) acts as Lewis bases. The anion vacancies which expose coordinately unsaturated Al^{3+} (cus) ions function as a Lewis acid.⁶

The choice of metal oxide used is important as Hucul and Brenner reported that maximum activity of a catalysts is achieved when the preparation allows for the full decarbonylation and low-valent state of the metal carbonyl. Standard alumina does not allow this; thus, it is necessary to dehydroxylate the alumina as seen in reaction (1).



Reaction (1) illustrates complete decarbonylation along with oxidation. When a highly dehydroxylated alumina is used, this is advantageous as it allows for the synthesis of catalysts with an average oxidation state near zero.⁸

Alumina has a surface that is fully hydroxylated. The extent of dehydroxylation can be decreased by heating. The process of dehydroxylation of

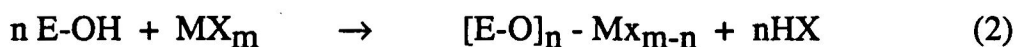
fully hydroxylated alumina begins at just above 200 °C in the case of γ -alumina. It is unclear at which temperature full dehydroxylation occurs; however, it has been determined that at a temperature of approximately 950 °C nearly complete dehydroxylation is reached. At this stage, the γ -alumina has been partially converted to δ -alumina. Partial dehydroxylation of alumina occurs at approximately 475 °C.⁹ This is illustrated in Table I.

Table I. Temperature Effect on Surface Activity of Alumina

TEMPERATURE	PROCESS	SURFACE ACTIVITY
200 °C	initiation of dehydration	$2\sigma\text{-H} \rightarrow \text{H}_2\text{O} + \sigma\text{-O}^-$ The oxygen lattice now contains a vacancy in the surface and expand a Al^{3+} ion that is a coordinately unsaturated surface species.
475 °C	partially hydroxylated	The original 15 approximately 4 of 15 $\sigma\text{-OH}/\text{nm}^2$.
950 °C	nearly completely dehydroxylated	approximately 0.12 $\sigma\text{-OH}/\text{nm}^2$ remains.

Interaction of the Metal Oxide Support and Organometallic Complexes

The deposition of organometallic complexes on a metal oxide support results in the partial retention of the organic ligand.¹⁰ The groups present on the surface of the alumina are responsible for the formation and stabilization of the catalytically active supported complex. The organometallic complex interacts with surface groups of alumina thus resulting in the binding of the complex to the supported system.¹¹ This binding with the surface of an oxide is illustrated in reaction (2).

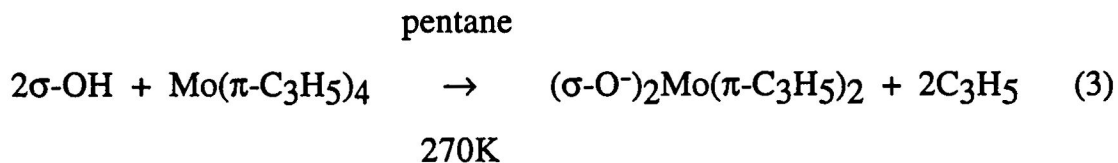


where E = Al, and

MX_m = organometallic compound or transition metal compound

When reaction (2) occurs, the product formed is a highly active, well dispersed, supported metal catalyst.

Yermakov and co-workers illustrated the binding of an organometallic complex on alumina using a molybdenum compound. The complex is anchored onto the support surface by a reaction that occurs with the σ -OH species which is acidic as shown in reaction (3).¹²



This process occurs as a result of the basic character of the π -allyl ligands which behave as monoanions.¹³ The use of allyl complexes for the preparation of supported catalyst also has been studied by Iwasawa and coworkers.¹⁴

With reference to mononuclear compounds where the carbonyl groups are terminal, binding can occur at a ligand site. This process is illustrated in reaction (4).¹⁵



Where R = Al

Burwell, using $\text{Mo}(\text{CO})_6$, showed the substitution of CO by surface ligands of alumina. This substitution occurred at room temperature when partially or strongly dehydroxylated alumina was used. In this case a COOH^- species was formed via a nucleophilic attack of a $\sigma\text{-OH}$ group on a CO ligand.¹⁶ The basicity of the surface hydroxyl groups is responsible for the extent to which decarbonylation occurs.¹⁷ The formation of the surface complex $\text{Rh}^+(\text{CO})_2$ with evolution of hydrogen resulting from the oxidation of the zero valent rhodium in $\text{Rh}_6(\text{CO})_{16}$ also show the importance of basic $\sigma\text{-OH}$ groups in reactions of metal carbonyls.¹⁸

Kazusaka and Howe discussed the binding and reactivity of $\text{W}(\text{CO})_6$, which is similar to that of $\text{Mo}(\text{CO})_6$. However, in the case of $\text{W}(\text{CO})_6$ when heating occurs, in addition to the formation of sub-carbonyl species, bimolecular species are formed. These bimolecular species contain bridging carbonyl ligands that are coordinated to Lewis acid sites on the support.¹⁹

Infrared data from temperature programmed decomposition analyses indicated the loss of three carbonyls for $\text{Mo}(\text{CO})_6$ and six for $\text{W}(\text{CO})_6$ per metal atom. The sub-carbonyl species $\text{M}(\text{CO})_3$ is formed at 200 °C in both cases, but at higher temperatures $\text{W}(\text{CO})_6$ formed the bimolecular species $\text{W}_2(\text{CO})_6$.²⁰

Temperature programmed decomposition studies carried out with $\text{Cr}(\text{CO})_6$ on alumina illustrated that this metal carbonyl first undergoes loss of carbon

monoxide. However, as the temperature is increased, this causes further loss of CO resulting in the formation of sub-carbonyl species in addition to the evolution of hydrogen.^{21,22} Similarly in the case of Mo(CO)_6 , most of the metal carbonyl is desorbed while the remainder forms subcarbonyl species such as $[(\text{Al-O})(\text{CO}_2\text{Mo}(\mu\text{-CO}\rightarrow\text{Al})_2\text{Mo(CO)}_2(\text{O-Al}))]$. In this species, the bridging carbonyl ligands are coordinated to Lewis acids sites on alumina.²³

Bjorklund and Burwell conducted studies using nickel tetracarbonyl on γ -alumina. Initial binding on the alumina surface resulted in a yellow complex. The color change, from white to yellow, was due to the loss of carbonyl upon binding. Further loss of the carbonyl resulted in a gray color complex. When temperature programmed decomposition was carried out the extent of CO/Ni present in the grey complex was decreased. This was achieved at a temperature of 100 °C.²⁴ Further heating to 450 °C liberated hydrogen, carbon dioxide and carbon monoxide. This process occurred when partially dehydroxylated alumina was used. However, when highly dehydroxylated alumina was used and temperature programmed decomposition carried out hydrogen was not evolved.²⁵

In the case of polynuclear compounds which have both a terminal and a bridging carbonyl, binding can occur at either carbonyl. However, binding at the bridging carbonyl allows for the formation of the most stable species. This binding is illustrated in Fig. 2 with the iron species $\text{Fe}_3(\text{CO})_{12}$. The bonding of this anion involves coordination to a Lewis acid site.²⁶

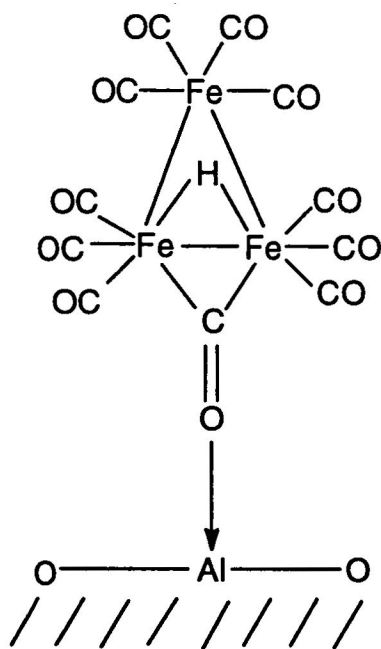
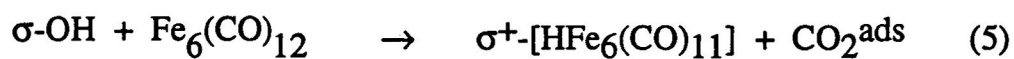


Fig. 2. Binding at a bridging carbonyl for the iron species $\text{Fe}_3(\text{CO})_{12}$.

In the case of the compounds $\text{Fe}_3(\text{CO})_{12}$, $\text{Fe}_2(\text{CO})_9$, and $\text{Fe}(\text{CO})_5$, the formation of the anionic hydride cluster $[\text{HFe}_3(\text{CO})_{11}]^-$ was detected and seen in reaction (5).²⁷



The formation of the $[\text{HFe}_3(\text{CO})_{11}]^-$ species occurs via the reaction as shown in Fig. 3.

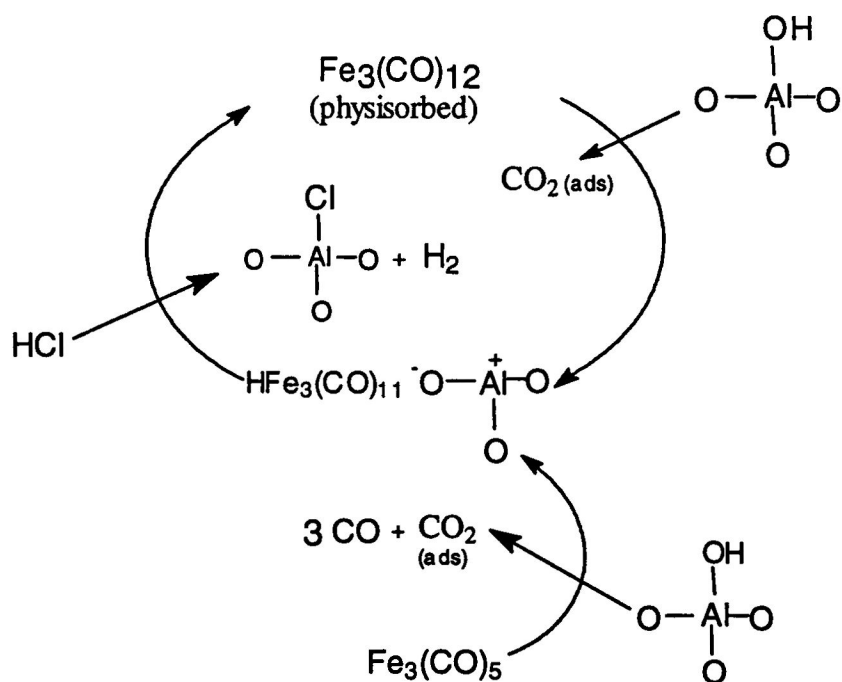


Fig. 3. Diagram depicting the formation of the anionic hydride cluster $[\text{HFe}_3(\text{CO})_{11}]^-$

According to Hugues et al., since dehydroxylated alumina was used, it is the hydroxyl groups of alumina that are responsible for the nucleophilic attack on the carbonyls.²⁸

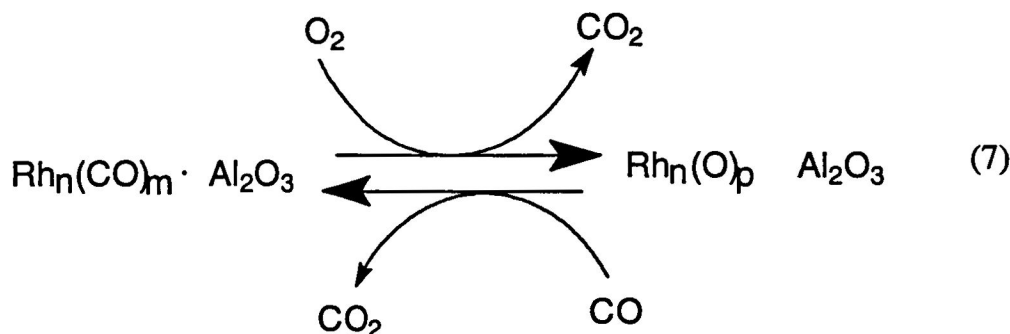
When temperature programmed decomposition was carried out on $\text{Fe}_3(\text{CO})_{12}$, this compound decomposed at 420 K to form Fe^{3+} on the surface.

Smith et al showed the binding of $\text{Os}_3(\text{CO})_{12}$ on alumina as seen in reaction 6.²⁹



The deposition of $\text{Rh}_6(\text{CO})_{16}$ on alumina and exposure to oxygen gave rise to a yellow or tan complex indicative of decarbonylation. This decarbonylation compound could be regenerated to the carbonylated form by allowing contact with

less than one atmosphere of CO. When this occurred the original pale violet color was restored. This process of decarbonylation/ carbonylation of $\text{Rh}_6(\text{CO})_{16}/\gamma\text{-Al}_2\text{O}_3$ results in the evolution of carbon dioxide as seen in reaction 7.³⁰



The compound $\text{Rh}_6(\text{CO})_{16}$ on alumina retains its character, and form $[\text{Rh}_6(\text{C})]_{16-n}(\text{O}_2)_n/\gamma\text{-Al}_2\text{O}_3$. Upon heating the sample to 250 °C, all carbonyl groups are lost and only the Rh_6 cluster remains.³¹ The $\text{Rh}_6(\text{CO})_{16}$ species is not stable as carbon dioxide is lost upon exposure to air or oxygen.³²

Research by Du and associates focused on the polynuclear species $[\text{Pt}(\text{CO})_6]_5[\text{N}(\text{C}_2\text{H}_5)_4]_2$. The infrared spectra of this compound, when placed on alumina, remains unchanged. However, when temperature programmed decomposition is carried out in vacuum at 150 °C the terminal and bridging carbonyls disappear. Further exposure to CO for 30 min. at a pressure of 5.3 KPa results in the reappearance of terminal carbonyl only.^{33,34}

Infrared studies carried out using rhodium compounds indicated that $\text{Rh}_2\text{CO}_2(\text{CO})_{12}$ is adsorbed initially on γ -alumina with loss of the bridging carbonyls. Experiments carried out above 27 °C showed that the remaining carbonyls are also lost. Decarbonylation also occurs when this compound is left standing in air at room temperature.³⁵

According to Psaro and coworkers, supported metal clusters of the first and second row transition metals are more catalytically active than those of the third row.³⁶ In contrast to $\text{Fe}_3(\text{CO})_{12}$ and $\text{Rh}_5(\text{CO})_{16}$, the compound $\text{Os}_3(\text{CO})_{12}$ is stable up to 70 °C when supported on alumina. Smith and coworkers also provide evidence that illustrates the fact that the surface Os carbonyl species supported on alumina is stable up to approximately 300 °C.³⁷

According to Guczi and Beck, bimetallic clusters when placed on an alumina support forms mononuclear species. The metal framework of compounds such as $\text{FeRu}_2(\text{CO})_{12}$, $\text{Fe}_2\text{Ru}(\text{CO})_{12}$, and $\text{H}_2\text{FeRu}_3(\text{CO})_{13}$ cleaved via sub-carbonyl species as $\text{MCO}---\text{M}$, $\text{M}(\text{CO})_x$ and $[\text{HM}(\text{CO})_x]^-$. In this case where $x = 1-5$ and $\text{M}=\text{Fe}$ or Ru , the original cluster formed $\text{Ru}_3(\text{CO})_{12}$ and $\text{Fe}(\text{CO})_5$. When temperature programmed decomposition was carried out, further decomposition occurred giving rise to anchored $\text{Ru}(\text{O})(\text{CO})_2$, $\text{Ru}(\text{II})(\text{CO})_2$, and $\text{Ru}(\text{III})(\text{CO})_2$ in addition to Fe^{2+} and Fe^{3+} . These products were stable over a range of 273-573K.³⁸

Shriver and coworkers also carried out studies on the interaction of organometallic complexes incorporating cyclopentadienyl groups as ancillary ligands. These species are of interest due to the special reactivity and stability that occur as a result of a strong six electron multi-centered bond that forms with the cyclopentadienyl group and the transition metal. Surface adducts are formed in the case of organometallic complexes incorporating the cyclopentadienyl group. Compounds such as $[\text{CpFeCO}]_4$, $\text{Cp}_3\text{Ni}(\text{CO})_2$, and $[\text{CpNiCO}]_2$ bind to the surface by means of a donor-acceptor interaction between the oxygen of the carbonyl and the Al^{3+} ions present on alumina surface as seen in Fig. 4.³⁹

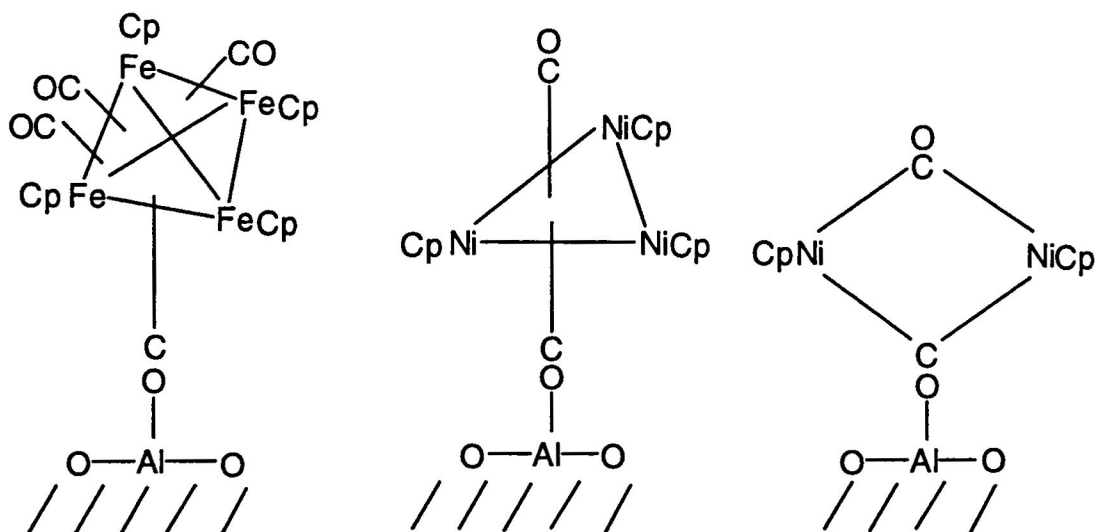
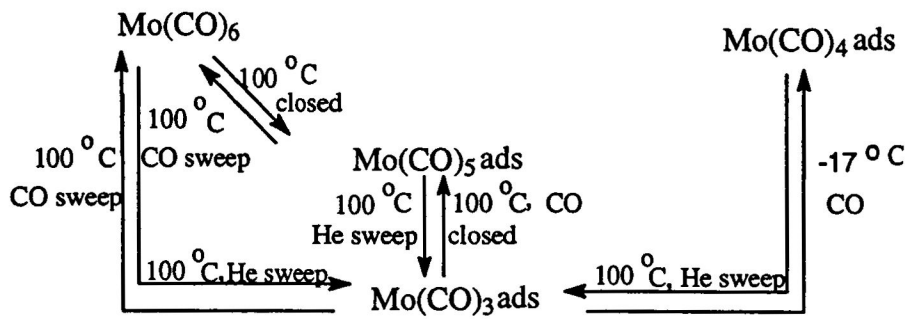


Fig. 4. Diagram showing binding to the surface via a donor-acceptor interaction.

The stability of the surface adducts was found to increase as shown:
 $[\text{CpFeCO}]_4 > \text{Cp}_3\text{Ni}(\text{CO})_2 > [\text{CpNiCO}]_2$.

Temperature programmed decomposition of supported metal carbonyls result in either partial or complete decarbonylation of the compound. While the result of this process is the formation of sub-carbonyl species, the process of decarbonylation is not permanent. Brenner and Burwell suggest that the removal of CO can be reversed by introducing a flow of CO gas into the system. This process can occur as seen in reaction scheme 1.



Scheme 1. Diagram illustrating the reversible process of decarbonylation/carbonylation.

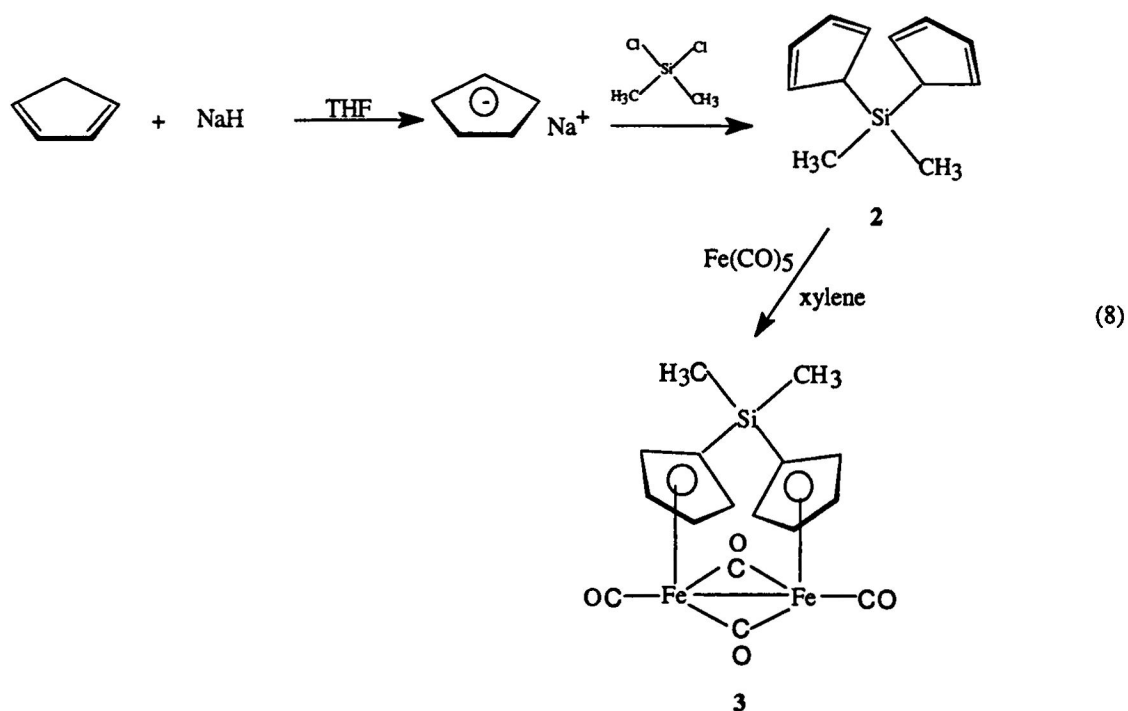
CHAPTER 2

EXPERIMENTAL

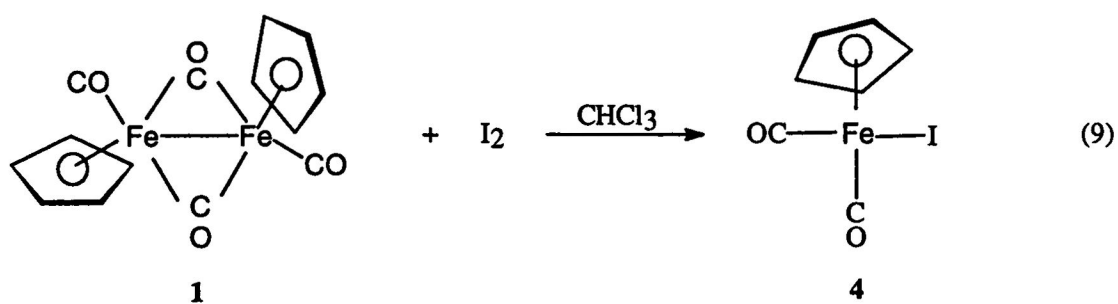
General: All reactions and subsequent manipulations were carried out using standard Schlenk techniques under a purified nitrogen atmosphere.

Cyclopentadienyliron dicarbonyl dimer (**1**) was purchased from Aldrich Chemical Co. and Gamma alumina, with a surface area of 110 m²/g, was purchased from Goodfellow. The alumina was pretreated by heating it to 500 °C to ensure partial dehydroxylation.

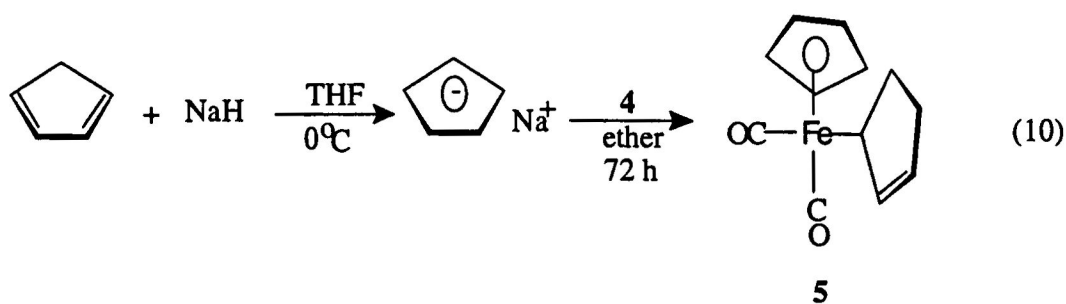
Biscyclopentadienyldimethylsilane, (**2**),⁴² and di- μ -carbonyl-cis-(1-5- η -1'-5'- η '-dicyclopentadienyldimethylsilane)bis(carbonyldiiron)(FeFe) (**3**),⁴³ were synthesized as shown in reaction 8.



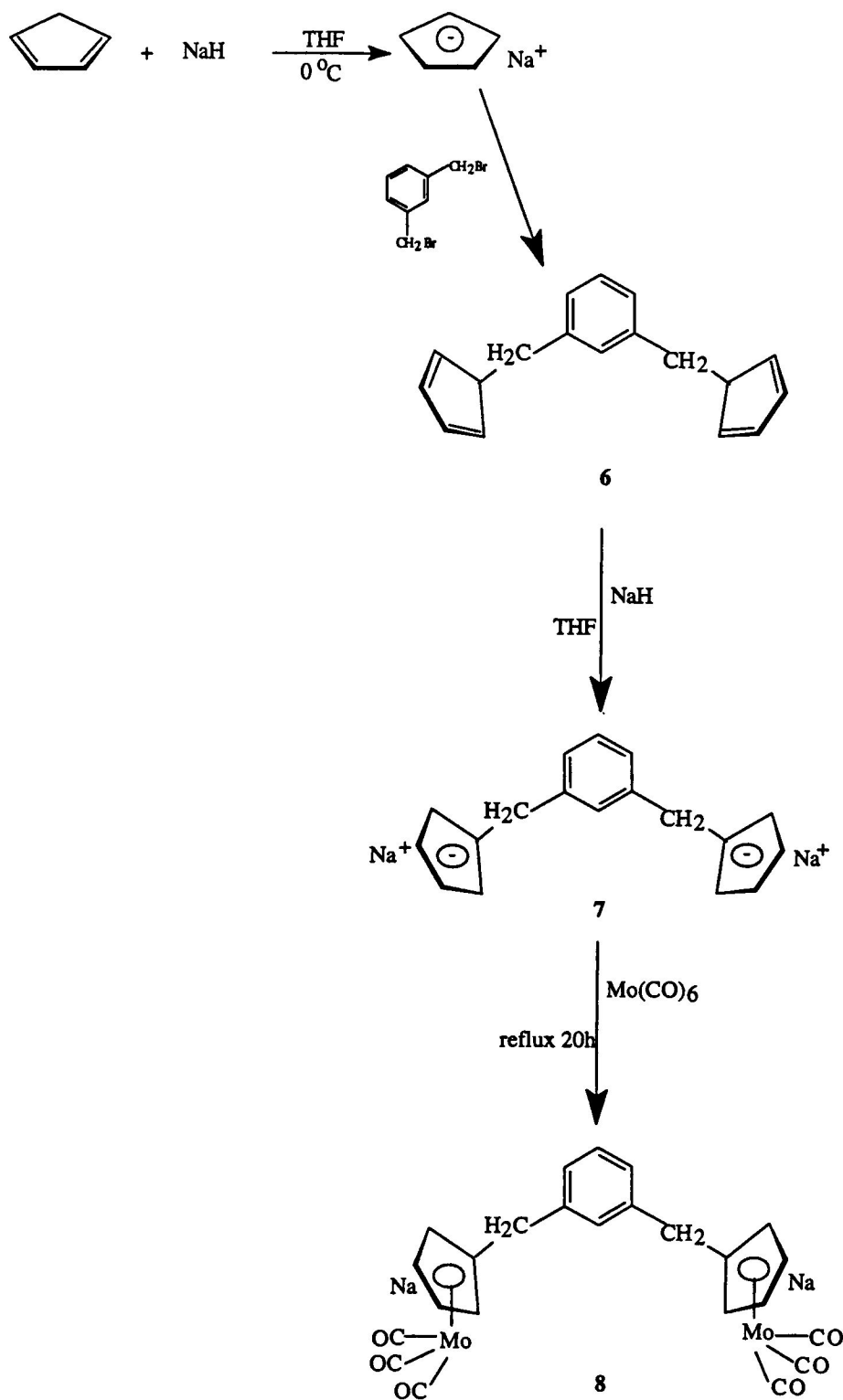
Reaction 9 shows the synthesis of cyclopentadienyldicarbonyliodoiron (II), (4).⁴⁴



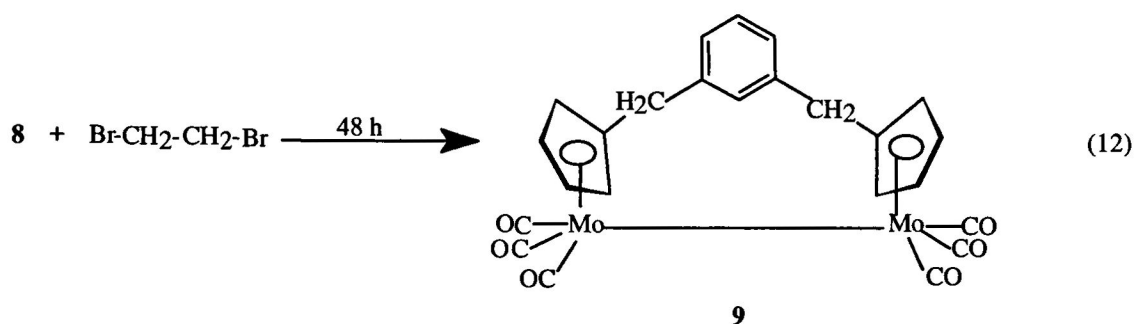
Reaction 10 shows the synthesis of cyclopentadienyl-dicarbonyl-2,4-cyclopentadienyliron, (5).⁴⁵



Reactions 11 and 12 shows the synthesis of the compounds α,α' -dicyclopentadienyl-m-xylene, (6),⁴⁶ disodium(m-phenylene)dicyclopentadienide, (7),⁴⁷ disodium[(m-phenylenedimethylene)bis(η^5 -cyclopentadienyl)][tricarbonylmolybdate (1-)], (8),⁴⁸ and [α,α' -m-xylenebis(η^5 -cyclopentadienyl)]bis[tricarbonylmolybdenum], (9).⁴⁹



(11)



The organometallic complexes, **1**, **3** (**1** and **3**), **4**, **5**, and **9** were impregnated on γ -alumina using the incipient wetness method.⁵⁰

Impregnation of cyclopentadienyliron dicarbonyl dimer, **1, on γ -alumina:** In a typical experiment 0.0258 g (0.0729 mmol) of **1** was dissolved in 3.6 mL of hexane and 1.001 g of Goodfellow γ -alumina 110 m²/g was added and the mixture was stirred for 4 h at room temperature. The solvent was removed by passing dry N₂ over the mixture overnight. Assuming four OH⁻ groups per binding site and 4.4 x 10²⁰ of these sites/m², this corresponded to a coverage of approximately 1/10 of the surface sites. Samples of approximately 1/20, 2/10, 3/10, and 4/10 coverage were prepared in a similar manner as described in Table II.

Table II. Complex Characteristics of **1** for Specified Alumina Coverage

complex (grams)	complex (moles)	γ -alumina (grams)	coverage
0.0129	3.64 x 10 ⁻⁵	1.003	0.0499
0.0516	1.46 x 10 ⁻⁴	1.002	0.199
0.0774	2.19 x 10 ⁻⁴	1.001	0.299
0.1032	2.916 x 10 ⁻⁴	1.003	0.3991

Impregnation of di- μ -carbonyl-cis- μ -(1-5- η :1'-5'- η '-dicyclopentadienyl-dimethyl silane) bis(carbonyldiiron)(FeFe), 3, on γ -alumina: Di- μ -carbonyl-cis- μ -(1-5- η :1'-5'- η '-dicyclopentadienyldimethylsilane)bis(carbonyldiiron) (FeFe) was impregnated on Goodfellow γ -alumina 110 m²/g as described above. Samples of approximately 1/20, 1/10, 2/10, 3/10, and 4/10 coverage were prepared as shown in Table III.

Table III. Complex Characteristics of 3 for Specified Alumina Coverage

complex (grams)	complex (moles)	γ -alumina (grams)	coverage
0.0149	3.65×10^{-5}	1.002	0.0498
0.0299	7.30×10^{-5}	1.002	0.0999
0.0598	1.46×10^{-4}	1.001	0.199
0.0897	2.19×10^{-4}	1.002	0.299
0.1196	2.919×10^{-4}	1.003	0.3995

Impregnation of cyclopentadienyliron dicarbonyl dimer and di- μ -carbonyl-cis- μ -(1-5- η :1'-5'- η '-dicyclopentadienyldimethylsilane)bis(carbonyldiiron) (FeFe), (1 and 3), on γ -alumina: Cyclopentadienyliron dicarbonyl dimer 0.116 g (3.153×10^{-4} mol) and di- μ -carbonyl-cis- μ -(1-5- η :1'-5'- η '-dicyclopentadienyldimethylsilane)bis(carbonyldiiron)(FeFe) 0.1116 g (2.724×10^{-4} mol) were impregnated on 1.003 g of Goodfellow γ -alumina 110 m²/g as described in the method above, to give a combined coverage of 0.400.

Impregnation of cyclopentadienyldicarbonyliron(II), 4, on γ -alumina: Samples of cyclopentadienyldicarbonyliron(II) were impregnated on Goodfellow γ -alumina 110 m²/g as described above. Samples of approximately 1/20, 1/10, 2/10, 3/10 and 4/10 coverage were prepared as shown in Table IV.

Table IV. Complex Characteristics of 4 for Specified Alumina Coverage

complex (grams)	complex (moles)	γ -alumina (grams)	coverage
0.0111	3.65×10^{-5}	1.003	0.0500
0.0222	7.31×10^{-5}	1.003	0.100
0.0444	1.46×10^{-4}	1.001	0.200
0.0666	2.19×10^{-4}	1.003	0.300
0.0888	2.92×10^{-4}	1.002	0.400

Impregnation of cyclopentadienyl-dicarbonyl-2,4-cyclopentadienyliron, 5, on γ -alumina: A sample of cyclopentadienyl dicarbonyl-2,4-cyclopentadienyliron was impregnated on 101mg of Goodfellow γ -alumina 110m²/g.

Impregnation of $[\alpha,\alpha'$ -m-xylenebis(η^5 -cyclopentadienyl)]bis[tricarbonylmolybdenum], 9, on γ -alumina: Samples of $[\alpha,\alpha'$ -m-xylenebis(η^5 -cyclopentadienyl)]bis[tricarbonylmolybdenum], were impregnated on Goodfellow γ -alumina 110 m²/g as described above. Samples of approximately 1/20, 1/10, 2/10, 3/10 and 4/10 coverage were prepared as shown in Table V.

Table V. Complex Characteristics of **9** for Specified Alumina Coverage

complex (grams)	complex (moles)	γ -alumina (grams)	coverage
0.0216	3.65×10^{-5}	1.002	0.0499
0.0432	7.30×10^{-5}	1.003	0.0999
0.0864	1.46×10^{-4}	1.001	0.199
0.1296	2.190×10^{-4}	1.003	0.2997
0.1728	2.919×10^{-4}	1.002	0.3996

DRIFTS spectra of samples **1**, **3**, (**1** and **3**), and **4** on γ -alumina were obtained using a Nicolet 510 FTIR with a mercury-cadmium-telluride (MCT) detector, an 18-bit A/D converter, and an updated 680 data station. Spectra of **5** and **9** on γ -alumina were obtained using the same kind of detector and converter along with a Magna-IR 750 data station. The samples were prepared by loading KBr (previously sieved with a 63 microns mesh) into a HVC-DR2 environmental cell manufactured by Herrick Scientific Corporation. The surface was carefully leveled with a spatula. A thin layer of impregnated alumina was then placed on top of the KBr layer and leveled. Samples of **1** were also prepared by mixing 5% by weight impregnated alumina and 95% KBr. The cell was enclosed and purged with nitrogen, supplied from a glass vacuum manifold. Electrical supply and thermocouple connections were made to a thermostat heating system. Spectra were obtained at room temperature and at elevated temperatures under an

atmosphere of 6 torr of nitrogen. The samples of 1/20 and 1/10 surface coverage were too dilute to obtain any useful information. However, the significant spectra are shown.

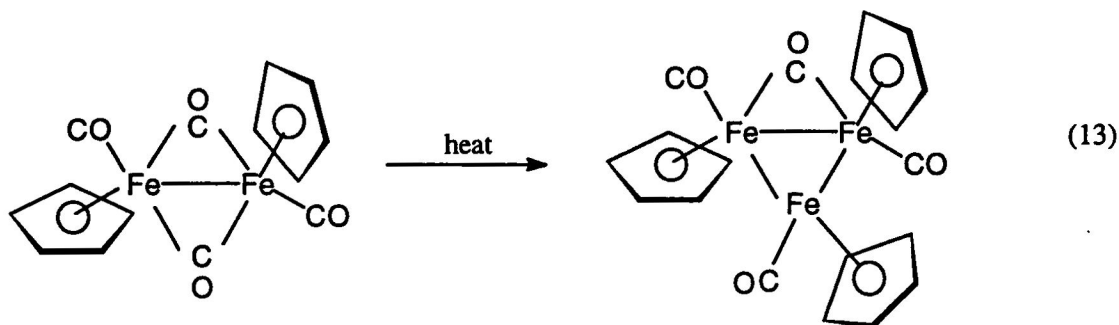
CHAPTER 3

RESULTS AND DISCUSSION

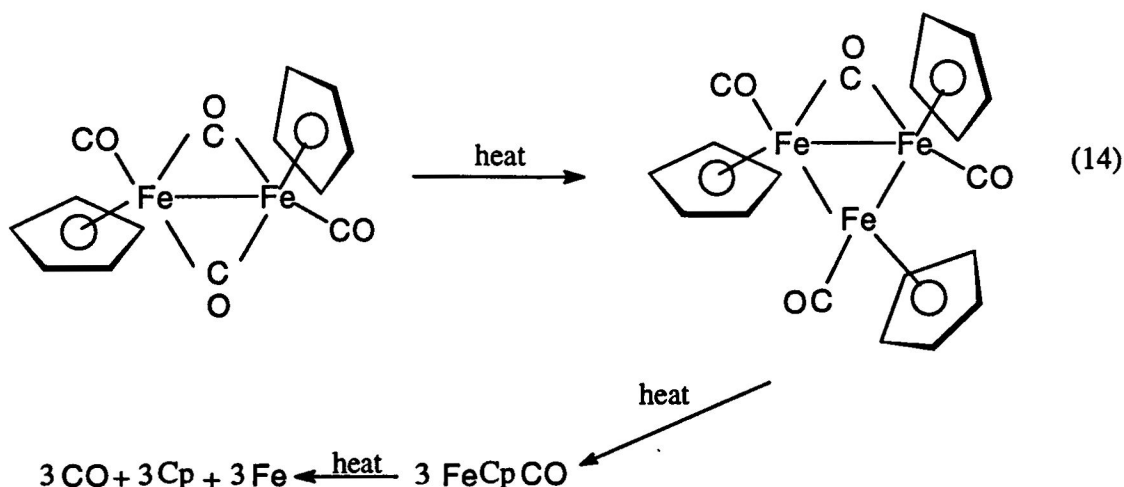
Diffuse Reflectance Infrared Fourier Transform Spectroscopy (DRIFTS) and temperature programmed decomposition (TPDE) were utilized to obtain spectral data of cyclopentadienyliron dicarbonyl dimer, (1); di- μ -carbonyl-cis- μ -(1-5- η :1'-5'- η '-dicyclopentadienyldimethylsilane)bis(carbonyldiiron)(Fe:Fe), (3); cyclopentadienyliron dicarbonyl dimer and di- μ -carbonyl-cis- μ -(1-5- η :1'-5'- η '-dicyclopentadienyldimethylsilane)bis(carbonyldiiron)(FeFe), (1 and 3); cyclopentadienyldicarbonyliodoiron (II), (4); cyclopentadienyl-dicarbonyl-2,4-cyclopentadienyliron (5); and [α,α' -m-xylenebis(η^5 -cyclopentadienyl)]bis[tricarbonylmolybdenum] (9); on γ -alumina as function of coverage and temperature. Assuming four OH⁻ groups per binding site and 4.4×10^{20} of these sites/m², samples of approximately 1/10, 1/20, 2/10, 3/10, and 4/10 coverage were prepared and analyzed. Each of the compounds were analyzed in terms of decarbonylation as a function of temperature. Comparisons of decarbonylation were made with respect to pure compounds and compounds supported on γ -alumina and non-supported compounds. The carbonyl bands were monitored because they have been shown to be diagnostic for determining the structure and bonding in this type of complexation. In addition, the carbonyl bands are by far the most intense band in the spectra of these complexes and can be conveniently monitored when other bands are too weak to even be observed.

Cyclopentadienyliron dicarbonyl dimer: 1

The solution spectrum of **1** (Fig. 10) exhibited bands at 2041.0, 2000.7, 1973.3, and 1960.5 cm^{-1} due to terminal carbonyls and at 1774.0 cm^{-1} due to the bridging carbonyls. When DRIFTS employing TPDE was carried out on **1**, the spectrum at room temperature (Fig. 11) exhibited broad terminal carbonyl bands at 2040.6, 1974.0, 1938.9 and 1910.4 cm^{-1} . A bridging carbonyl band was observed at 1779.5 cm^{-1} and a shoulder at 1737.5 cm^{-1} . Upon heating to 40 $^{\circ}\text{C}$ (Fig. 12) the band at 1974.0 cm^{-1} disappeared and the bridging carbonyl shoulder decreased in intensity. The spectrum remained unchanged upon further heating to 80 $^{\circ}\text{C}$ (Fig. 13) where the 1909.7 and 2040.0 cm^{-1} peaks decreased in intensity. The bridged carbonyl band at 1779.5 cm^{-1} shifted to a lower wavenumber of 1764.9 cm^{-1} and the 1737.5 cm^{-1} band steadily decreased in intensity upon further heating to 100 $^{\circ}\text{C}$ (Fig. 14) which exhibited the presence of only two bands in the terminal carbonyl region at 1955.0 and 1936.0 cm^{-1} . The bridging carbonyl band seen at 1764.9 cm^{-1} was also present. This shift of the carbonyl bands to lower wavenumbers is consistent with the formation of a trimer (reaction 13) as reported by Shriver (ref. 39).



It was expected that if sufficient heat was applied this would result in complete decarbonylation leaving behind a metal cluster and the cyclopentadienyl fragment as seen in reaction 14. However, this was not observed.



When **1** was placed on partially dehydroxylated gamma alumina the spectrum at room temperature was different from that of the pure compound. The spectrum for the 2/10 (Fig. 21), 3/10 (Fig. 18) and 4/10 (Fig. 15) coverage on γ -alumina exhibited an increase in wavenumber for all terminal carbonyl bands and one bridging carbonyl band. However, there was a decrease in wavenumber for the other bridging carbonyl band. This was indicative of Lewis acid binding at a bridging carbonyl (Fig 5). Binding at this site would be expected to cause the bridging carbonyl where binding occurred to be shifted to a lower wavenumber, relative to **1** above. The terminal carbonyls would then be shifted to a higher wavenumber. This in fact occurred.

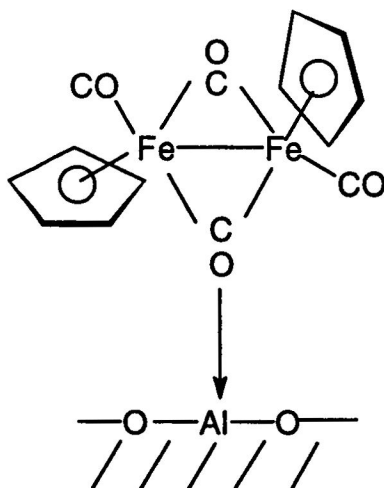
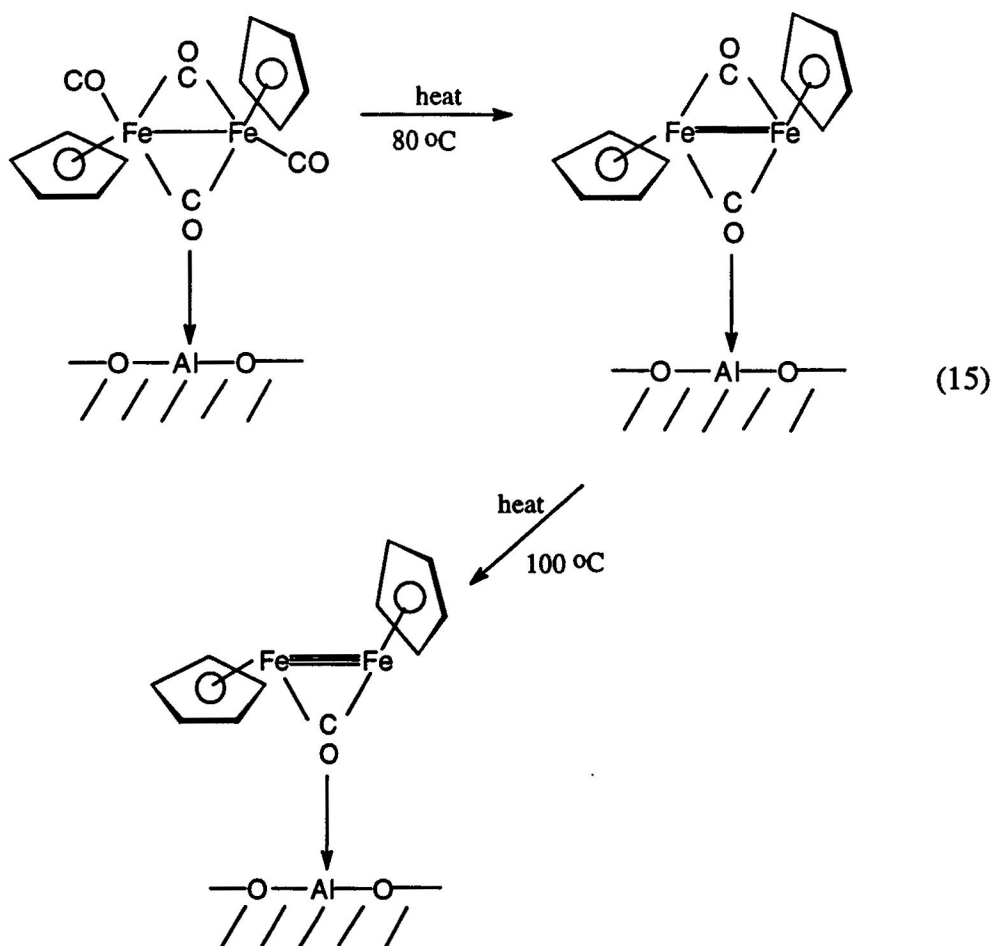


Fig. 5. Diagram illustrating binding to alumina at a bridging carbonyl site in **1**.

The band at 2059.6 cm^{-1} in the 2/10 sample decreased in intensity upon heating from room temperature (Fig. 21) to $40\text{ }^{\circ}\text{C}$ (Fig. 22). As the temperature was increased to $80\text{ }^{\circ}\text{C}$ (Fig. 23) the 1837.3 cm^{-1} band disappeared. No further changes were observed upon heating to $100\text{ }^{\circ}\text{C}$. In the case of the 4/10 coverage the spectrum remained unchanged up to $60\text{ }^{\circ}\text{C}$. As the temperature was increased to $80\text{ }^{\circ}\text{C}$ (Fig. 16) all terminal carbonyl bands disappeared while the bridging carbonyl bands remained. The bridging carbonyl band at 1772.2 cm^{-1} disappeared upon heating to $100\text{ }^{\circ}\text{C}$ (Fig. 17) while the band at 1714.4 cm^{-1} remained as seen in reaction 15 (ref 39). The same was true for the 3/10 sample.



Analysis of 2/10, 3/10 and 4/10 samples at room temperature prepared on a 95% KBr and 5% alumina support exhibited the presence of terminal and bridging carbonyls. The samples showed spectral data consistent with Lewis acid binding at a bridging carbonyl. As the coverage increased so did the intensity of the peaks

The DRIFTS data indicate that when 1 was placed on γ -alumina, the introduction of this Lewis acid catalyzed decarbonylation of the compound. On alumina, decarbonylation occurred more readily because of a complexation with a Lewis acid site that removed electron density directly or indirectly from the iron, thus decreasing backbonding, causing the carbonyl bond to metal bond to weaken.

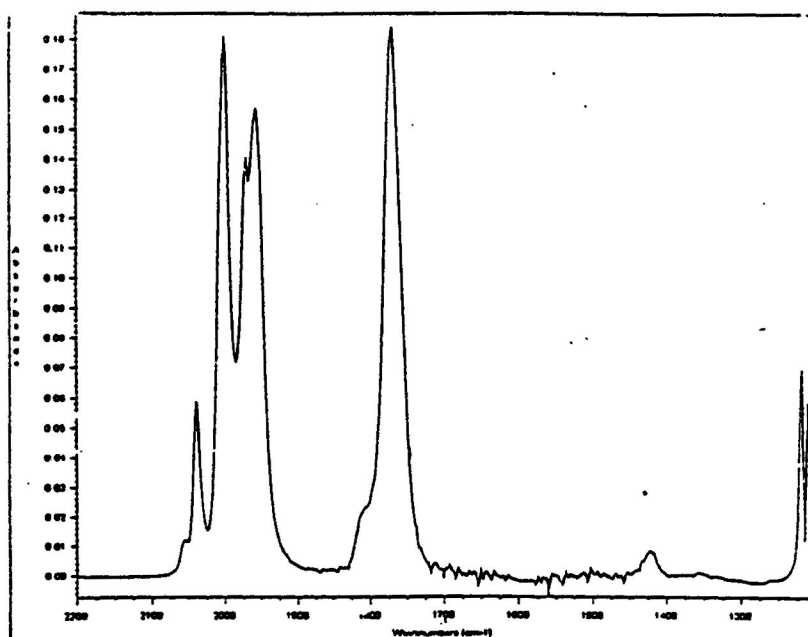


Fig. 10. FT-IR of cyclopentadienyliron dicarbonyl dimer, (1), in hexane

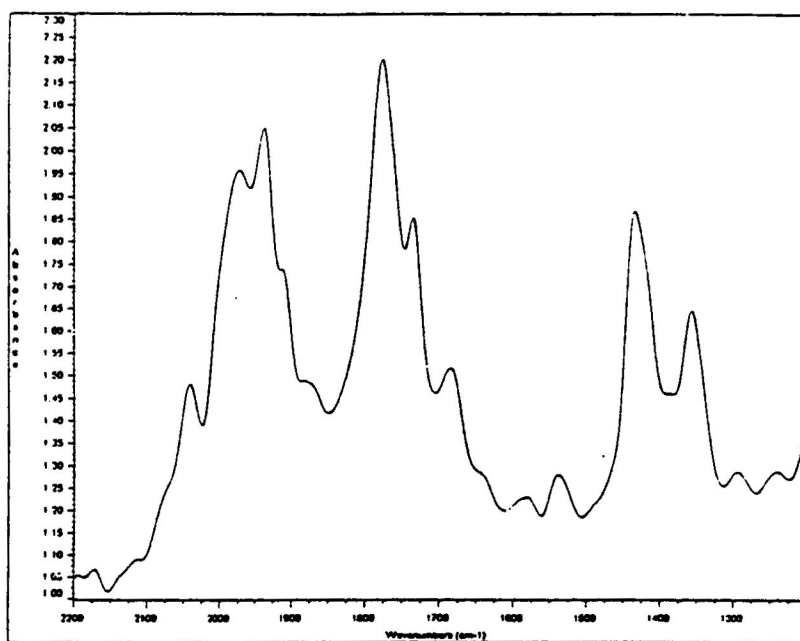


Fig. 11. DRIFTS Spectrum of (1) at Room Temperature.

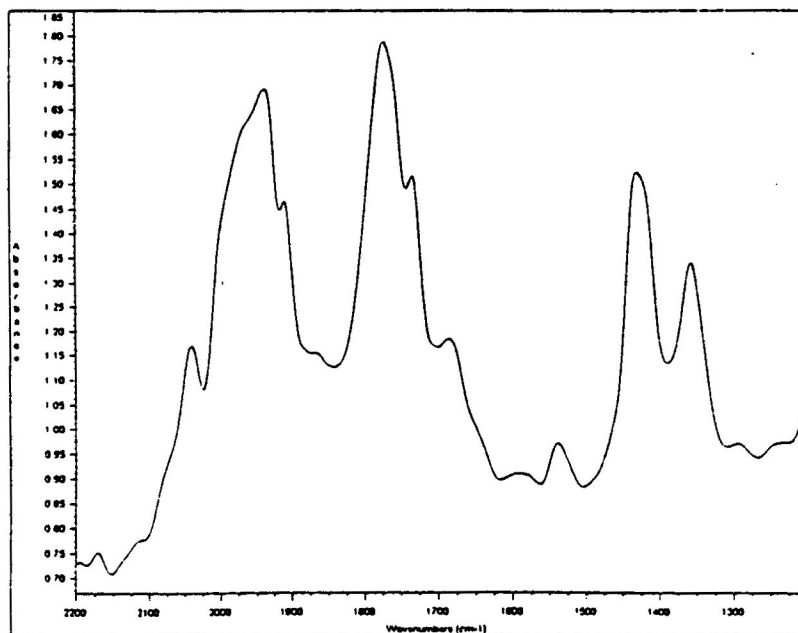


Fig. 12. DRIFTS Spectrum of (1) at 40 °C.

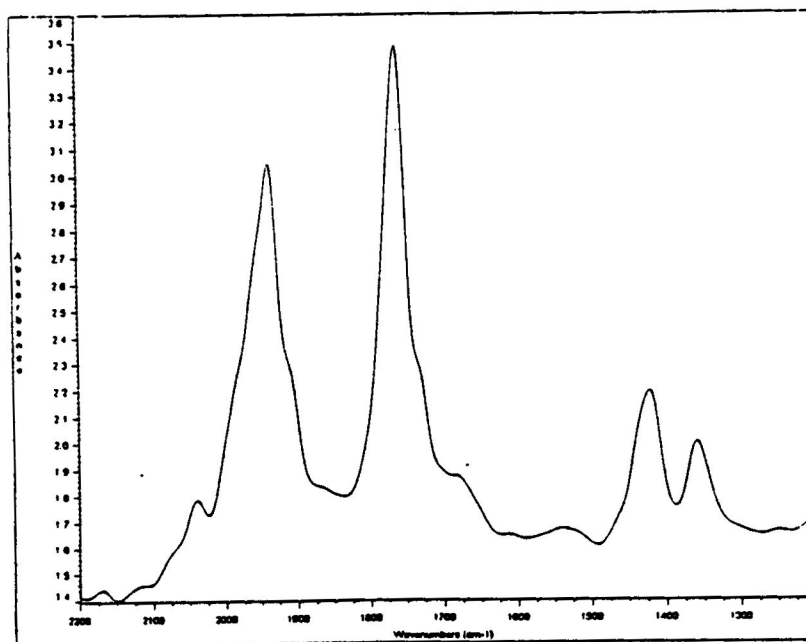


Fig. 13. DRIFTS Spectrum of (1) at 80 °C .

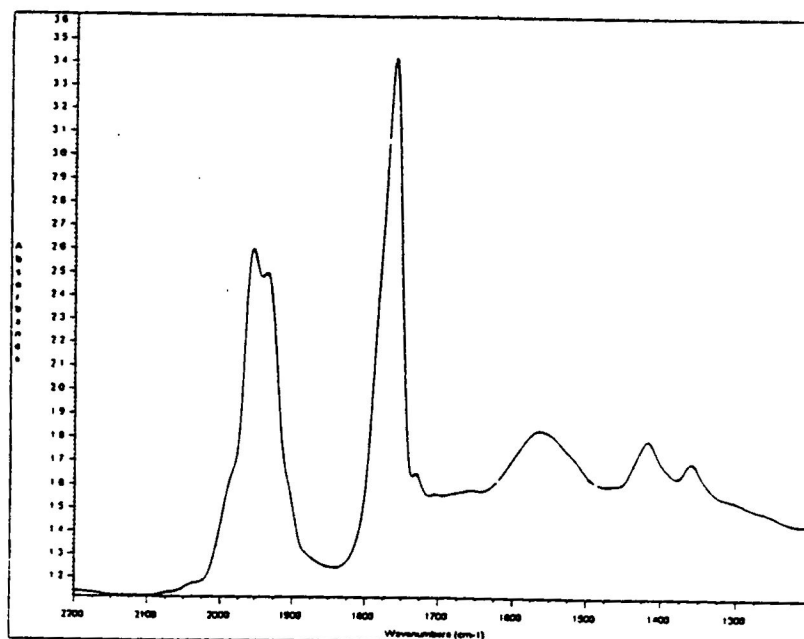


Fig. 14. DRIFTS Spectrum of (1) at 100 °C .

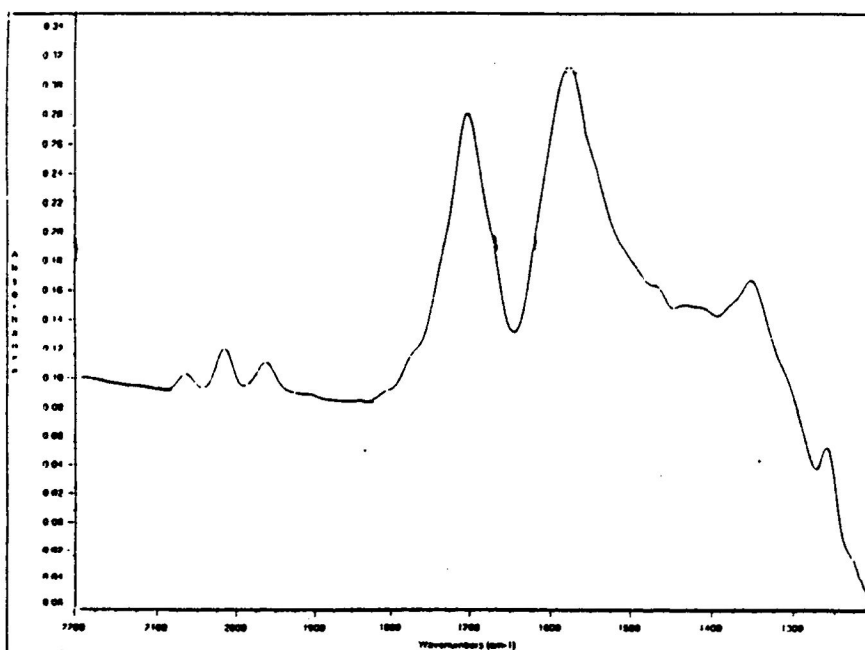


Fig. 15. DRIFTS Spectrum of (1) on $\gamma\text{-Al}_2\text{O}_3$ (4/10 coverage) at Room Temperature.

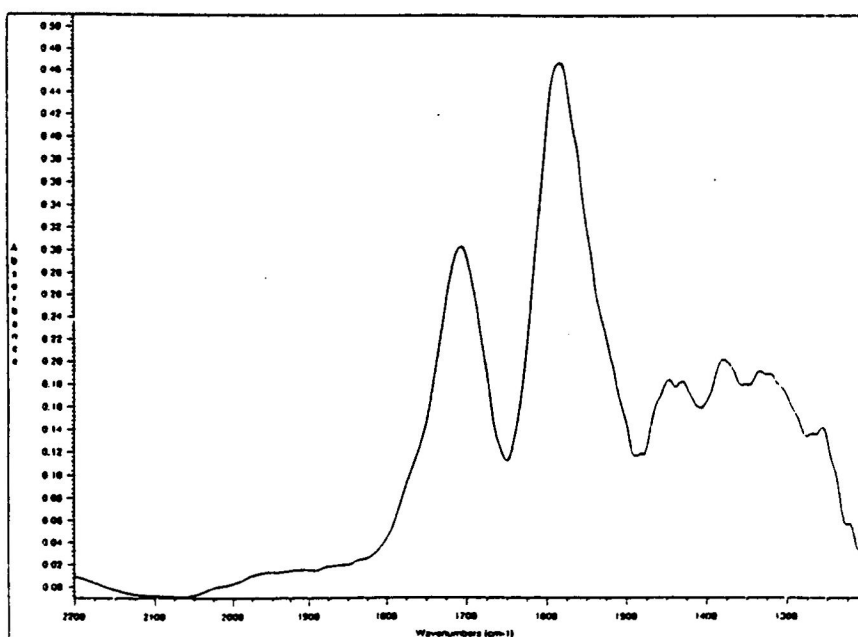


Fig. 16. DRIFTS Spectrum of (1) on $\gamma\text{-Al}_2\text{O}_3$ (4/10 coverage) at 80 °C.

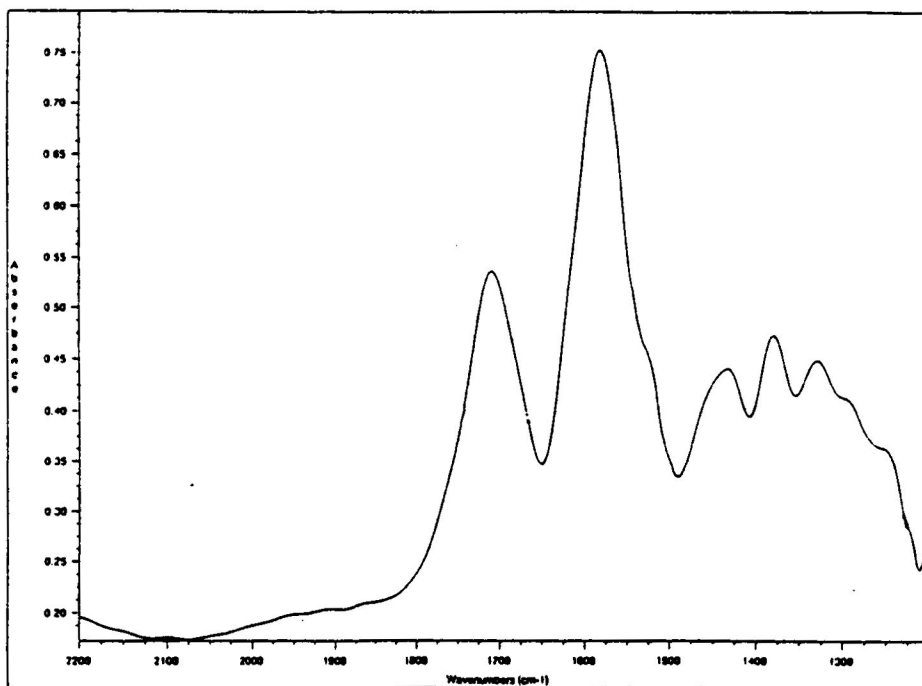


Fig. 17. DRIFTS Spectrum of (1) on γ -Al₂O₃ (4/10 coverage) at 100 °C.

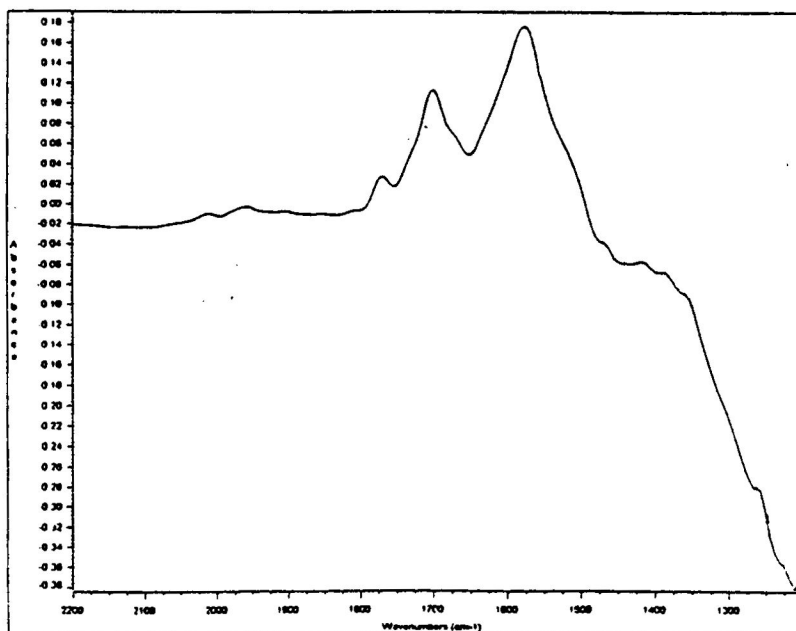


Fig. 18. DRIFTS Spectrum of (1) on γ -Al₂O₃ (3/10 coverage) at Room Temperature.

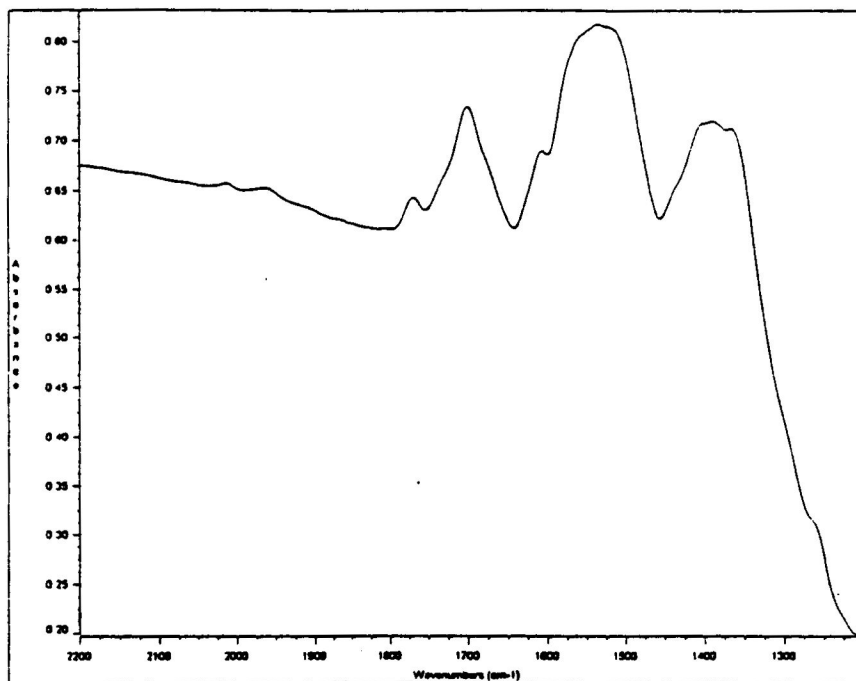


Fig. 19. DRIFTS Spectrum of (1) on γ -Al₂O₃ (3/10 coverage) at 60 °C.

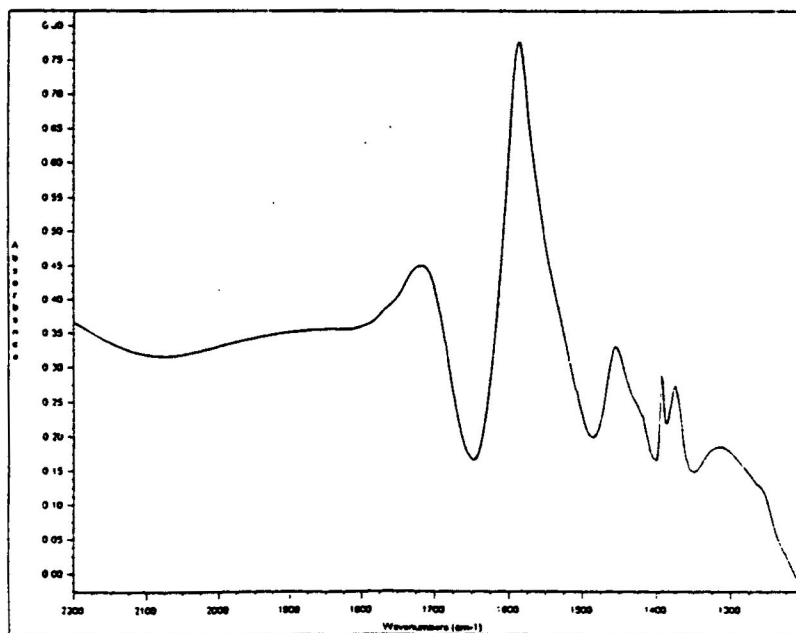


Fig. 20. DRIFTS Spectrum of (1) on γ -Al₂O₃ (3/10 coverage) at 100 °C.

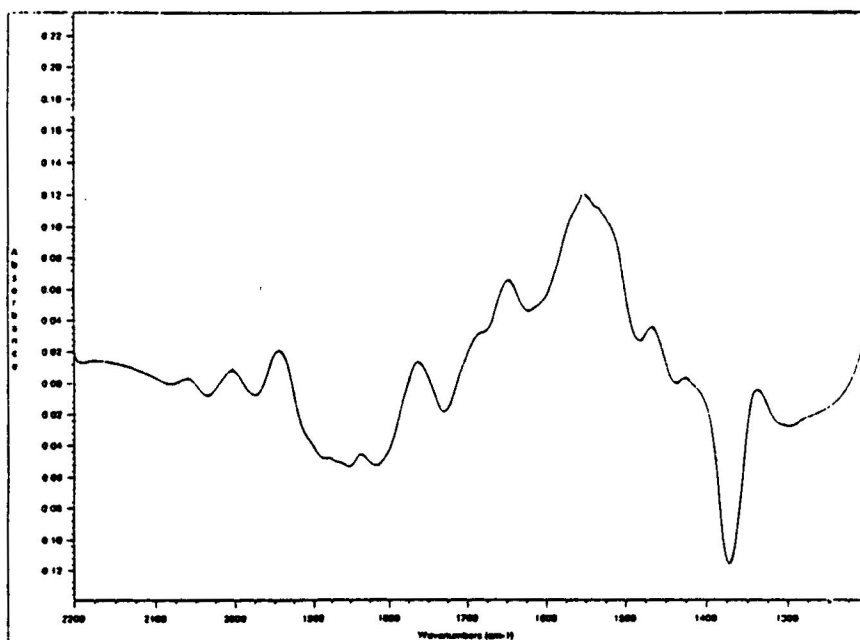


Fig. 21. DRIFTS Spectrum of (1) on $\gamma\text{-Al}_2\text{O}_3$ (2/10 coverage) at Room Temperature.

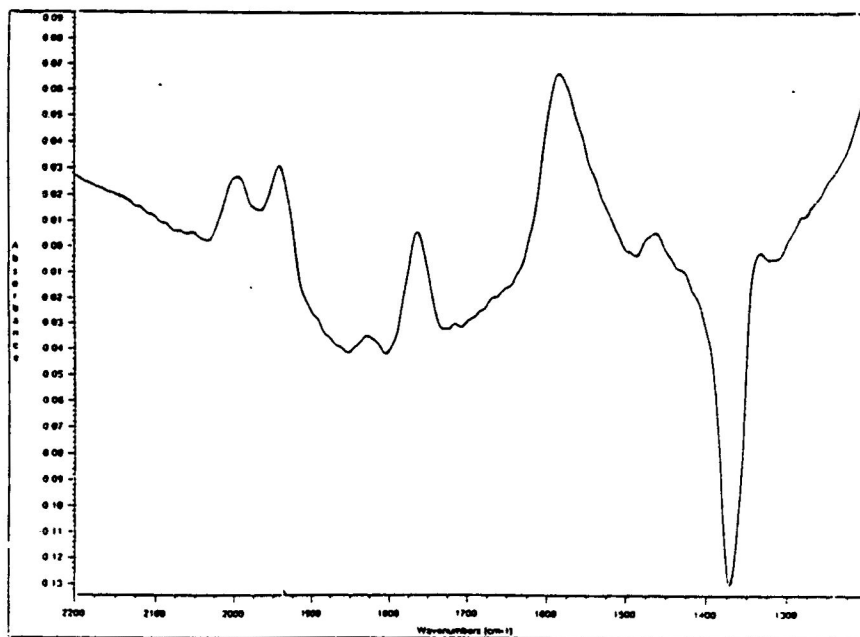


Fig. 22. DRIFTS Spectrum of (1) on $\gamma\text{-Al}_2\text{O}_3$ (2/10 coverage) at 40 °C.

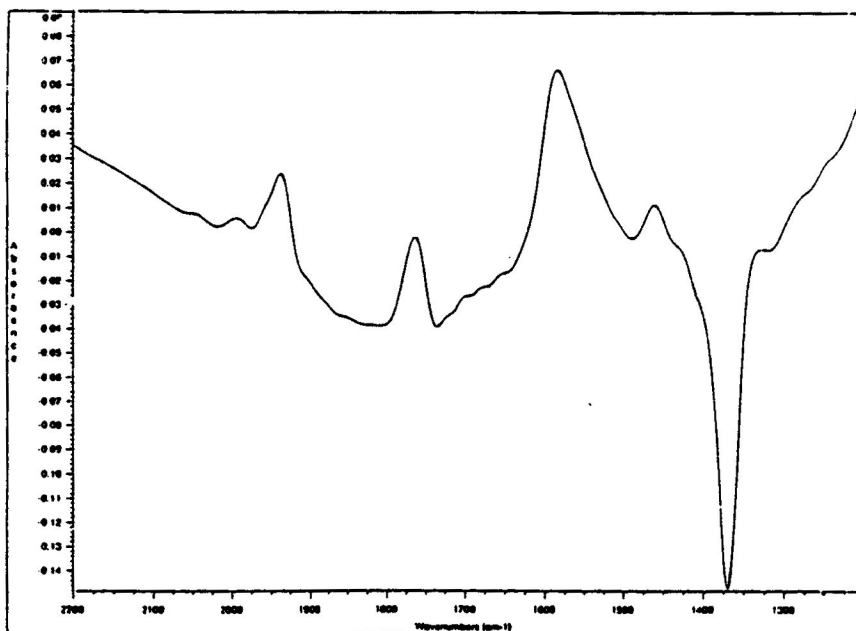


Fig. 23. DRIFTS Spectrum of (1) on γ -Al₂O₃ (2/10 coverage) at 80 °C .

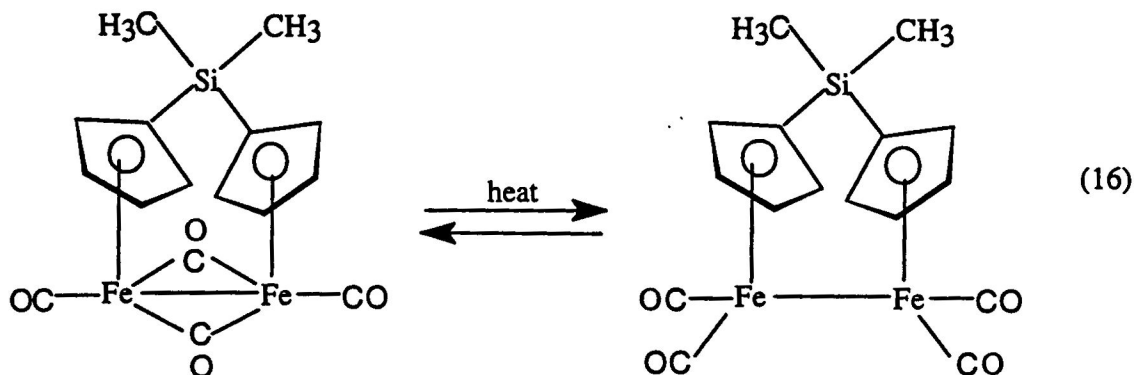
Table VI. DRIFTS data for (1) as a function of temperature and coverage (in wavenumbers)

Temperature in degree Celsius	Pure compound dissolved in hexane	Pure compound	Coverage on gamma alumina		
			4/10	3/10	2/10
Room Temperature	2041 (w)	2040.6 (m)	2066.2 (m)	2013.5 (w)	2059.6 (w)
	2000.7 (m)	1974 (s)	2015.7 (m)	1961.7 (w)	2002.6 (w)
	1973.3 (vs)	1938.9 (s)	1967.5 (m)	1772.2 (m)	1944.8 (w)
	1960.5 (s)	1910.4 (vs)	1708.2 (vs)	1710 (s)	1837.3 (vw)
	1774 (vs)	1779.5 (m)			1764.9 (w)
40		1737.5 (m)			
		2040.6 (m)	2066.2	2014.3	2059 (m)
		1940.4 (s)	2015.7	1963.1	1999.9 (m)
		1938.9 (s)	1964.5	1772.2	1942 (vw)
		1910.4 (vs)	1708.2	1710	1939.7 (m)
60		1779.5 (s)			1827 (w)
		1737.5 (s)			1764 (m)
		2040.6	2066.2	1772.2 (m)	2059 (vw)
		1938.9	2015.7	1710 (s)	1999.9 (vw)
		1910.4	1964.5		1941.1 (w)
80		1779.5	1708.2		1827.1 (w)
		1737.5			1764.9 (w)
		2040.6 (w)	2066.2 (vw)	1713.7 (m)	1938.9
		1938.2 (vs)	2015.7 (vw)		1766.7
		1909.7 (vs)	1964.5 (vw)		
100		1764.9 (vw)	1708.2 (s)		
		1737.5 (vw)			
		1955 (s)	1708.2 (s)	1713.7	1714.4
		1936 (s)			
		1764.9 (vs)			

Di- μ -carbonyl-cis- μ -(1-5- η :1'-5'- η '-dicylopentadienyl)dimethylsilane)bis (carbonyl)diiron)(Fe:Fe), **3**

The nujol spectrum of **3** (Fig. 24) exhibited terminal carbonyl bands at 1998.9 and 1955.8 cm^{-1} . The bridged carbonyls exhibited a stretching frequency of 1785.0 cm^{-1} . The DRIFTS spectra of **3** exhibited terminal carbonyl bands at 1993.8 and 1952.1 cm^{-1} (Fig. 25). A shoulder was observed at 1911.9 and 1805.9 cm^{-1} (Fig. 17) and a bridging carbonyl band at 1775.9 cm^{-1} . When TPDE was carried out on this compound, at 40 $^{\circ}\text{C}$ the spectrum

slightly higher wavenumber. This also occurred for the terminal carbonyl bands at 100 °C (Fig. 28) where the higher band had a greater intensity and the shoulder band disappeared along with the band at 1805.9 cm^{-1} . Upon heating to 140 °C (Fig. 29) only three bands remained at 1995.2, 1950.6 and 1788.6 cm^{-1} . Overall, as the temperature increased there was a decrease in intensity of each carbonyl band. The shift of the terminal carbonyls to lower wavenumbers along with the shift to a higher wavenumber for the bridging carbonyl suggests fluxional behavior of this compound between the bridged and unbridged species as seen in reaction 16.



When **3** was placed on partially dehydroxylated gamma alumina distinct changes occurred in the IR spectra relative to the parent compound. The room temperature spectra exhibited an overall increase in wavenumber for the terminal and bridging carbonyls. This increase in wavenumber for all carbonyl groups was indicative of Lewis acid binding at a metal site (Fig. 6).

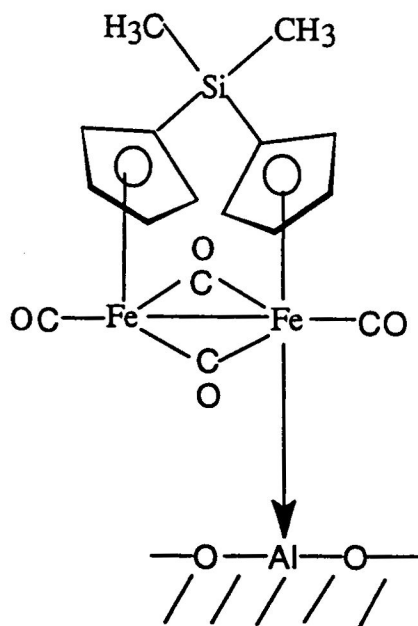
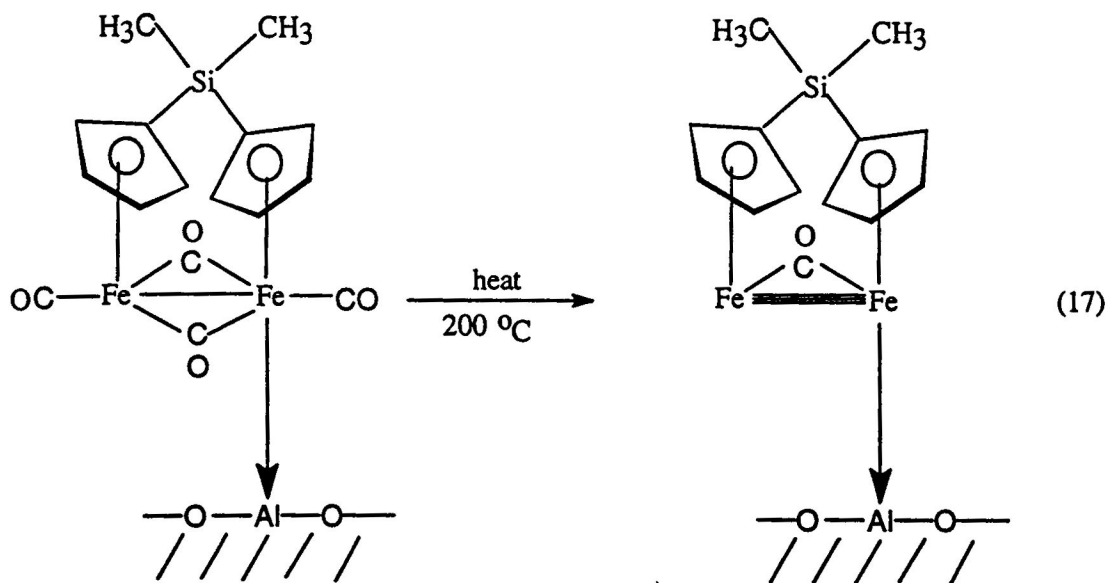


Fig. 6. Diagram illustrating binding to alumina at metal site in 3.

This binding to the metal site was also observed for the 2/10 (Fig. 35), 3/10 (Fig. 33) and 4/10 (Fig. 30) coverage on the alumina support. In the case of all three coverages the spectra remained slightly unchanged from 40 °C to 100 °C as seen in reaction 17. In all three coverages analyzed the band at 2059 cm^{-1} was present but as the temperature was increased it decreased considerably in intensity. This band disappeared in both the 2/10 and 3/10 samples but in the 4/10 sample the band at 2034.5 cm^{-1} decreased steadily and shifted upon heating to 150 °C (Fig. 31) to 2037 cm^{-1} . The band at 2037 cm^{-1} disappeared upon heating to 200 °C, (Fig. 32). The 4/10 sample, which was heated up to 400 °C, exhibited decarbonylation of terminal carbonyls occurring at 200 °C, while the band at 1708 cm^{-1} remained. The spectra remained unchanged upon heating from 200 °C to 400 °C. No further changes were observed upon cooling to room temperature.

Overall, as TPDE was carried out there was a decrease in intensity of each spectral band.



The DRIFTS data indicate that when 3 was placed on γ -alumina, the introduction of this Lewis acid catalyzed decarbonylation of the compound. On alumina, decarbonylation occurred more readily because of a complexation with a Lewis acid site that removed electron density directly or indirectly from the iron, thus decreasing backbonding, causing the carbonyl bond to metal bond to weaken.

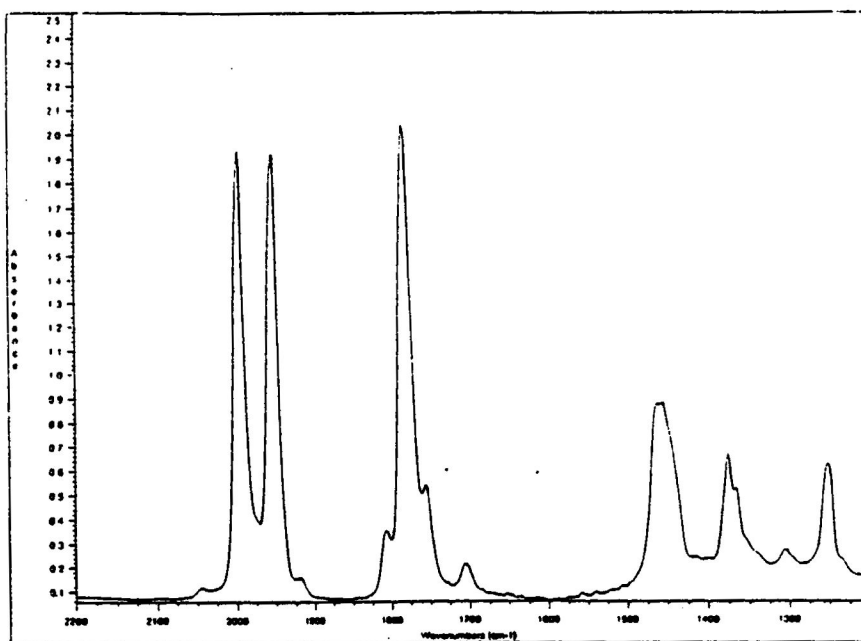


Fig. 24. FT-IR Spectrum of di- μ -carbonyl-cis- μ (1-5- η :1'-5'- η '-dicyclopentadienyldimethylsilane)bis(carbonyldiiron)(FeFe), (3), in nujol.

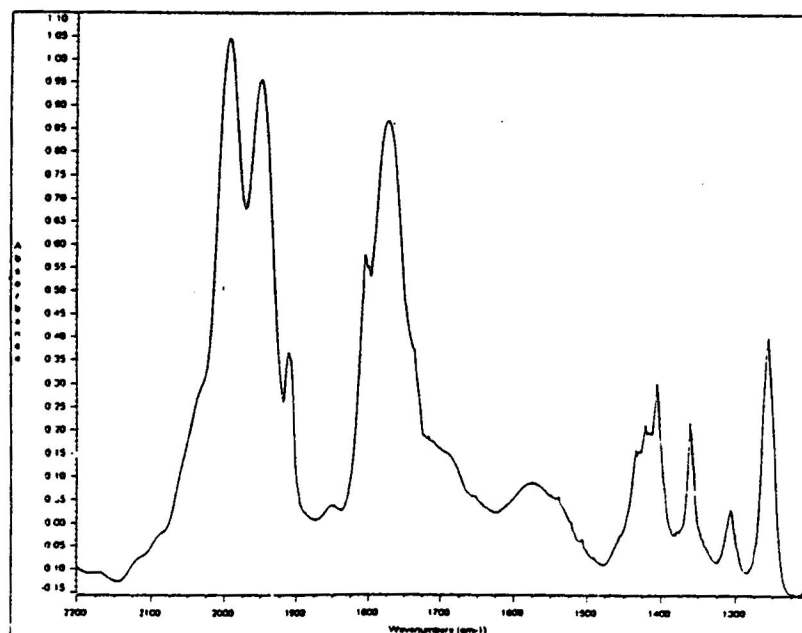


Fig. 25. DRIFTS Spectrum of (3) at Room Temperature.

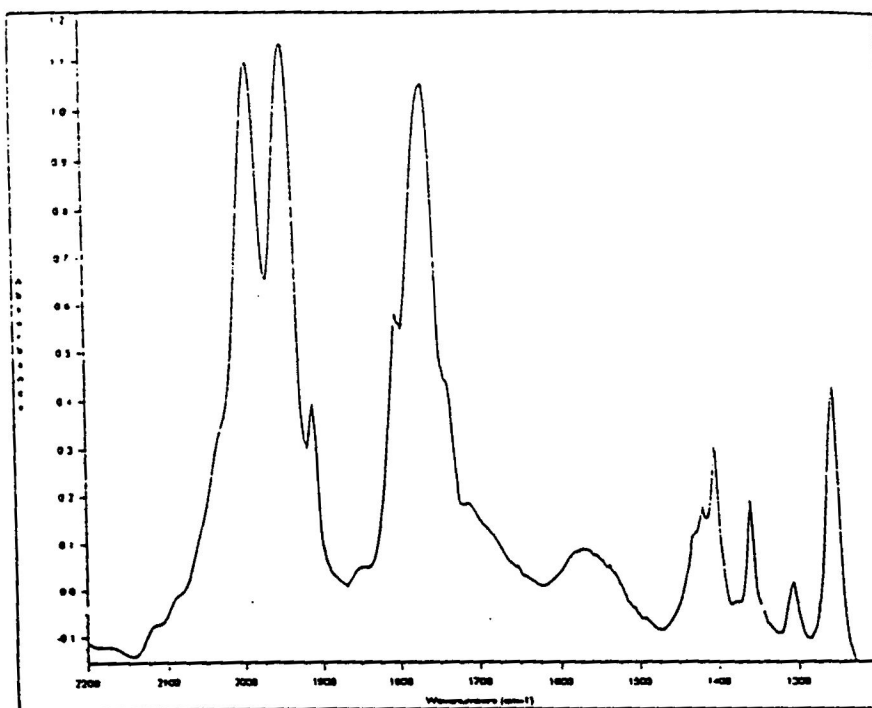


Fig. 26. DRIFTS Spectrum of (3) at 60 °C.

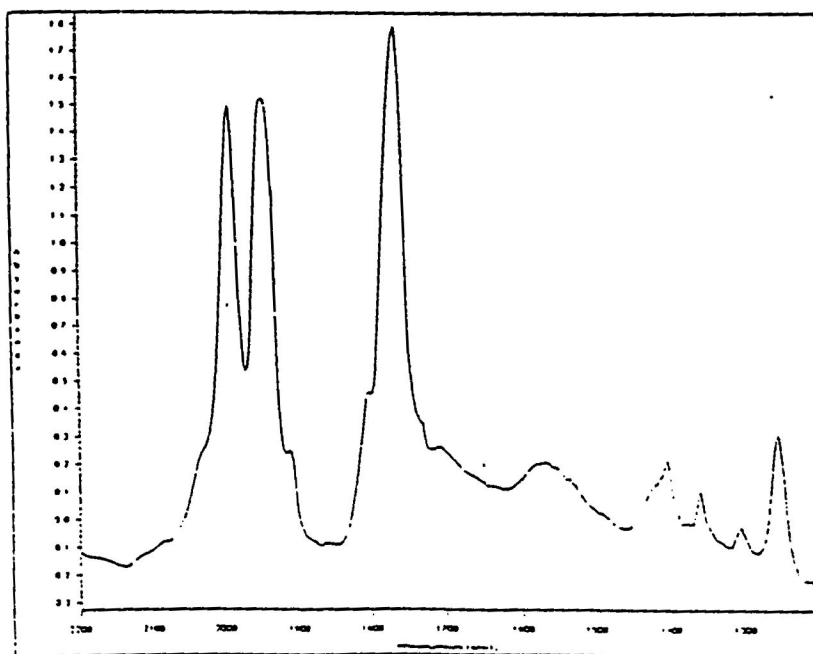


Fig. 27. DRIFTS Spectrum of (3) at 80 °C.

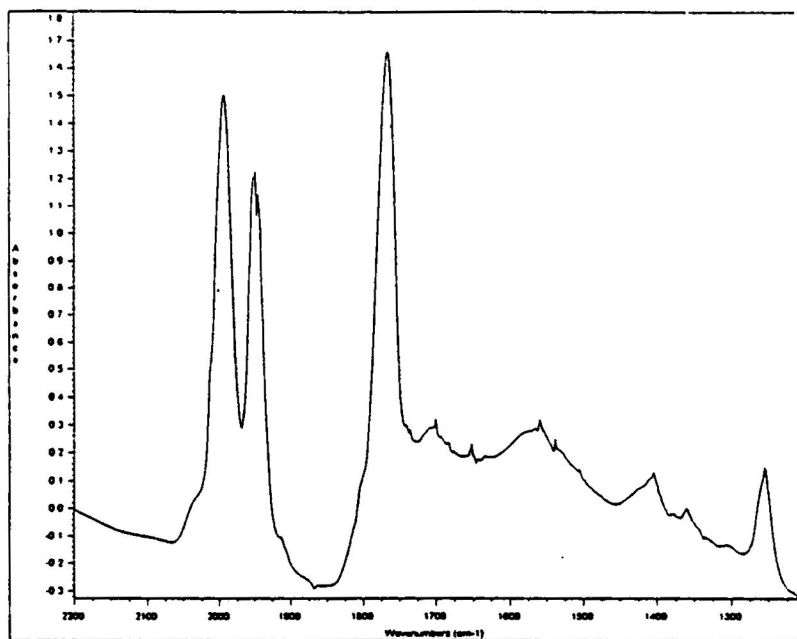


Fig. 28. DRIFTS Spectrum of (3) at 100 °C.

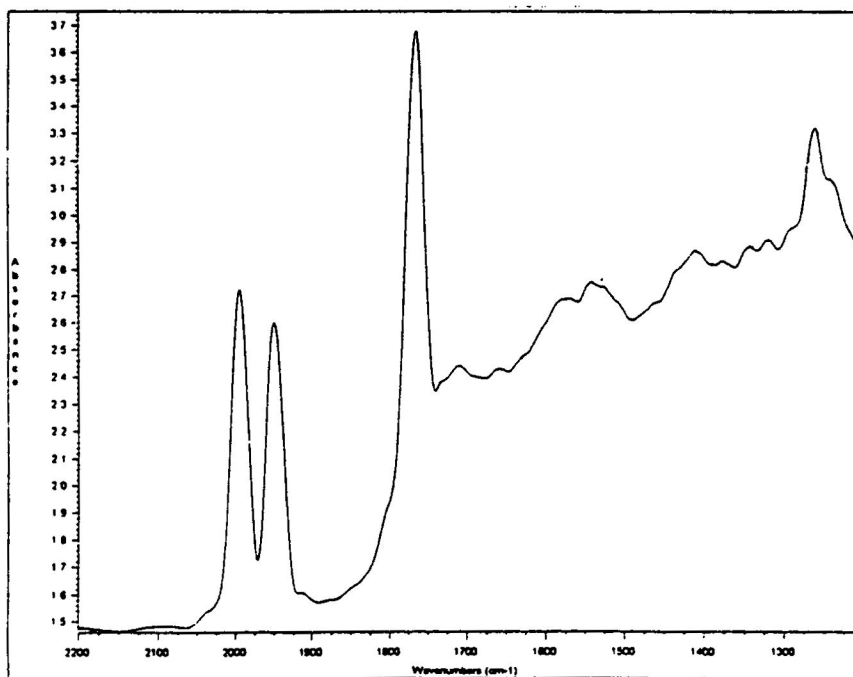


Fig. 29. DRIFTS Spectrum of (3) at 140 °C.

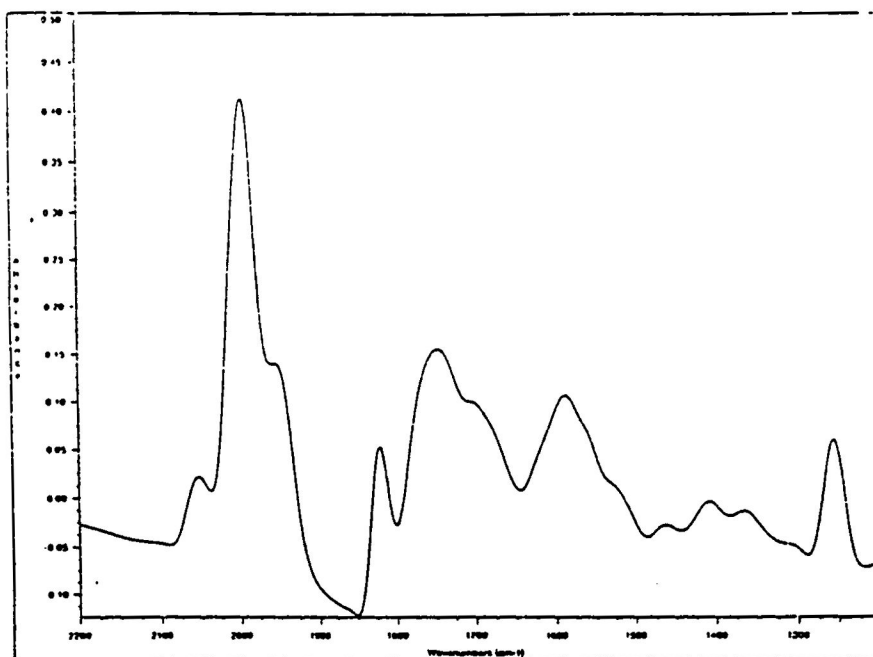


Fig. 30. DRIFTS Spectrum of (3) on $\gamma\text{-Al}_2\text{O}_3$ (4/10 coverage) at Room Temperature.

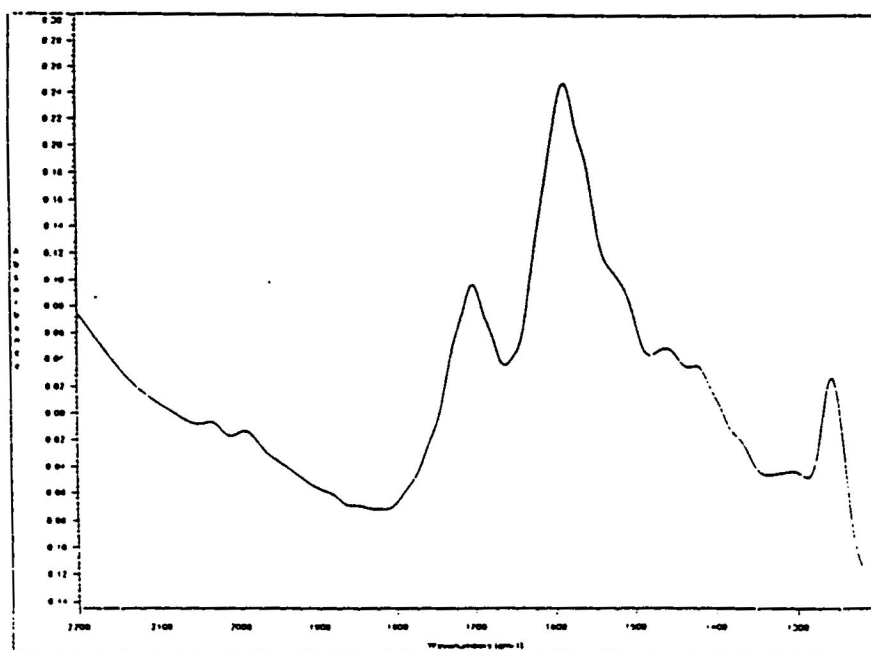


Fig. 31. DRIFTS Spectrum of (3) on $\gamma\text{-Al}_2\text{O}_3$ (4/10 coverage) at 150 °C.

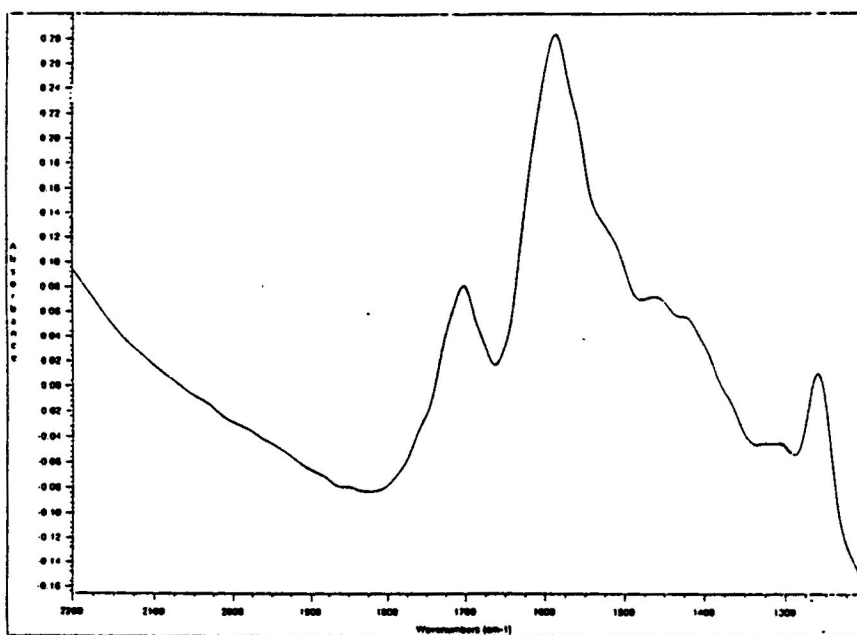


Fig. 32. DRIFTS Spectrum of (3) on γ -Al₂O₃ (4/10 coverage) at 200 °C.

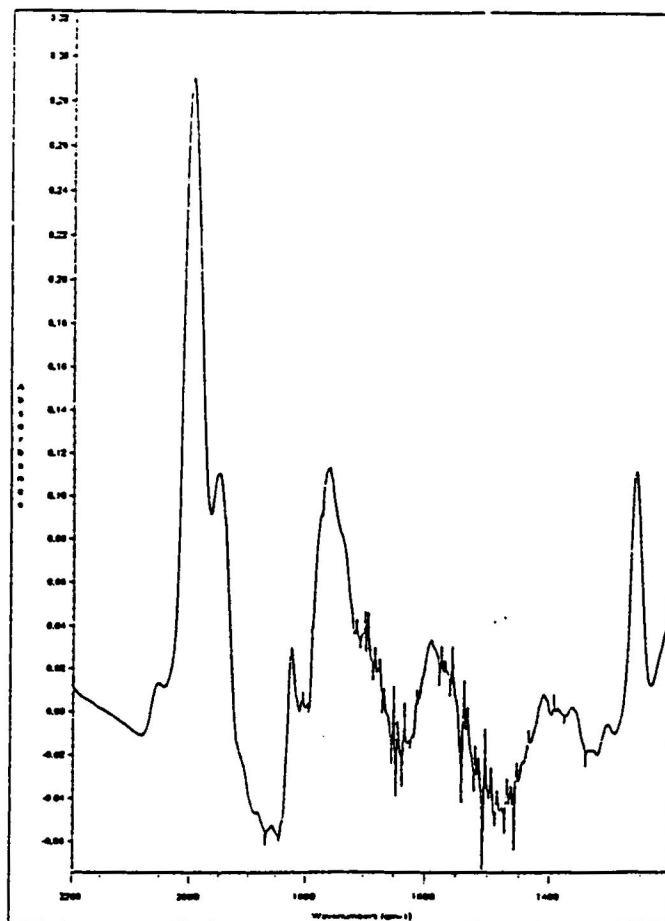


Fig. 33. DRIFTS Spectrum of(3) on $\gamma\text{-Al}_2\text{O}_3$ (3/10 coverage) at Room Temperature.

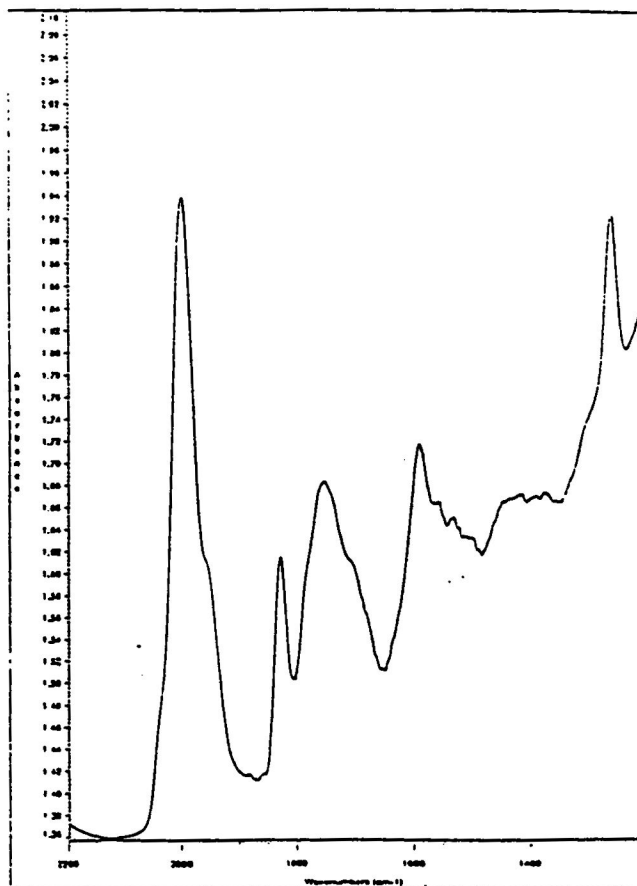


Fig. 34. DRIFTS Spectrum of (3) on γ -Al₂O₃ (3/10 coverage) at 100 °C.

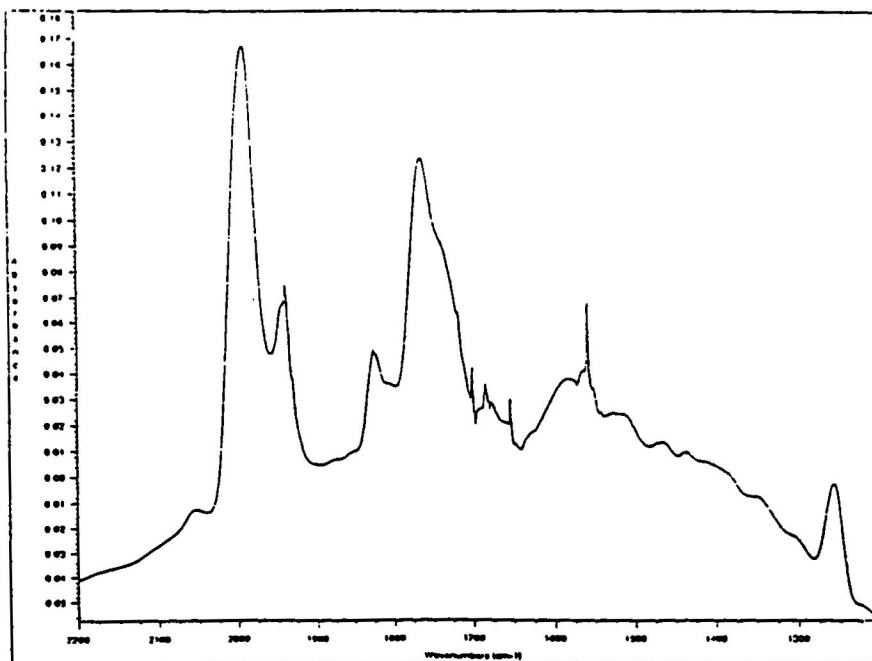


Fig. 35. DRIFTS Spectrum of (3) on $\gamma\text{-Al}_2\text{O}_3$ (2/10 coverage) at Room Temperature.

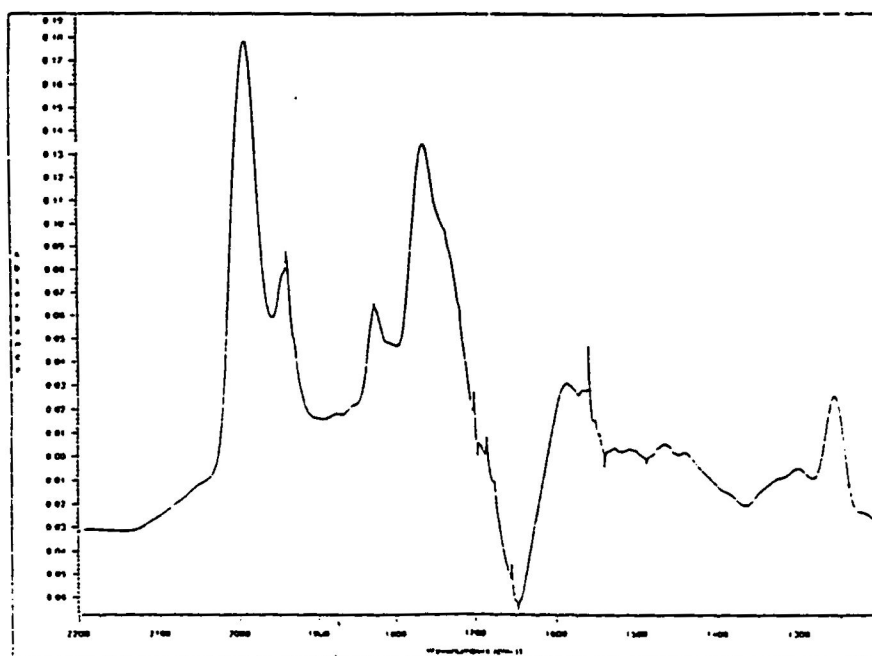


Fig. 36. DRIFTS Spectrum of (3) on $\gamma\text{-Al}_2\text{O}_3$ (2/10 coverage) at 40 °C.

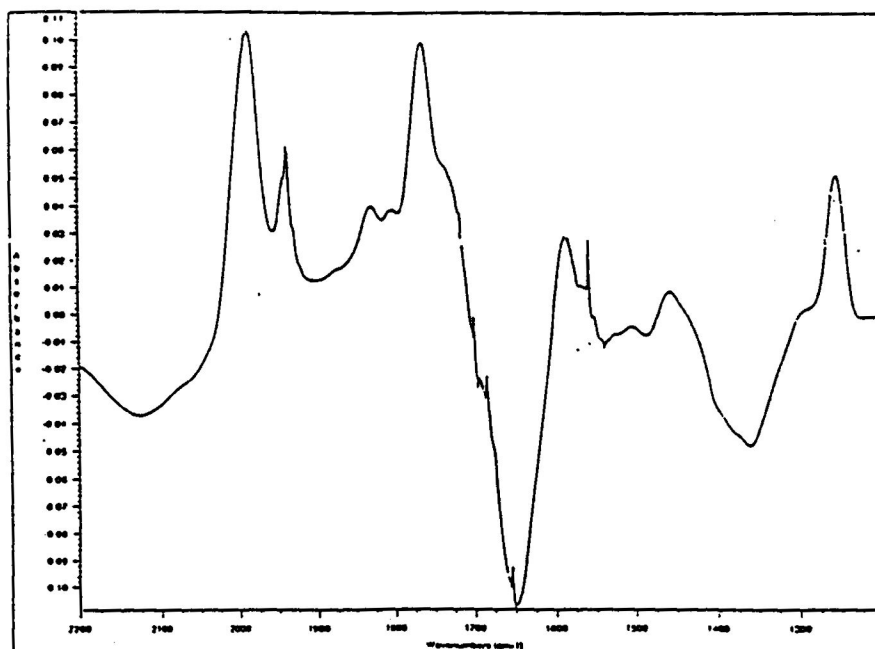


Fig. 37. DRIFTS Spectrum of (3) on $\gamma\text{-Al}_2\text{O}_3$ (2/10 coverage) at 100 °C.

Table VII. DRIFTS data for (3) as a function of temperature and coverage (in wavenumbers)

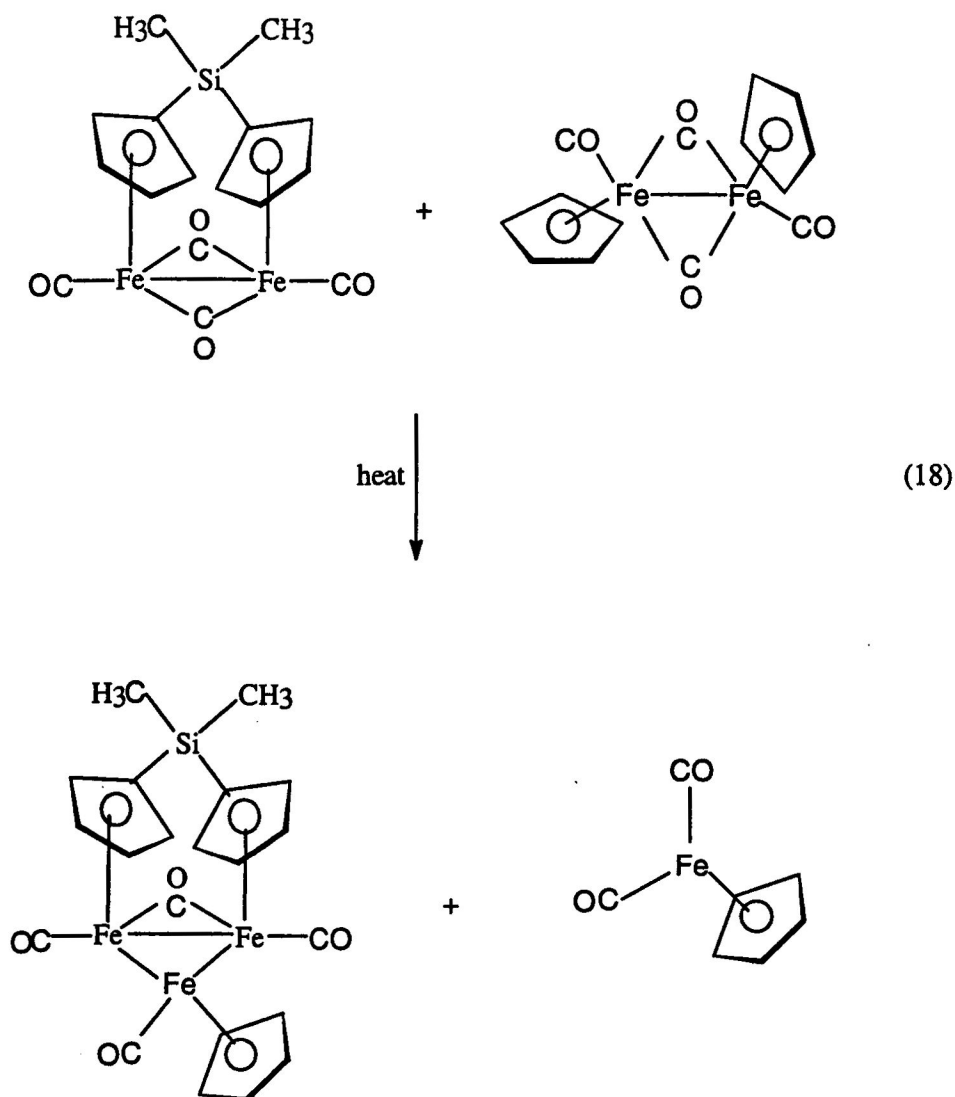
Temperature in degree Celsius	Pure compound (nujol)	Pure compound	Coverage on gamma alumina		
			4/10	3/10	2/10
Room Temperature	1998.9 (vs)	1993.8 (s)	2059.6 (m)	2059.6 (w)	2059.6 (w)
	1955.8 (vs)	1952.1 (s)	1997.4 (vs)	1999.6 (vs)	1995.2 (s)
	1785 (vs)	1911.9 (m)	1953.6 (s)	1952.8 (m)	1941.1 (m)
		1805.9 (m)	1822.7 (m)	1827.1 (w)	1805.1 (s)
		1775.9 (s)	1748.4 (s)	1766.7 (m)	1827.1 (m)
40					1768.6 (s)
		1993.8 (s)	2045	2045	1994.5 (s)
		1952.1 (s)	1998.9	1998.2	1941.1 (m)
		1911.9 (m)	1952.8	1953.6	1827.8 vw
		1805.9 (m)	1824.1	1827.1	1805 (m)
60		1775.9 (s)	1748.4	1764.9	1766.7 (s)
		1993.1	2044.2	1999.6	1994.5
		1947.7	1998.9	1953.6	1941.1
		1911.9	1950.6	1827.8	1827.8
80		1805.9	1825.6	1757.6	1805.1
		1770.4	1750.3		1766.7
		1993.1 (vs)	2037.7	1999.6 (vs)	1992.3
		1947.7 (vs)	1994.5	1955 (m)	1940.4
100		1911.9 (w)	1954.3	1827.8 (m)	1829.3
		1805.9 w	1826.3	1759.4 (m)	1805.1
		1768.6 (vs)	1783.2		1768.6
			1737.5		
		1996 (vs)	2037	1999.6	1990 (s)
120		1950.6 (s)	1996	1953.6	1941.1 (m)
		1768 (vs)	1950.6	1827.8	1833.6 (w)
			1827.1		1805.9 (w)
					1768.6 (s)
120		1996.7			
		1950.6			
		1770.4			

Table VII. (continued)

140		1995.2 (s)		
		1950.6 (s)		
		1768.6 (vs)		
80				
60			2036.9	
			1995.2	
			1950.6	
			1827.8	
			1783.2	
40			2036.8	
			1996	
			1824.1	
			1783.2	
Room Temperature			2036.9	
			1996	
			1823.4	
			1781.4	
100			2036.2	
			1995.2	
			1824.9	
			1786.8	
150			2037 (vw)	
			1991.6 (vw)	
			1881.9 (vw)	
200				
300				
400				
300				
200				
100				
Room Temperature				

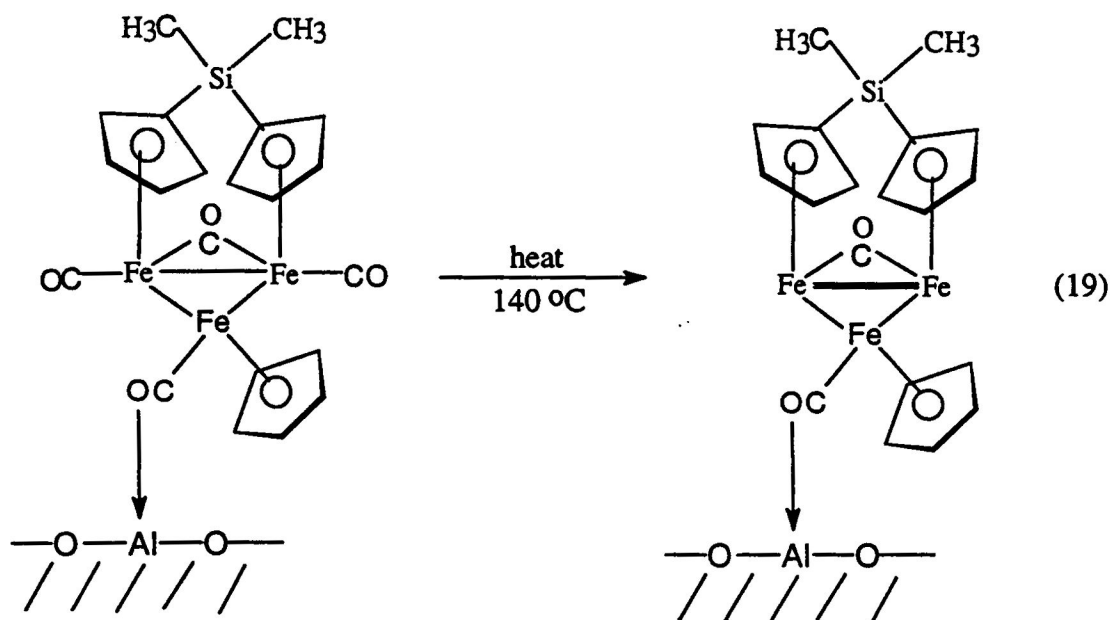
Cyclopentadienyliron dicarbonyl dimer and di- μ -carbonyl-cis- μ -(1-5- η :1'-5'- η ':-dicyclopentadienyldimethylsilane)bis(carbonyldiiron)(FeFe): (1 and 3)

A mixture of **1** and **3** was analyzed by DRIFTS and TPDE. Three samples were prepared by (i) combining separately finely powdered **1** and **3**, (ii) finely powdering a mixture of **1** and **3** with an agate mortar and pestle, (iii) impregnating partially dehydroxylated gamma alumina by the incipient wetness technique to allow for 4/10 coverage using the mixture from (i). Spectral data for (i) and (ii) were similar $\pm 1.100\text{ cm}^{-1}$. The spectra exhibited contributions from both **1** and **3**, and individually. At room temperature (Fig. 38) the terminal carbonyl bands were observed at 2039.9 cm^{-1} (**3**), 1994.5 cm^{-1} (**1**), 1950.6 cm^{-1} (**1**), 1909.0 cm^{-1} (**1** and **3**) and 1805.9 cm^{-1} (**1**). The bridging carbonyl bands occurred at 1708.6 cm^{-1} (**1** and **3**) and 1733.8 cm^{-1} (**3**). The 2039.9 cm^{-1} band (**3**) disappeared upon heating to $80\text{ }^{\circ}\text{C}$ (Fig. 40) however at $100\text{ }^{\circ}\text{C}$ (Fig. 41) a new peak at 2012.9 cm^{-1} (**1** and **3**) appeared and remained upon heating to $140\text{ }^{\circ}\text{C}$. The 1994.5 cm^{-1} (**1**) band shifted to 1990.0 cm^{-1} upon heating to $60\text{ }^{\circ}\text{C}$ (Fig. 39) and remained upon heating to $140\text{ }^{\circ}\text{C}$. The intensity of the 1950.6 cm^{-1} (**1**), 1909 cm^{-1} (**1** and **3**) and 1768.8 cm^{-1} (**1** and **3**) bands increased and remained upon heating to $140\text{ }^{\circ}\text{C}$. The terminal carbonyl band at 1805.9 cm^{-1} (**1**) disappeared upon heating to $80\text{ }^{\circ}\text{C}$ (Fig. 40). The bridging carbonyl bands at 1733.8 cm^{-1} (**3**) shifted upon heating to $100\text{ }^{\circ}\text{C}$ (Fig. 41) to 1728.3 cm^{-1} (**1** and **3**) and remained upon heating to $140\text{ }^{\circ}\text{C}$. The shift of carbonyl bands to a lower wavenumber was indicative of the formation of a trinuclear species resulting from an insertion reaction between **1** and **3** as the temperature was increased as shown in reaction 18.



When (1 and 3) were placed on partially dehydroxylated gamma alumina the bands in the terminal carbonyl region shifted to a higher wavenumber and the bands in the bridging carbonyl shifted to a lower wavenumber. These shifts are consistent with Lewis acid binding at a terminal carbonyl. This sample exhibited a shift of the band at 2058.9 cm^{-1} to 2039.9 cm^{-1} from room temperature (Fig. 42) upon heating to $80\text{ }^{\circ}\text{C}$ (Fig. 43). This band then steadily decreased and disappeared upon heating to $140\text{ }^{\circ}\text{C}$ (Fig.45). The 1998.9 , 1954.3 , and 1825.6

cm^{-1} bands decreased in intensity upon heating to $120\text{ }^{\circ}\text{C}$ (Fig. 44) and disappeared upon heating to $140\text{ }^{\circ}\text{C}$ (Fig. 45). The terminal carbonyl band at 1708.2 cm^{-1} remained upon heating to $140\text{ }^{\circ}\text{C}$, however the 1746.6 cm^{-1} shifted to 1735.6 cm^{-1} upon heating to $80\text{ }^{\circ}\text{C}$ (Fig. 43) and disappeared upon heating to $140\text{ }^{\circ}\text{C}$ as shown in reaction 19.



The DRIFTS data indicate that when (1 and 3) was placed on γ -alumina, the introduction of this Lewis acid catalyzed decarbonylation of the compound. On alumina, decarbonylation occurred more readily because of a complexation with a Lewis acid site that removed electron density directly or indirectly from the iron, thus decreasing backbonding, causing the carbonyl bond to metal bond to weaken.

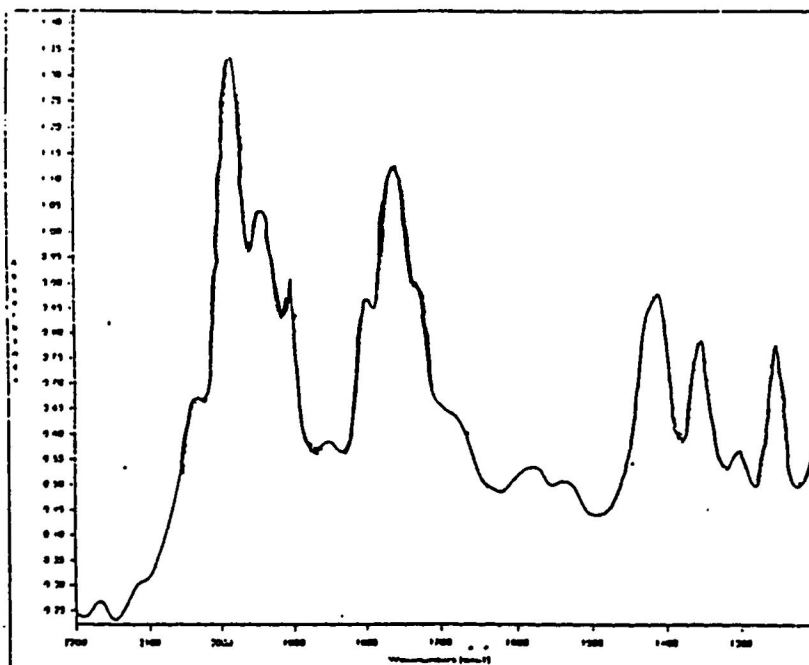


Fig. 38. DRIFTS Spectrum of cyclopentadienyliron dicarbonyl dimer and di- μ -carbonyl-cis- μ -(1-5- η :1'-5'- η' -dicyclopentadienyldimethylsilane)bis(carbonyldiiron)(FeFe), (1 and 3), at Room Temperature

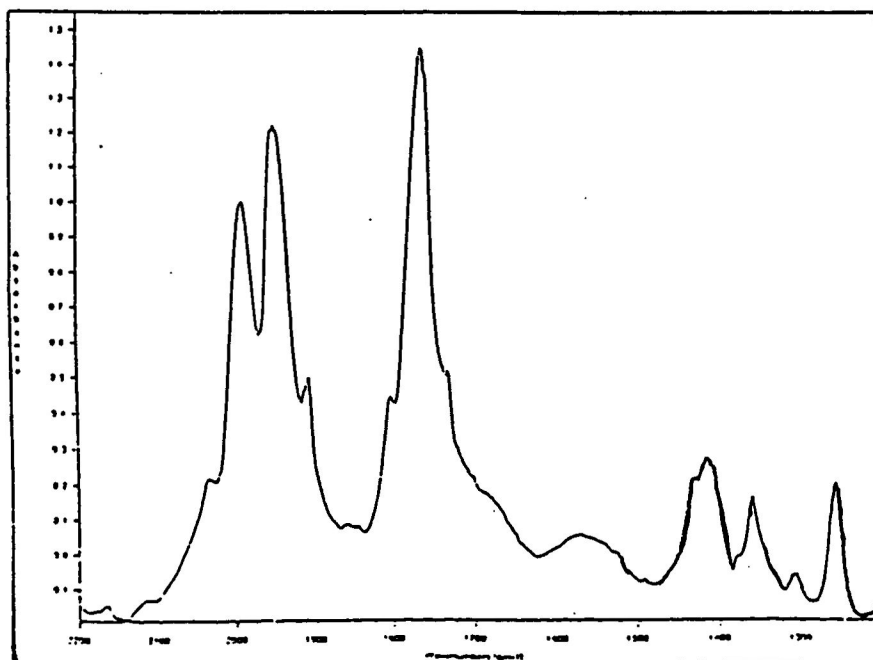


Fig. 39. DRIFTS Spectrum of (1 and 3) at 60 °C

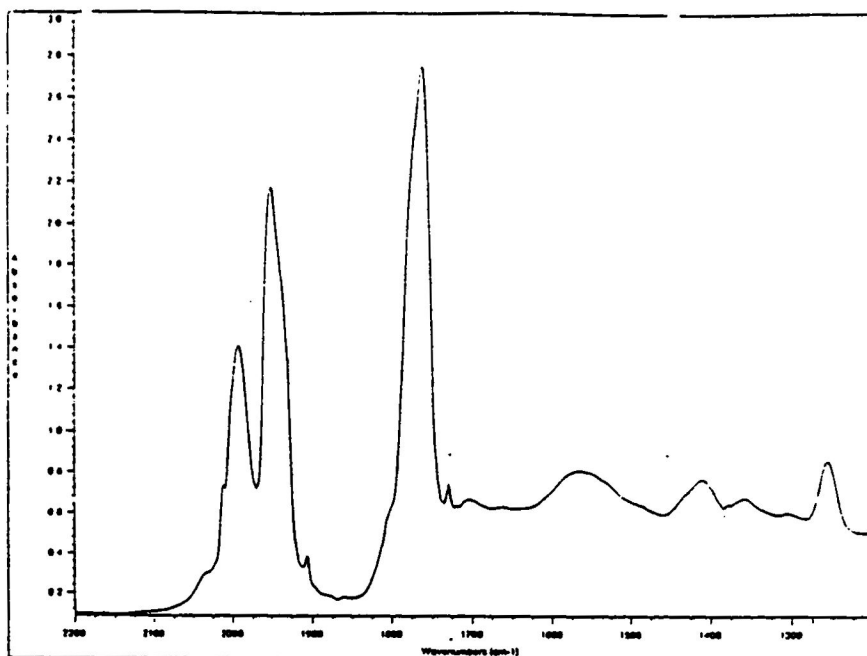


Fig. 40. DRIFTS Spectrum of (1 and 3) at 80 °C

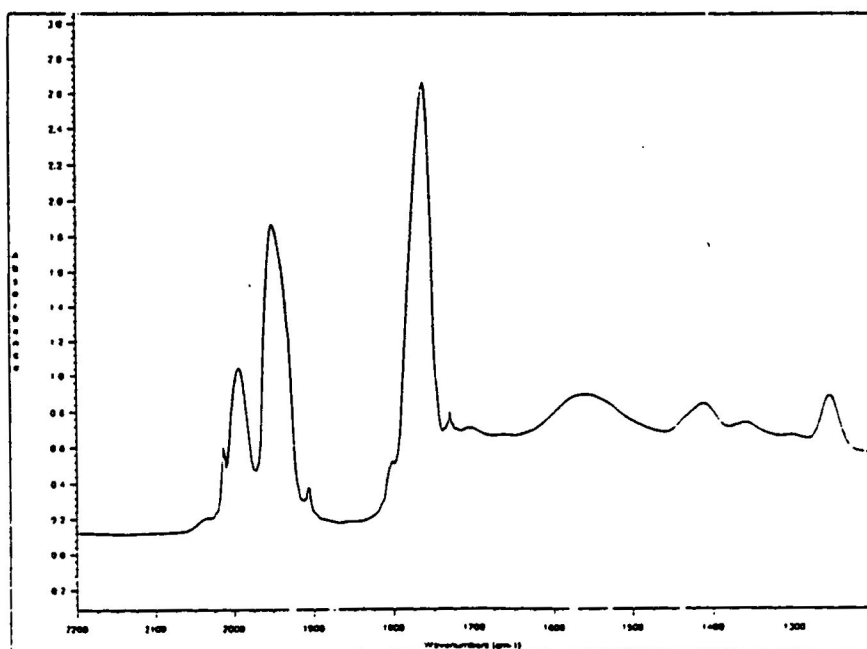


Fig. 41. DRIFTS Spectrum of (1 and 3) at 100 °C

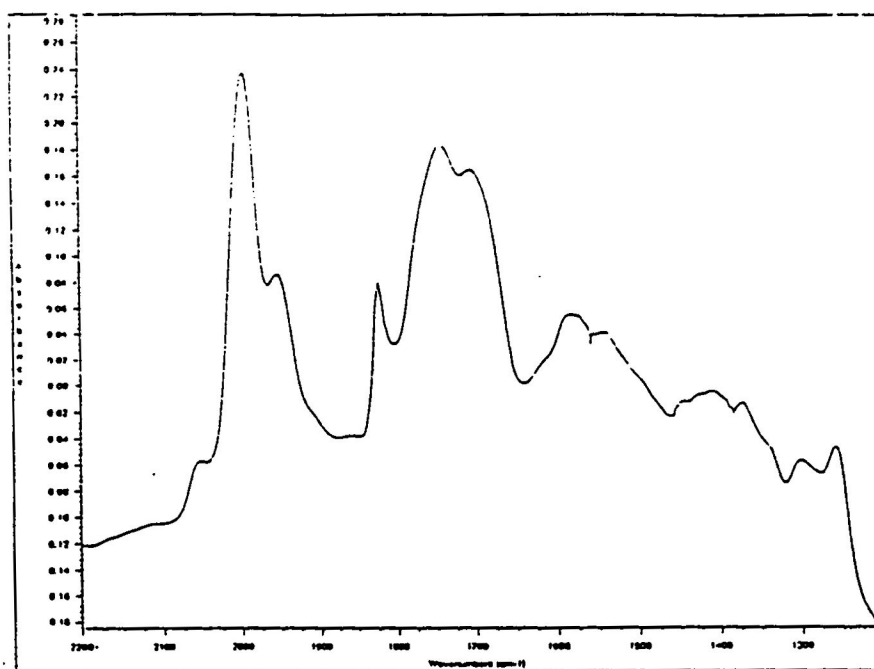


Fig. 42. DRIFTS Spectrum of (1 and 3) on $\gamma\text{-Al}_2\text{O}_3$ (4/10 coverage) at Room Temperature.

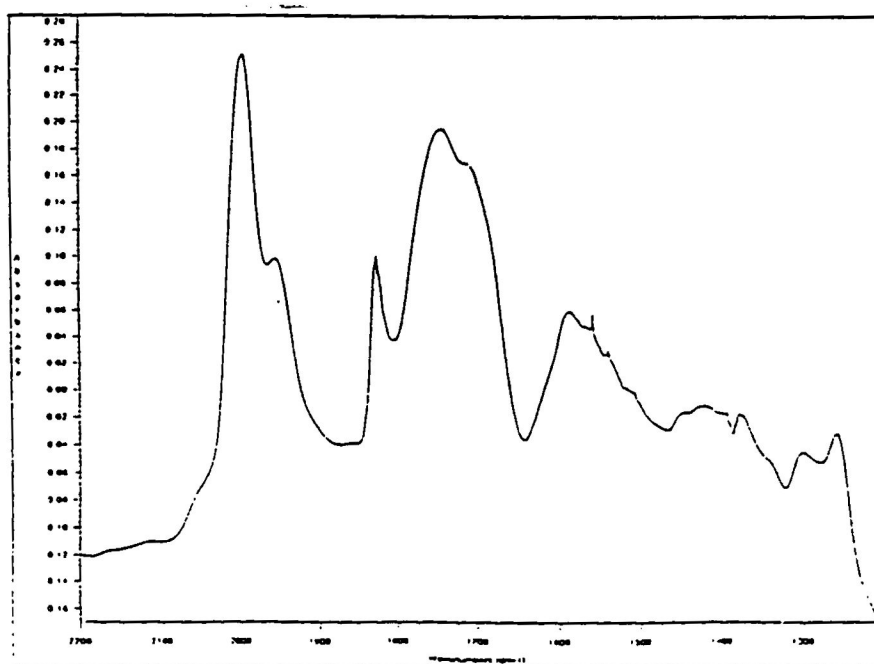


Fig. 43. DRIFTS Spectrum of (1 and 3) on $\gamma\text{-Al}_2\text{O}_3$ (4/10 coverage) at 80 °C.

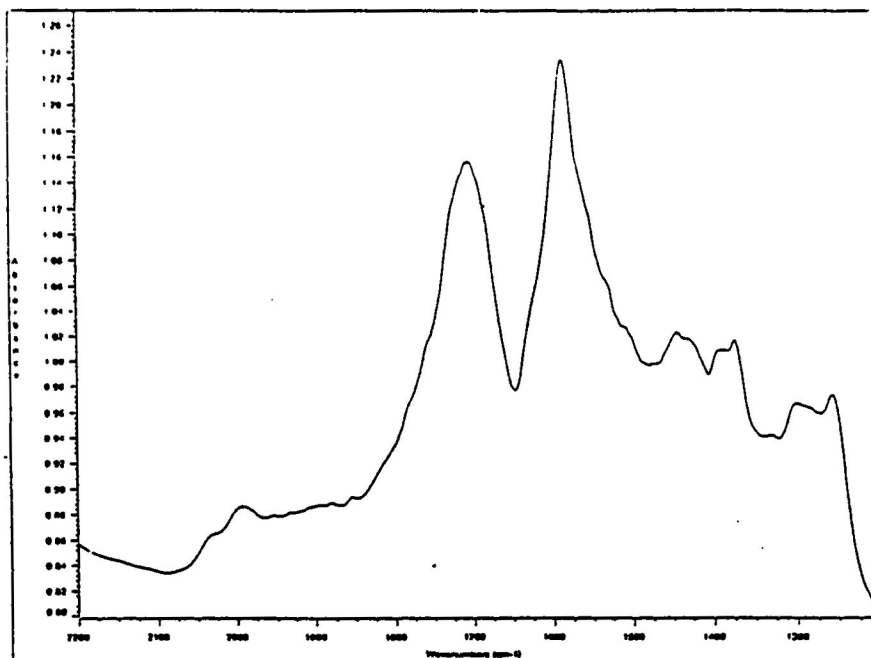


Fig. 44. DRIFTS Spectrum of (1 and 3) on γ -Al₂O₃ (4/10 coverage) at 120 °C

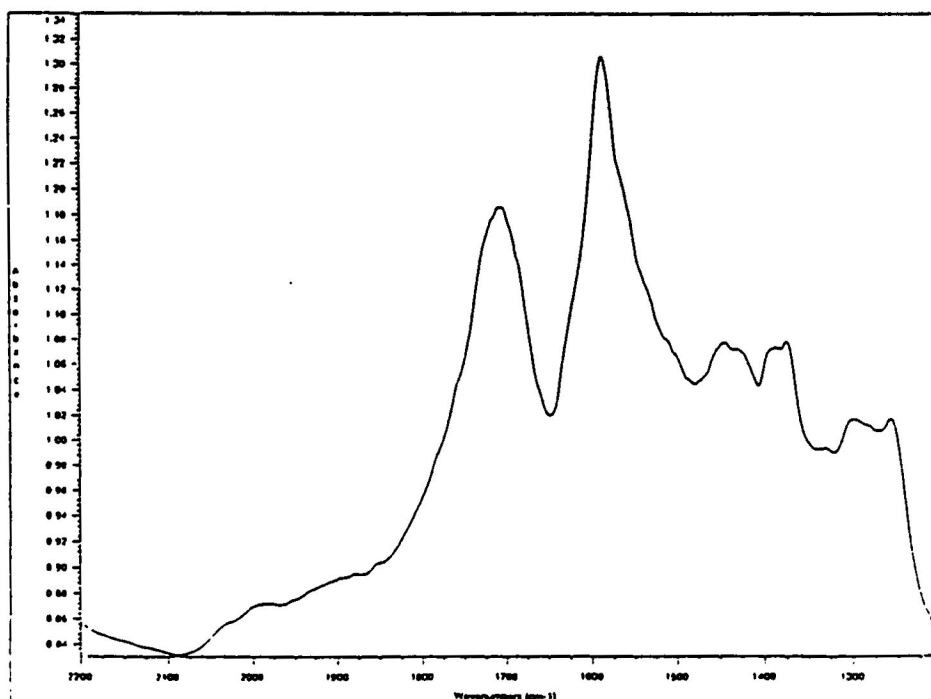


Fig. 45. DRIFTS Spectrum of (1 and 3) on γ -Al₂O₃ (4/10 coverage) at 140 °C

Table VIII. DRIFTS data for (1 and 3) as a function of temperature and coverage (in wavenumbers)

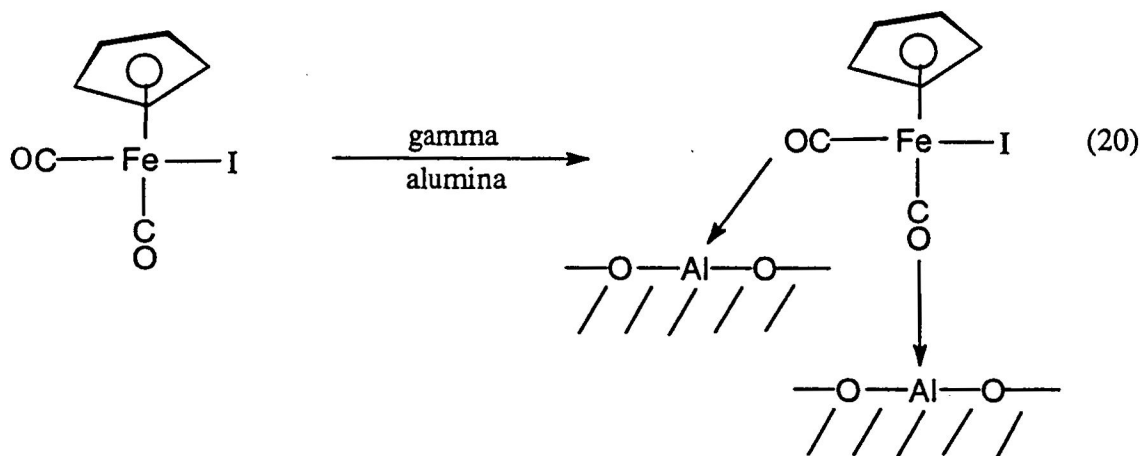
Temperature in degree Celsius	Pure (compound 1 and 3)	Pure (compound 1)	Pure (compound 3)	4/10 coverage using 1 and 3
Room Temperature	2040.6 (w)	1993.3	2039.9	2038.9
	1974 (vs)	1952.1	1994.5	1998.9
	1939.9 (s)	1911.9	1950.6	1954.3
	1910.4 (m)	1804.4	1909	1825.6
	1779.5 (vw)	1775.9	1805.9	1746.6
	1737.5 (m)		1708.6	1703
			1733.3	
40	2040.6	1993.8	2038.4	
	1974	1952.1	1994.5	2058.9
	1940.4	1912.6	1950.6	1998.9
	1910.4	1805.9	1909	1955
	1779.5	1775.9	1805.1	1825.6
	1737.5		1768.6	1746.6
			1735.6	1708
60	2040.6 (w)	1993.8	2038.4	
	1980.6 (s)	1949.2	1990.9	2058.9
	1938.9 (vs)	1911.9	1950.6	1998.2
	1909.7 (m)	1805.9	1909	1955
	1770.4 (m)	1770.4	1805.9	1927.1
	1737.5 (m)		1766.7	1746.4
			1732	1705.3
80	2042 (vw)	1993.1	1990.6	2039.9 (s)
	1938.2 (s)	1947.7	1950.6	1997.4 (m)
	1909.7 (vw)	1911.9	1907.5	1953.6 (m)
80	1764.9 (s)	1805.9	1764.9	1825.7 (s)
	1737.5 (w)	1768.6	1732	1735.6 (s)
100	1955 (vw)	1996	2012.9	2036.9
	1936 (w)	1950.6	1990.5	1997
	1764.9 (m)	1768.6	1950.6	1953.6
	1737.5 (s)		1907.5	1826.3
			1763.1	1706.4
			1728.3	
120			2012.9	2034.7 (vw)
			1990.5	1998.4 (vw)
			1950.6	1954.3 (vw)
			1908	1825.6 (vw)
			1770.4	1710.1 (s)
140		1995.2	2012.9	1708 (s)
		1950.6	1990	
		1768.6	1952.1	
			1908	
			1763.1	
			1728.3	

Cyclopentadienyldicarbonyliodoiron (II): 4

The solution IR spectrum of **4** (Fig. 46) exhibited bands which corresponded to terminal carbonyls at 2042 and 1999 cm^{-1} . The spectrum of the pure compound when DRIFTS was carried out at room temperature (Fig. 47) exhibited bands at 2130.5, 2069.8, 2018.6, 1951.4 and 1890.7 cm^{-1} . These bands corresponded to terminal carbonyls. The observation of four bands instead of the expected two bands is due to the packing of the crystal lattice. The spectrum upon heating to 60 $^{\circ}\text{C}$ (Fig. 48) exhibited carbonyl bands at 2038.4 and 1987.9 cm^{-1} . Further heating to 100 $^{\circ}\text{C}$ (Fig. 49) resulted in the disappearance of these carbonyl bands. Upon cooling the bands reappeared at 40 $^{\circ}\text{C}$ (Fig. 50), however, when cooled to room temperature bands were seen at 2047.2 and 1994.5 cm^{-1} (Fig. 51). This was indicative of the crystals having melted. When the compound was further heated to 100 $^{\circ}\text{C}$ (Fig. 52) all bands disappeared. Significant changes in the spectra were not observed upon further heating the sample to 400 $^{\circ}\text{C}$. When the sample was cooled to room temperature the spectrum exhibited bands at 2041.3 and 1985.0 cm^{-1} (Fig. 53). The number and shift of the carbonyls to lower wavenumbers was indicative of the crystals having melted.

When **4** was placed on partially dehydroxylated alumina the room temperature spectra of the 2/10 (Fig. 61), 3/10 (Fig. 58) and 4/10 (Fig. 54) samples exhibited carbonyls bands at lower wavenumbers than the pure compound. This was indicative of Lewis acid binding at both terminal carbonyls as shown in reaction 20. Upon heating the 2/10 sample to 60 $^{\circ}\text{C}$ (Fig. 62) the bands started to broaden and their intensity decreased. Further heating to 80 $^{\circ}\text{C}$ (Fig. 63) resulted in the disappearance of all bands. This same pattern of behaviour was also observed for the 3/10 coverage (Figs. 58-60). However, the 4/10 sample, upon heating to 80 $^{\circ}\text{C}$ (Fig. 55) exhibited a broadening and decrease in the intensity of

pattern of behaviour was also observed for the 3/10 coverage (Figs. 58-60). However, the 4/10 sample, upon heating to 80 °C (Fig. 55) exhibited a broadening and decrease in the intensity of the bands. Further heating to 100 °C (Fig. 56) resulted in the disappearance of all bands in the carbonyl region. Upon cooling the sample to room temperature (Fig. 57) carbonyl bands at 2042 and 1999cm⁻¹ reappeared. This indicated that while there was a continuous flow of nitrogen during the course of the experiment, the flow rate was not adequate to effect the removal of CO.



The DRIFTS data indicate that when **4** was placed on γ -alumina, the introduction of this Lewis acid catalyzed decarbonylation of the compound. On alumina, decarbonylation occurred more readily because of a complexation with a Lewis acid site that removed electron density directly or indirectly from the iron, thus decreasing backbonding, causing the carbonyl bond to metal bond to weaken.

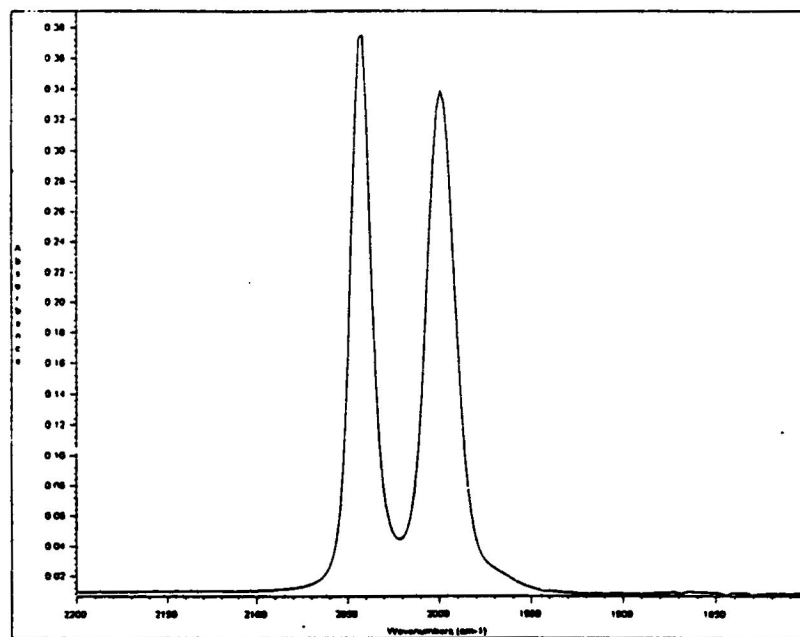


Fig. 46. FT-IR Spectrum of cyclopentadienyldicarbonyliodoiron (II), (4), in chloroform.

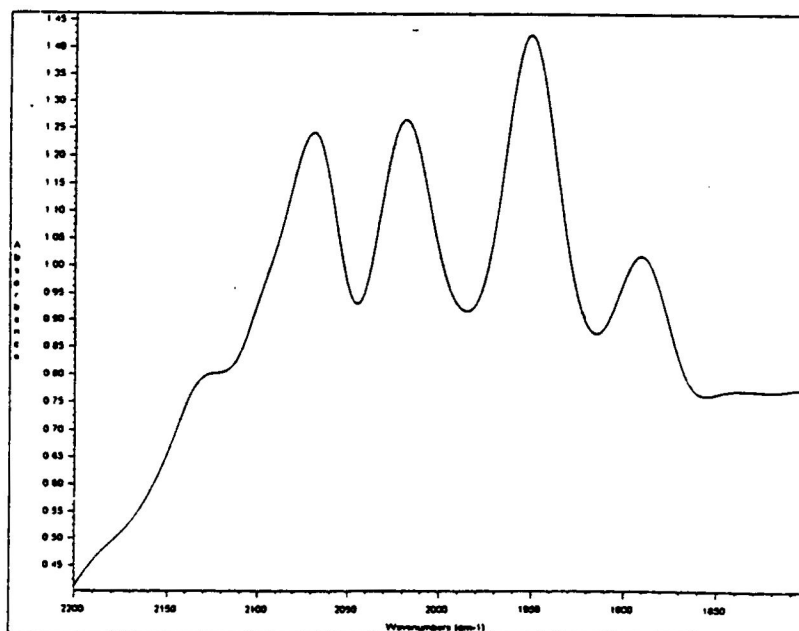


Fig. 47. DRIFTS Spectrum of (4) at Room Temperature.

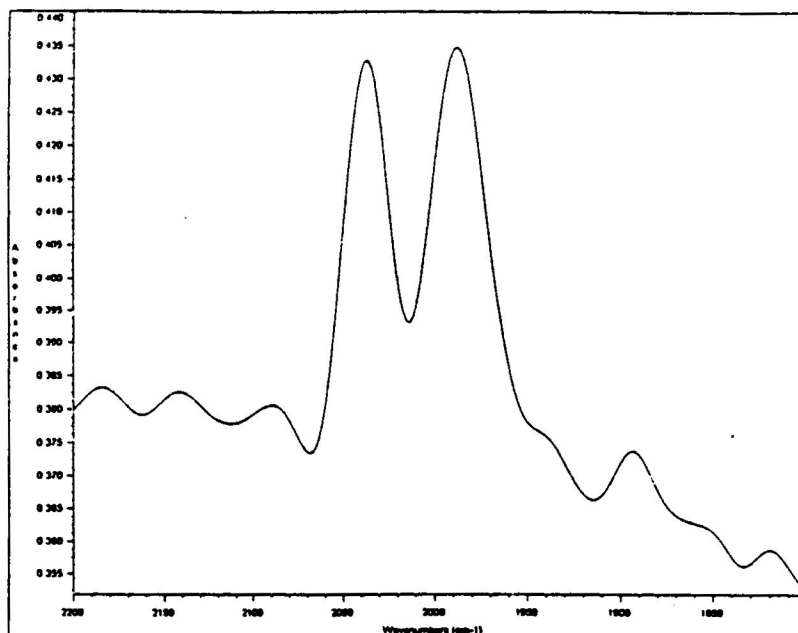


Fig. 48. DRIFTS Spectrum of (4) at 60 °C.

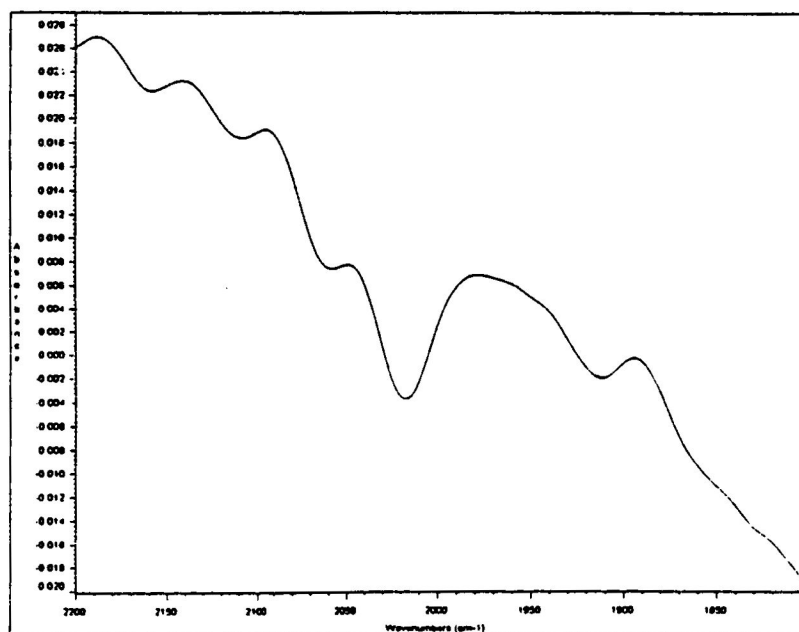


Fig. 49. DRIFTS Spectrum of (4) at 100 °C.

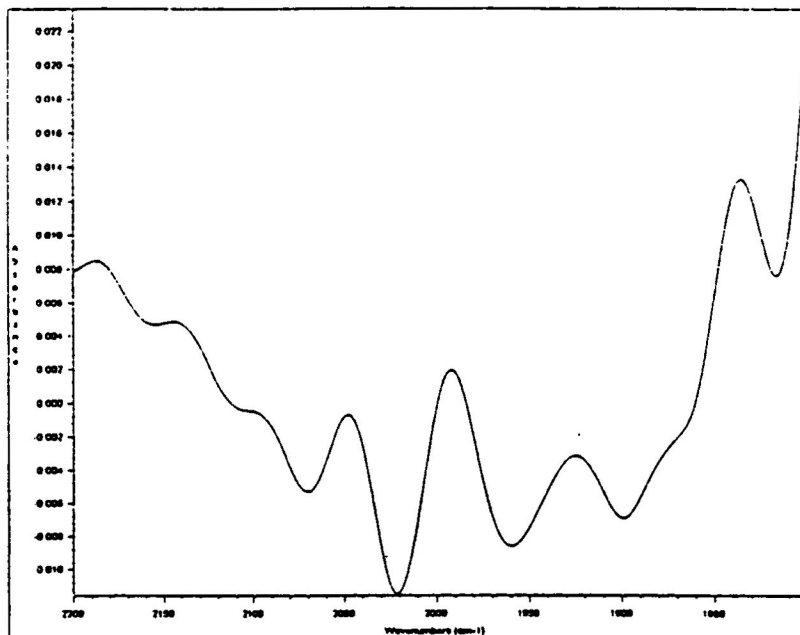


Fig. 50. DRIFTS Spectrum of (4) at 40 °C.

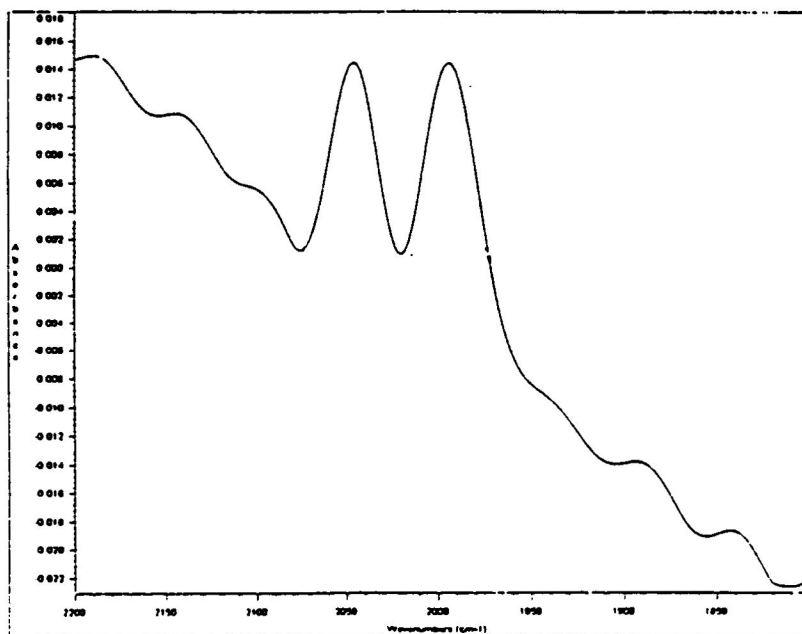


Fig. 51. DRIFTS Spectrum of (4) cooled to Room Temperature.

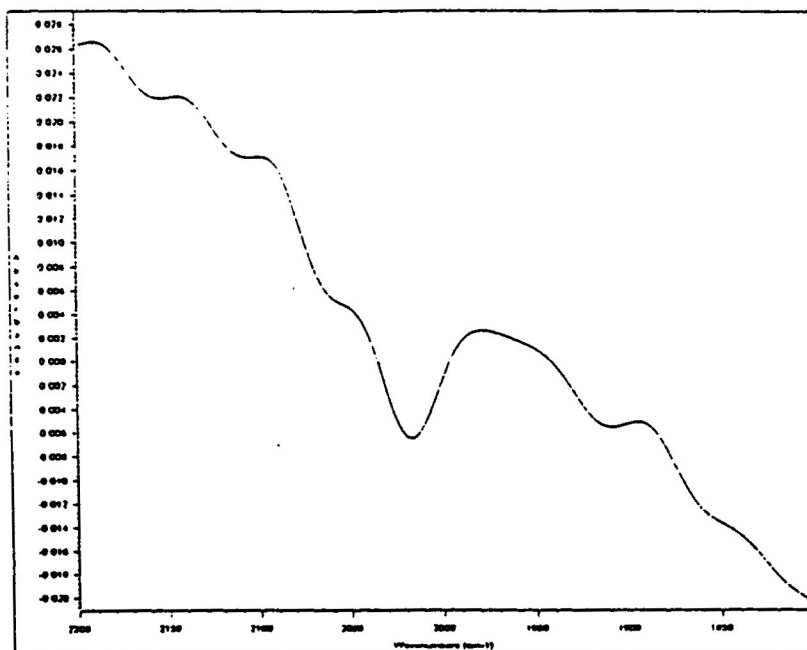


Fig. 52. DRIFTS Spectrum of (4) at 100 °C.

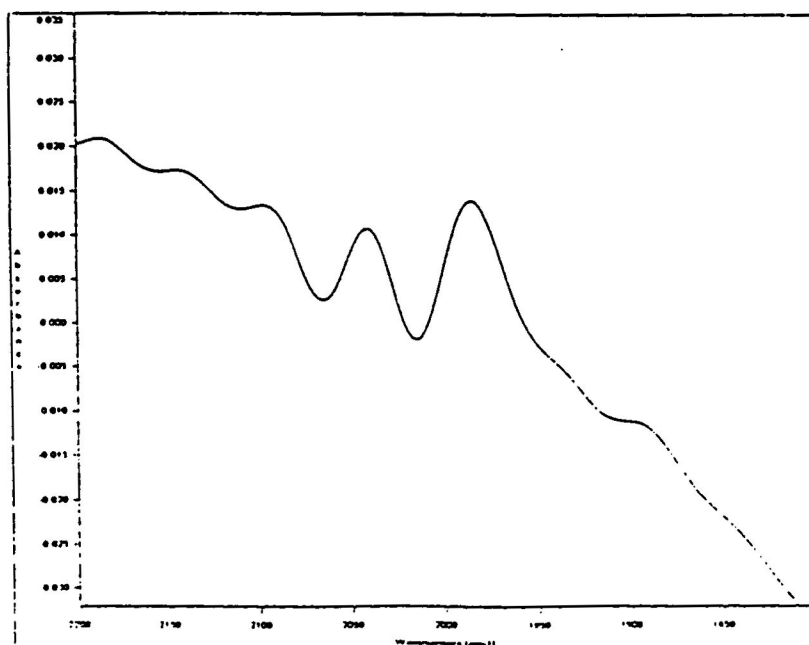


Fig. 53. DRIFTS Spectrum of (4) cooled to Room Temperature.

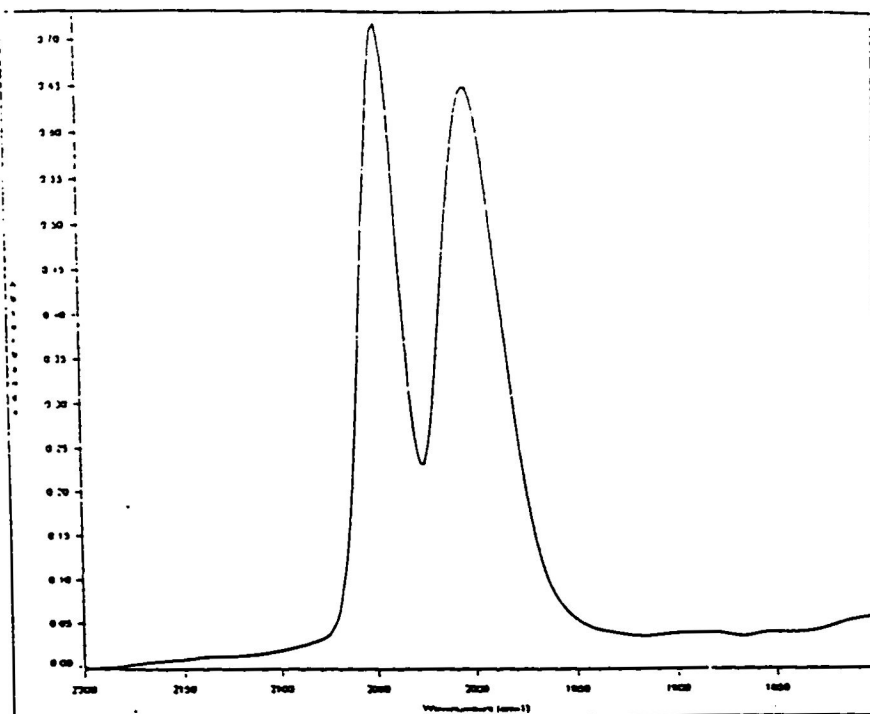


Fig. 54. DRIFTS Spectrum of (4) on γ -Alumina (4/10 coverage) at Room Temperature.

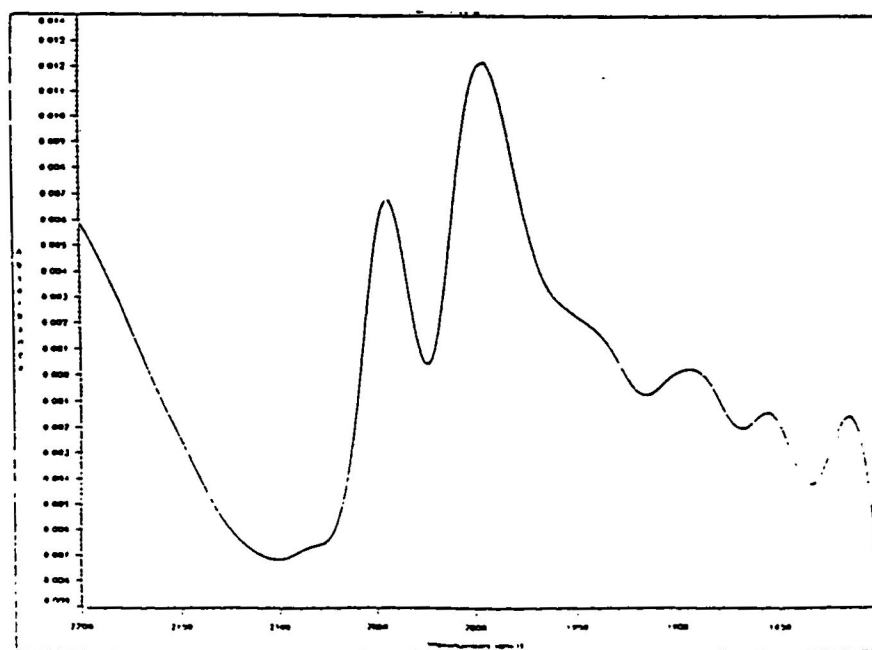


Fig. 55. DRIFTS Spectrum of (4) on γ -Alumina (4/10 coverage) at 80 °C.

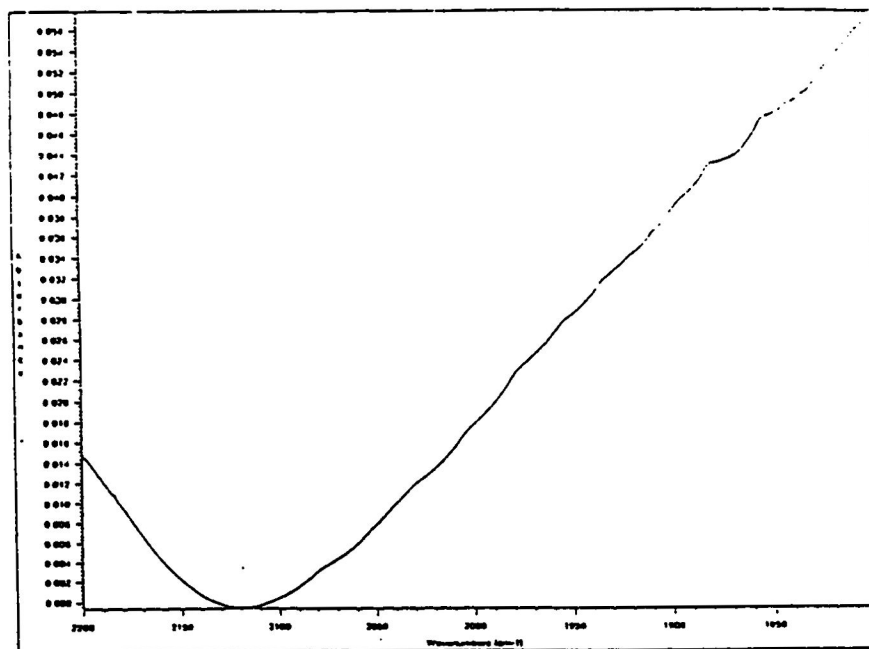


Fig. 56. DRIFTS Spectrum of (4) on γ -Alumina (4/10 coverage) at 100 °C.

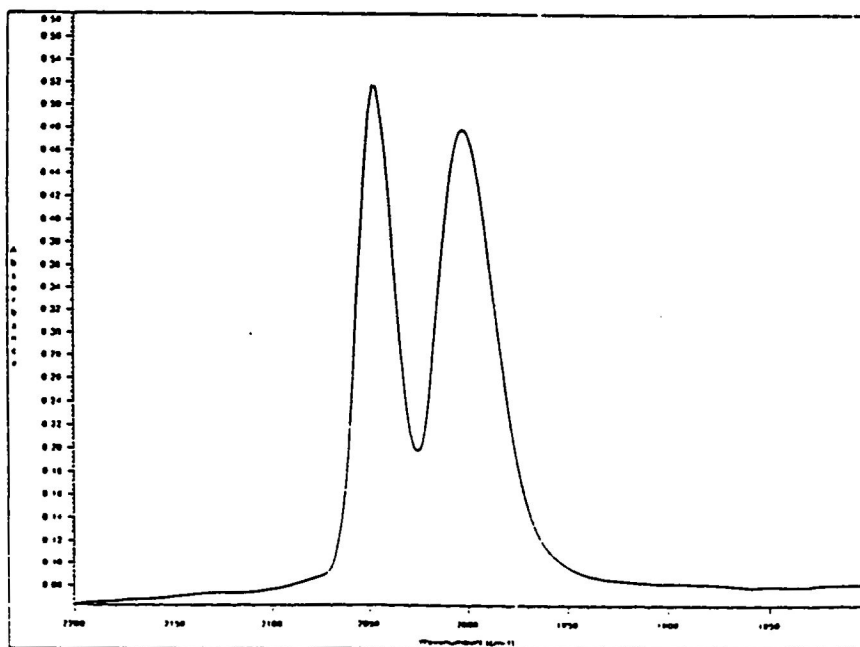


Fig. 57 DRIFTS Spectrum of (4) on γ -Alumina (4/10 coverage) at Room Temperature after cooling.

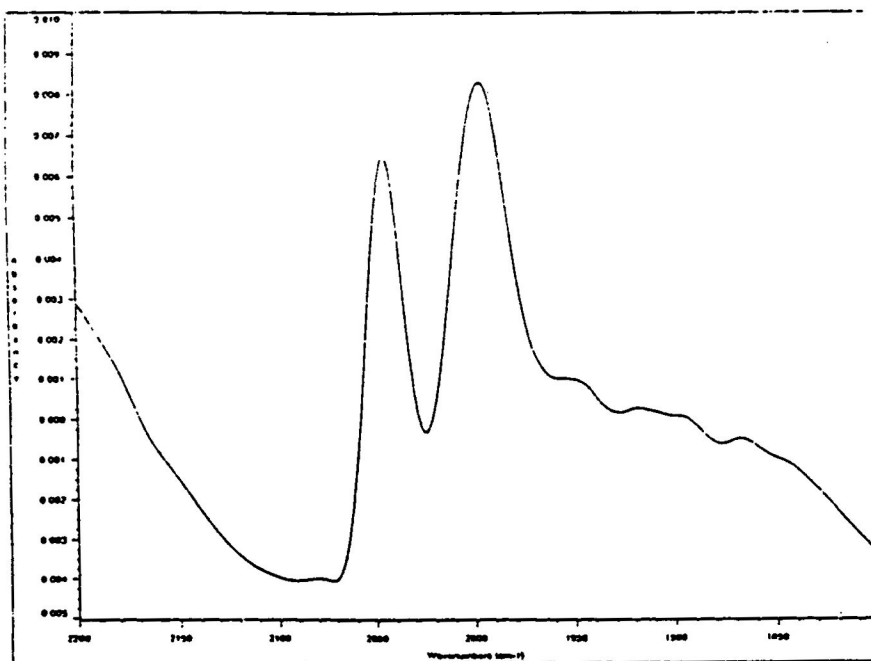


Fig. 58. DRIFTS Spectrum of (4) on γ -Alumina (3/10 coverage) at Room Temperature.

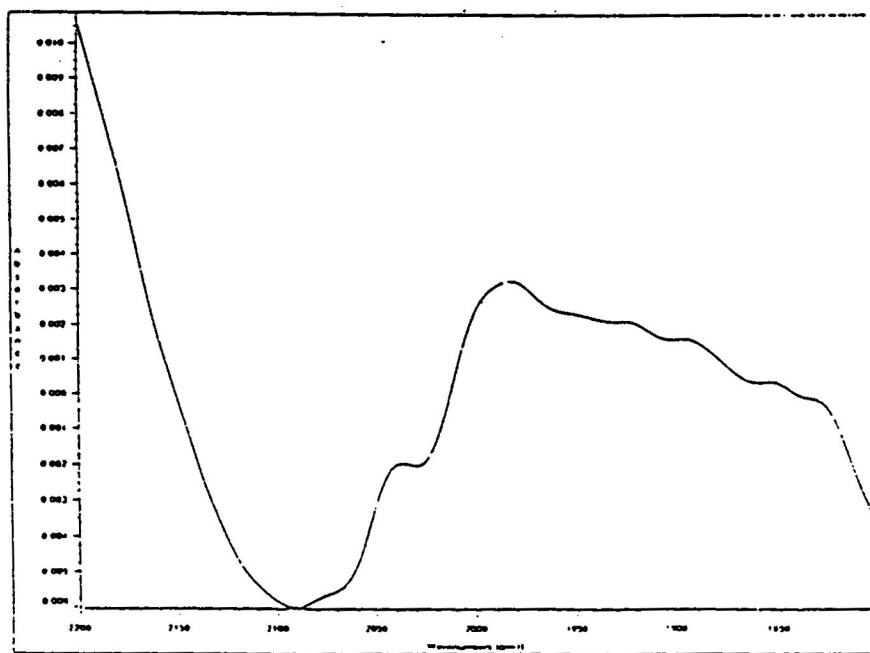


Fig. 59. DRIFTS Spectrum of (4) on γ -Alumina (4/10 coverage) at 60 °C.

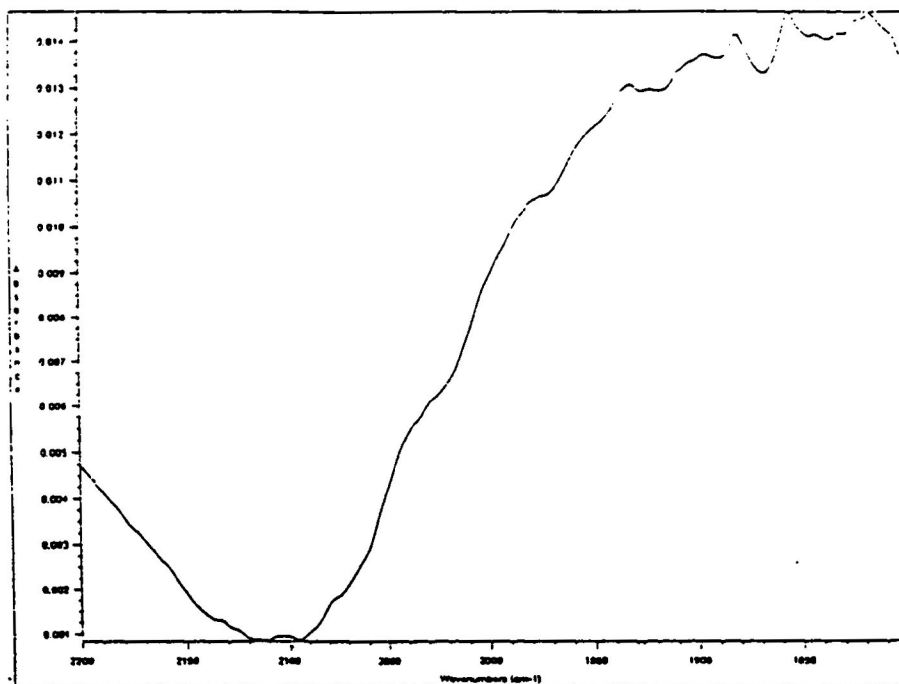


Fig. 60. DRIFTS Spectrum of (4) on γ -Alumina (4/10 coverage) at 80 °C.

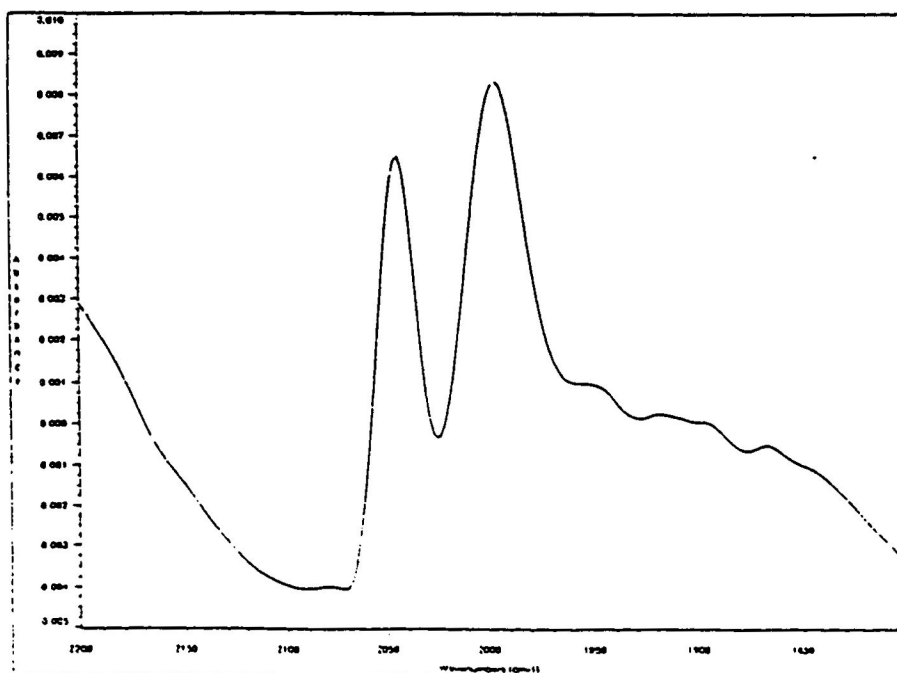


Fig. 61. DRIFTS Spectrum of (4) on γ -Alumina (2/10 coverage) at Room Temperature.

Table IX. DRIFTS data for (4) as a function of temperature and coverage (in wavenumbers)

Temperature in degree Celsius	Pure compound dissolved in chloroform	Pure compound	Coverage on gamma alumina		
			4/10	3/10	2/10
Room Temperature	2042 (vs)	2130.5 (vw)	2049.4 (vs)	2045 (m)	2045.7 (m)
	1999 (vs)	2069.8 (m)	2004.8 (vs)	1998.2 (m)	1999.6 (m)
		2018.6 (m)			
		1951.4 (m)			
40		1890.7 (w)			
		2132	2049.4	2045 (vw)	2045.7 (vw)
		2070.6	2004.8	1998.2 (w)	1999.6 (w)
		2023.8			
60		1953.6			
		1888.5			
		2038.4 (s)			
		1987.9 (s)			
80					
		2038.4			
		1987.9			
100			2047.4	2045	2045.7
			2004.8	1998.2	1999.6
80			2045 (w)		
			2004 (m)		
60					
40		2048.6 (w)			
		1993.8 (w)			
		1850 (m)			
Room Temperature		2047.2 (m)	2042		
		1994.5 (m)	1999		
100					
200					
300					
400					
Final		2041.3 (w)			
Room Temperature		1985 (w)			

Cyclopentadienyl-dicarbonyl-2,4-cyclopentadienyliron: 5

The carbonyl bands for this compound in solution are known to occur at 2013 and 1965 cm^{-1} .⁵¹ The carbonyl bands for this compound on partially dehydroxylated gamma alumina were observed at 2048.6, 2001.0, 1970.4, 1942.6, and 1888.5 cm^{-1} (Fig. 64). The shift of the bands to both a higher and a lower

wavenumber was indicative of Lewis acid binding at a terminal carbonyl (Fig. 7). The terminal carbonyl where binding occurred shifted to a lower wavenumber while the other terminal carbonyl was shifted to a higher wavenumber.

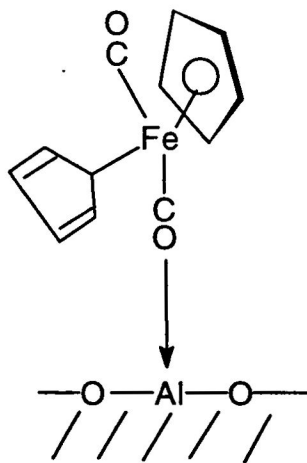


Fig. 7. Diagram illustrating binding to alumina at terminal carbonyl site in **5**.

The spectrum for this compound remained unchanged upon heating to 40 °C (Fig. 65). All carbonyl bands disappeared upon heating to 60 °C (Fig. 66). The spectrum remained unchanged upon heating to 80 °C and upon cooling to room temperature. Further analysis of the spectra showed that upon binding to the alumina and heating a reaction occurred resulting in the carbonyl groups leaving and the formation of ferrocene (Fig. 8). Thermal decarbonylation of **5** to ferrocene is known to occur at higher temperatures.⁵² The ferrocene bands at 2925.0, and 2856.3cm⁻¹ were unchanged upon heating to 80 °C (Fig. 67).⁵³

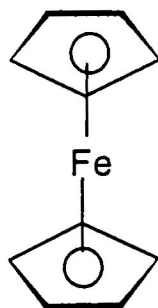


Fig. 8. Ferrocene.

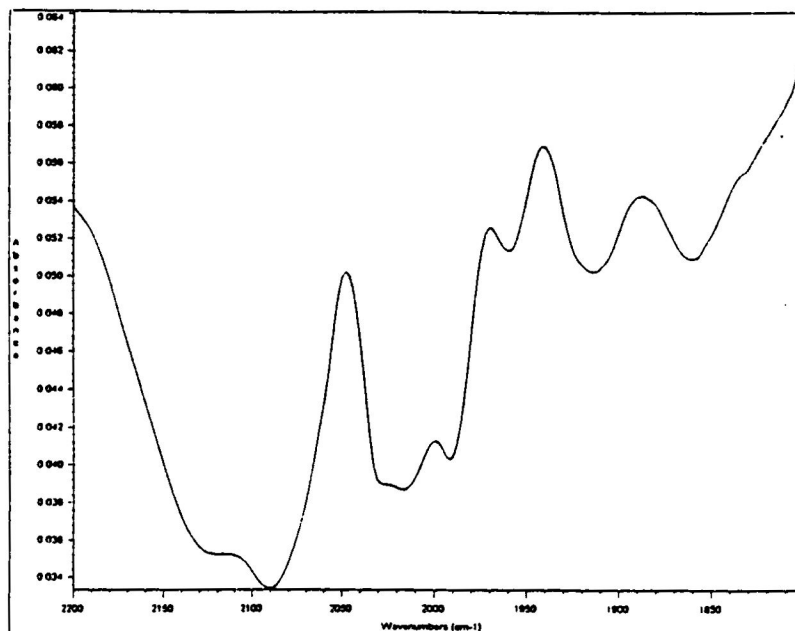


Fig. 64. DRIFTS Spectrum of Cyclopentadienyl-dicarbonyl-2,4-cyclopentadienyliron, (5), on 101 mg of γ - Al_2O_3 at Room Temperature.

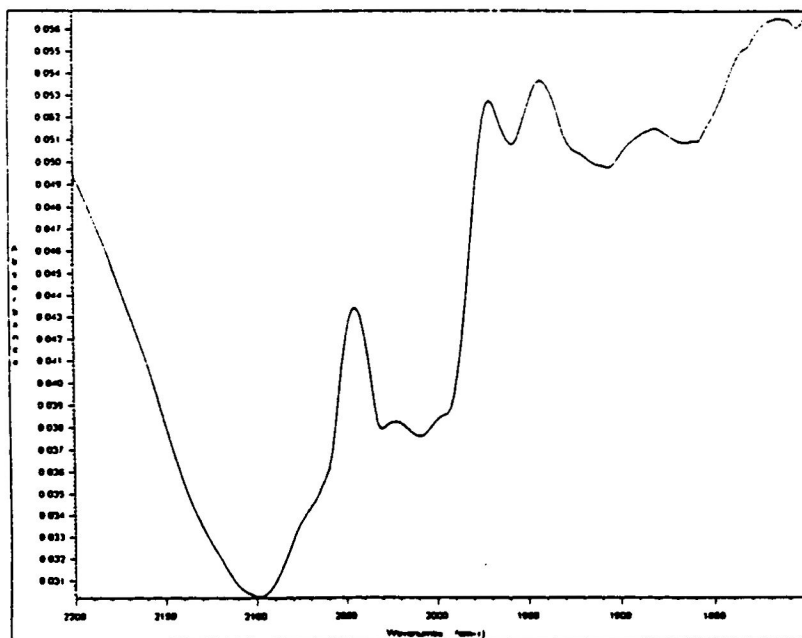


Fig. 65. DRIFTS Spectrum (5) on 101 mg of γ -Al₂O₃ at 40 °C

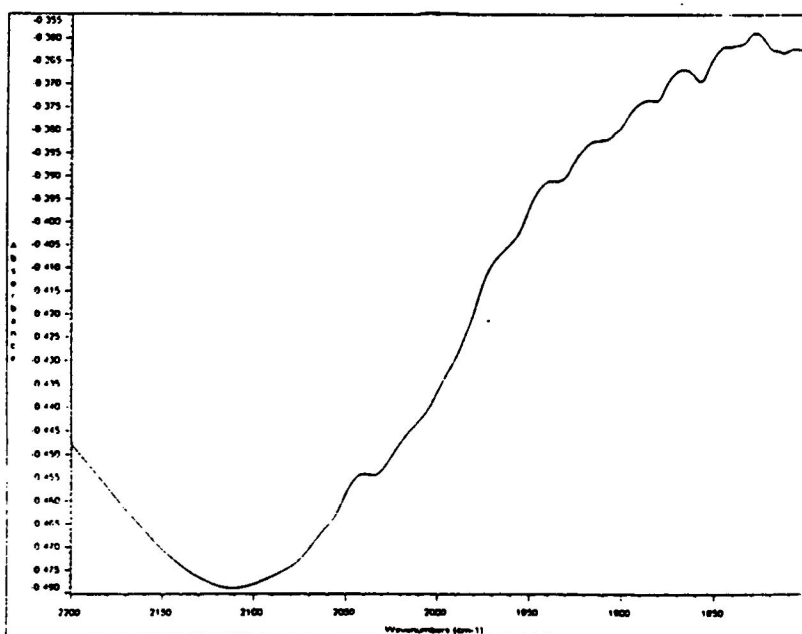


Fig. 66. DRIFTS Spectrum (5) on 101 mg of γ -Al₂O₃ at 60 °C

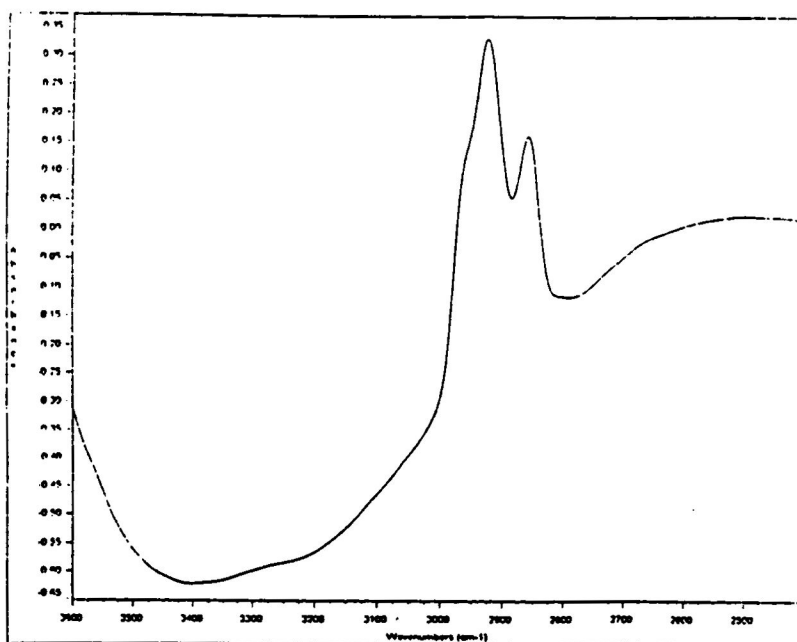


Fig. 67. DRIFTS Spectrum of (5) on 101mg γ -Al₂O₃ at 80 °C

Table X. DRIFTS data for (5) as a function of temperature and coverage (in wavenumbers)

Theoretical values	Room Temperature	Temperature in degree Celsius				Room Temperature
		40	60	80	60	40
2013	2048.6 (m)	2045 (m)		2925.0 (vs)		
1965	2001.1 (w)	1971.1 (s)		2856.3 (s)		
	1970.4 (m)	1943.3 (s)				
	1942.6 (s)	1883.4 (w)				
	1888.5 (m)					

[α,α' -m-xylenebis (η^5 -cyclopentadienyl)]bis[tricarbonylmolybdenum]: 9

The solution spectrum of 9 (Fig. 68) exhibited terminal carbonyl bands at 2045.7, 2009.9, 1978.4, 1952.8 and 1909.7cm⁻¹. DRIFTS analysis of this

compound exhibited carbonyl bands at 2047.2, 2011.3, 1975, 1926.5 and 1868.7 cm^{-1} at room temperature (Fig. 69). The spectrum remained relatively unchanged upon heating to 100 $^{\circ}\text{C}$ and cooling to room temperature. However, upon heating to 150 $^{\circ}\text{C}$ (Fig. 70) the bands considerably decreased in intensity and the 1975 cm^{-1} band broadened and shifted to 1958.0 cm^{-1} while the 1926.5 cm^{-1} shifted to 1891.4 cm^{-1} . Further heating to 350 $^{\circ}\text{C}$ (Fig. 71) resulted in the reappearance of carbonyl bands at 1951.4, 1887.0 and 1847.5 cm^{-1} . Upon further heating to 400 $^{\circ}\text{C}$ (Fig. 72) carbonyl bands were exhibited at 1951.4, 1925.8 and 1847.5 cm^{-1} . Upon cooling to room temperature the 1925.8 cm^{-1} band shifted to a higher wavenumber of 1932.4 cm^{-1} (Fig. 73). While there was a shift of the carbonyls to lower wavenumbers this is not fully understood at this time.

When **9** was placed on partially dehydroxylated gamma alumina the spectrum at room temperature differed from the pure compound. The 2/10 sample at room temperature (Fig. 88) exhibited bands at 2045.7, 2008.4, 1949.9 and 1899.5 cm^{-1} . In comparison to the pure compound, the 1975.5 and 1926.5 cm^{-1} bands disappeared or were masked due to shifting carbonyl bands. This spectral data suggested Lewis acid binding at a metal site (Fig. 9).

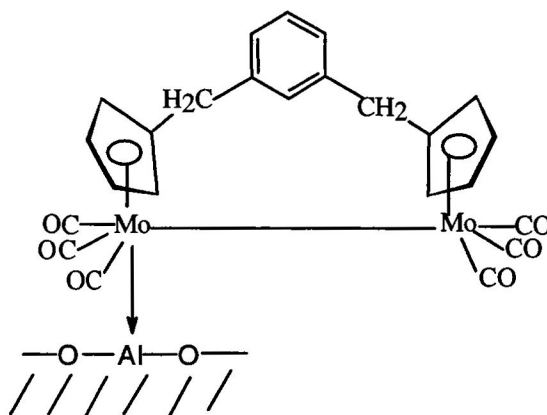


Fig. 9. Diagram illustrating binding to alumina at a metal in **9**.

Upon heating the 2/10 sample to 100 °C the 1898.7 cm^{-1} band shifted to 1893.6 cm^{-1} . When heated to 200 °C (Fig. 89) the carbonyl bands were observed at 1952.8, 1883.4, and 1845.3 cm^{-1} . Further heating to 300 °C (Fig. 90) resulted in complete decarbonylation. The spectrum was unchanged upon cooling to room temperature. Similarly, decarbonylation also occurred at 300 °C for the 3/10 coverage (Fig. 86). However, when the sample was cooled to 200 °C (Fig. 87) there was a slight reappearance of carbonyl bands at 1935.3 and 1831.4 cm^{-1} . These band were shifted to a higher wavenumber when compared to the room temperature spectrum (Fig. 81) that exhibited carbonyl bands at 2047.2, 2011.3, and 1869.5 cm^{-1} . This spectral data suggested binding at more than one site. Upon heating to 80 °C (Fig. 82) carbonyls bands were exhibited at 2045.0, 2008.4, and 1831.4 cm^{-1} . Upon further heating to 150 °C (Fig. 83) the spectrum exhibited carbonyl bands at 2000.4 and 1928.0 cm^{-1} . Further heating to 250 °C (Fig. 84) resulted in the carbonyl bands being shifted to a lower wavenumber, 1956.5, 1884.8 and 1825.7 cm^{-1} . The spectral data for the 4/10 coverage at room temperature exhibited an increase in carbonyl bands consistent with binding at the

metal, in addition to a decrease in a carbonyl band indicative of binding at a carbonyl. The terminal carbonyl bands at room temperature were observed at 2051.6, 2024.5, 1993.1, 1936.7, and 1842.4 cm^{-1} (Fig. 74). Upon heating to 80 $^{\circ}\text{C}$ (Fig. 75) the 1936.7 cm^{-1} band disappeared and the 1842.4 cm^{-1} bands shifted to 1830.0 cm^{-1} . Upon further heating to 100 $^{\circ}\text{C}$ (Fig. 76) carbonyl bands were observed at 2045.0 and 2009.1 cm^{-1} . As the temperature was increased to 150 $^{\circ}\text{C}$ (Fig. 77) these bands shifted to a lower wavenumber, 1956.5 and 1890.7 cm^{-1} . Further heating to 200 $^{\circ}\text{C}$ (Fig. 78) gave rise to carbonyl bands at 1955.8, 1885.6, and 1848.3 cm^{-1} . Upon heating to 350 $^{\circ}\text{C}$ (Fig. 79) decarbonylation occurred. When the sample was allowed to cool to 100 $^{\circ}\text{C}$ (Fig. 80) terminal carbonyl bands reappeared at 1938.9, 1885.6 and 1845.3 cm^{-1} . The spectrum remained unchanged as it was cooled to room temperature. This data suggests that while there was a continuous flow of nitrogen during the course of the experiment, the flow rate was not adequate enough to allow for the removal of CO.

The DRIFTS data indicate that when **9** was placed on γ -alumina, the introduction of this Lewis acid catalyzed decarbonylation of the compound. On alumina, decarbonylation occurred more readily because of a complexation with a Lewis acid site that removed electron density directly or indirectly from the molybdenum, thus decreasing backbonding, causing the carbonyl bond to metal bond to weaken.

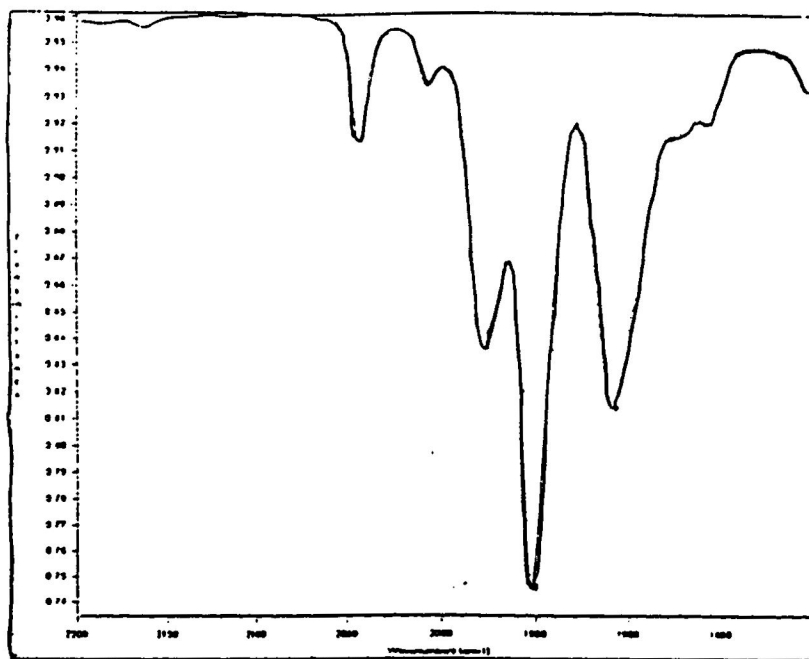


Fig. 68. FT-IR Spectrum of $[\alpha,\alpha'\text{-m-xylenebis}(\eta^5\text{-cyclopentadienyl})]\text{bis}[\text{tri-carbonylmolybdenum}]$, (9), in hexane

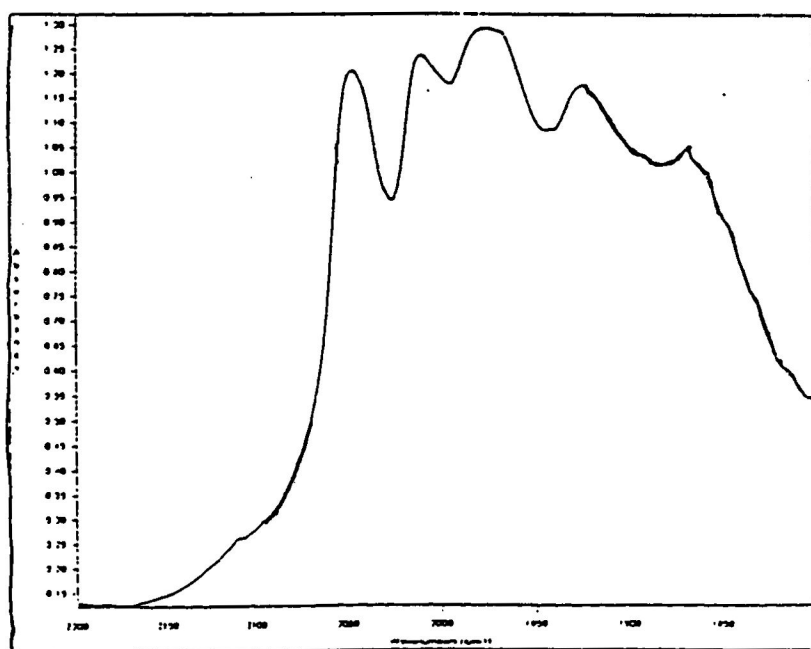


Fig. 69. DRIFTS Spectrum of (9) at Room Temperature

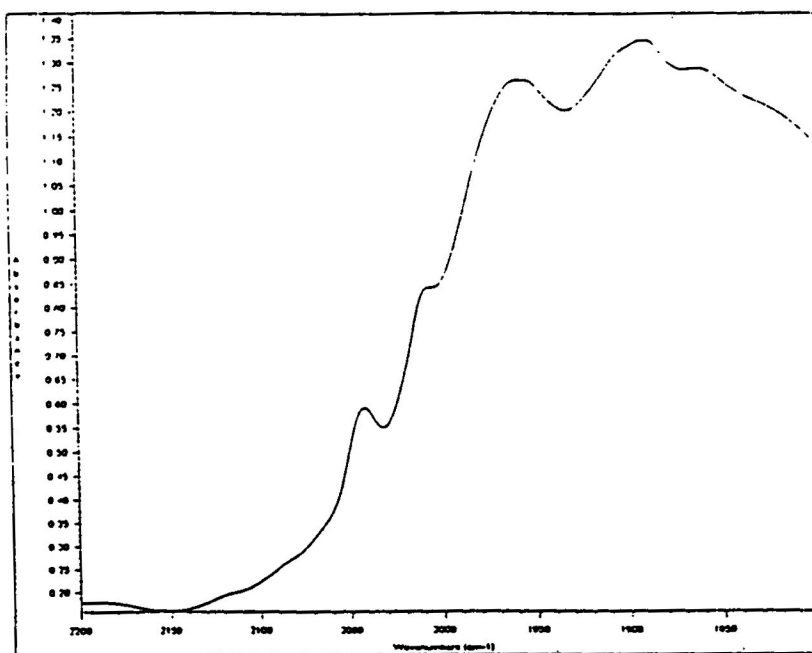


Fig. 70. DRIFTS Spectrum of (9) at 150 °C.

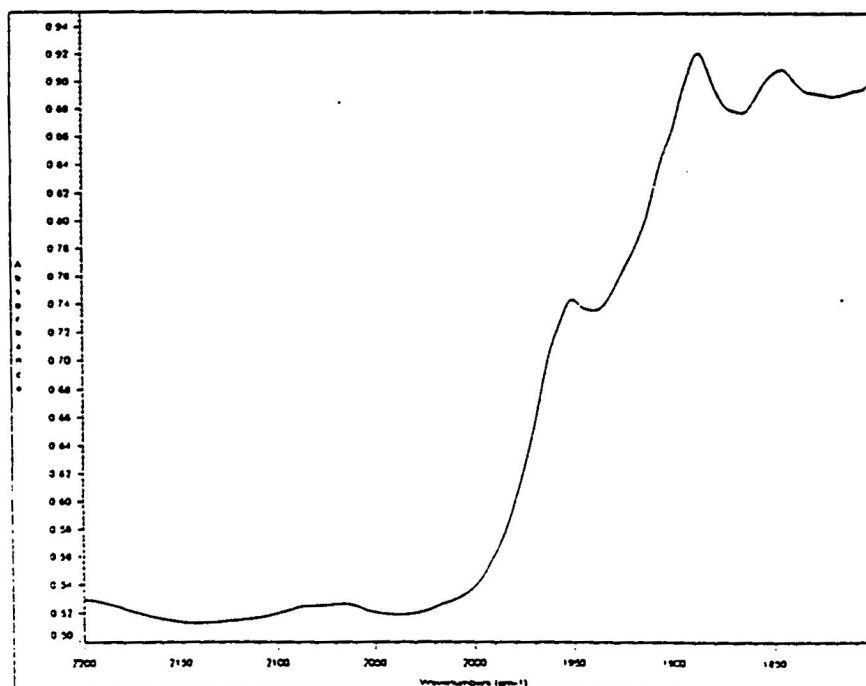


Fig. 71. DRIFTS Spectrum of (9) at 350 °C.

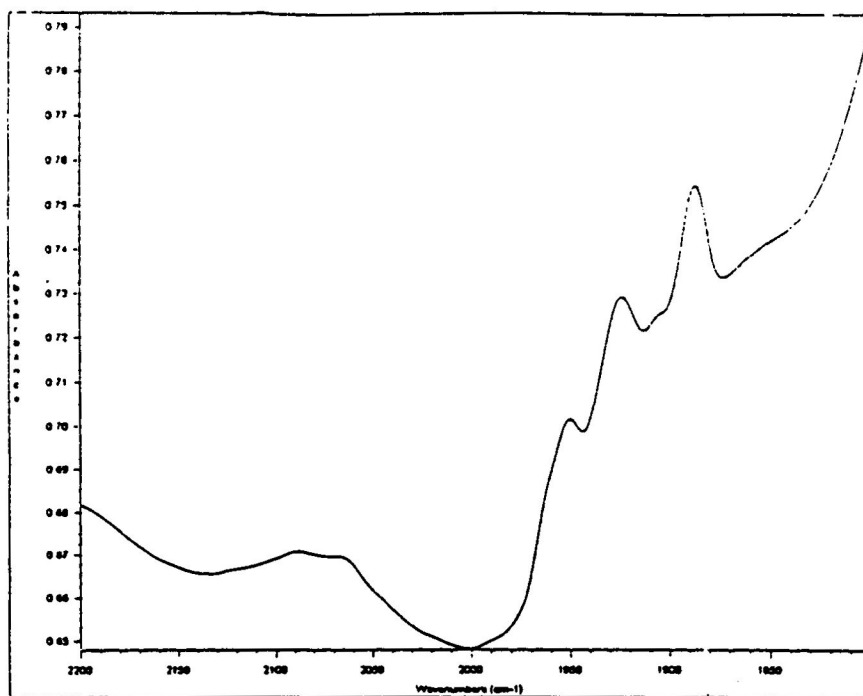


Fig. 72. DRIFTS Spectrum of (9) at 400 °C

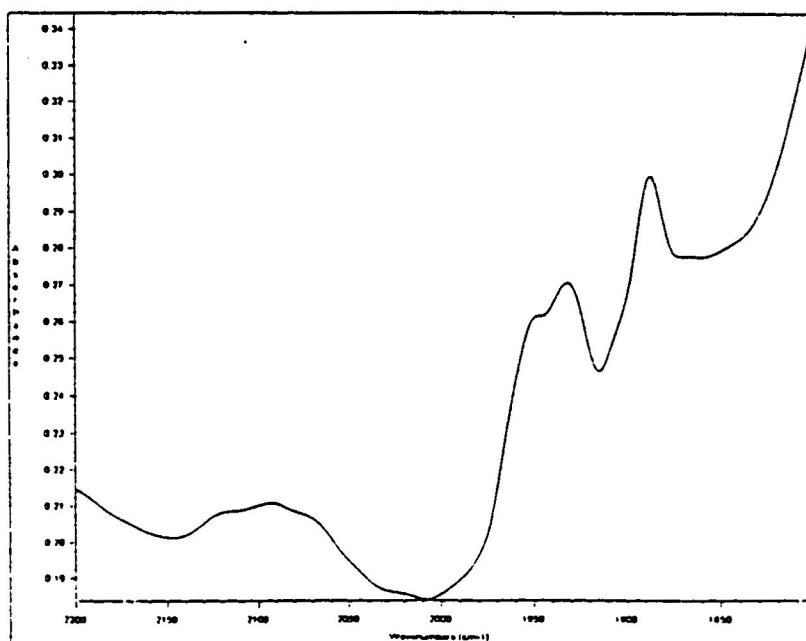


Fig. 73. DRIFTS Spectrum of (9) at Room Temperature after cooling

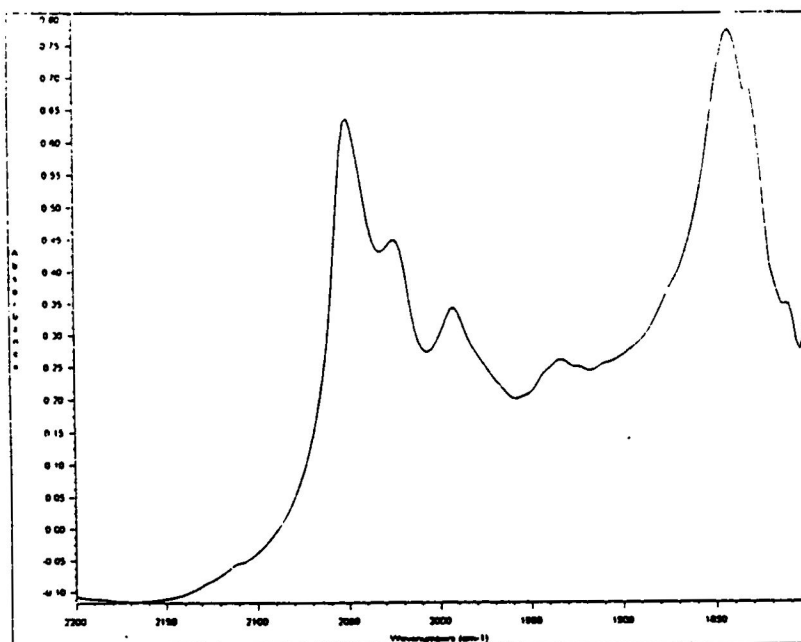


Fig. 74. DRIFTS Spectrum of (9) on γ -Alumina (4/10 coverage) at Room Temperature

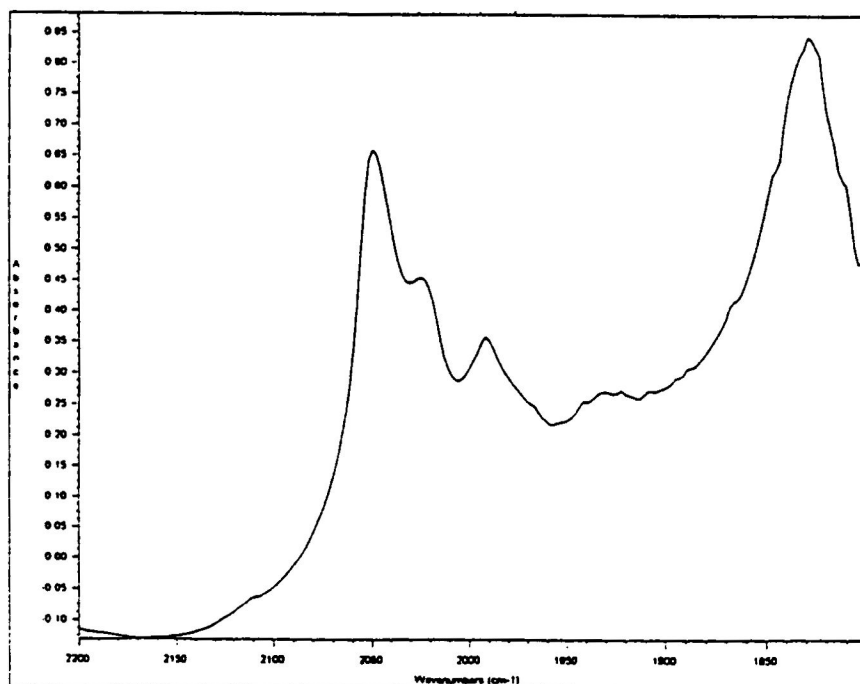


Fig. 75. DRIFTS Spectrum of (9) on γ -Alumina (4/10 coverage) at 80 °C

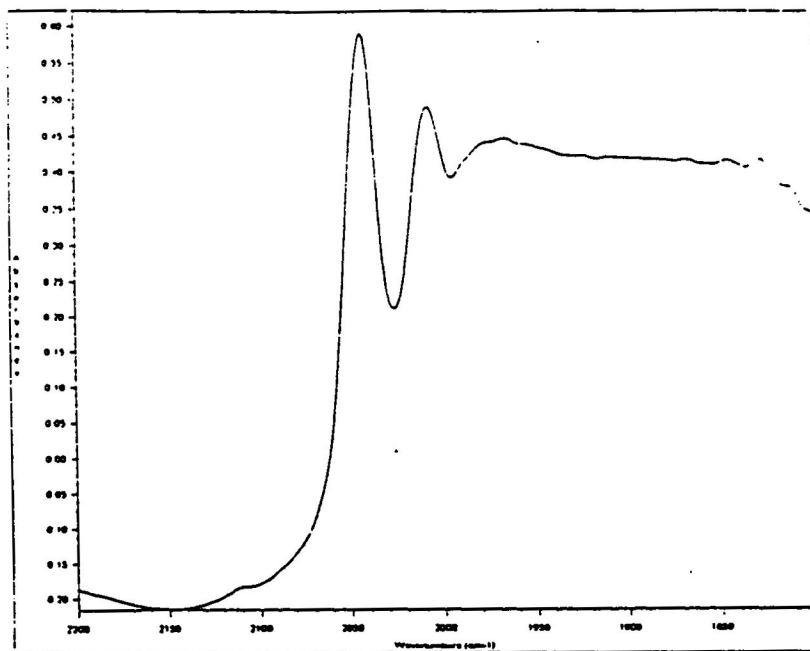


Fig. 76. DRIFTS Spectrum of (9) (4/10 coverage) at 100 °C.

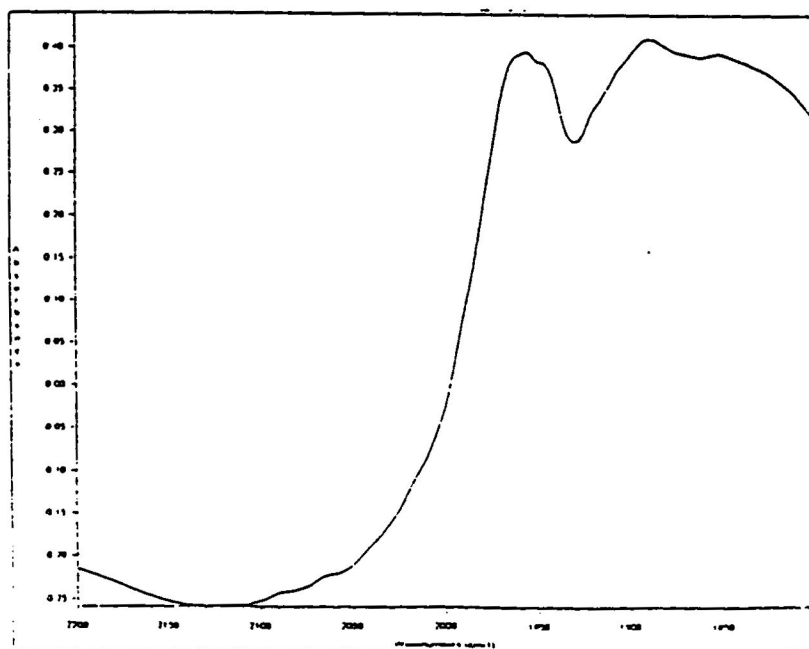


Fig. 77. DRIFTS Spectrum of (9) on γ -Alumina (4/10 coverage) at 150 °C.

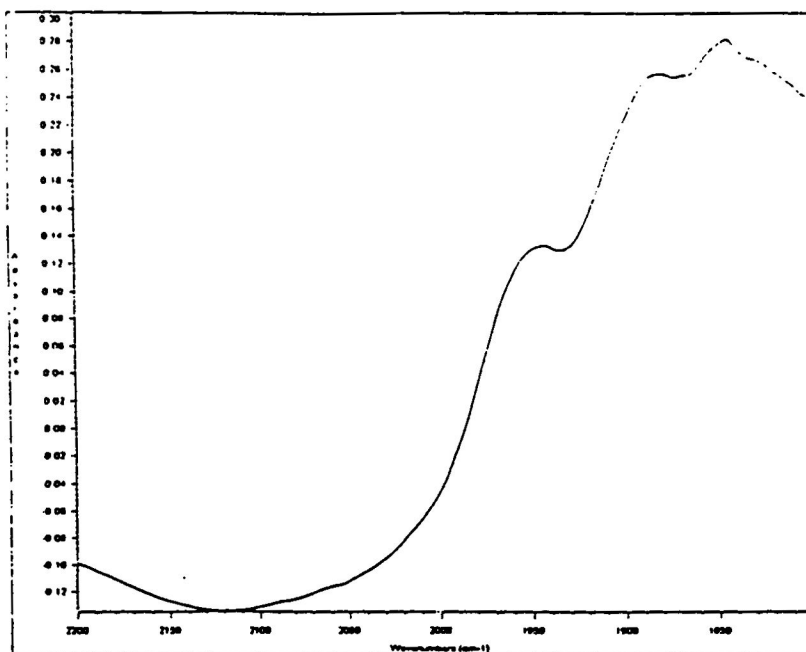


Fig. 78. DRIFTS Spectrum of (9) on γ -Alumina (4/10 coverage) at 200 °C.

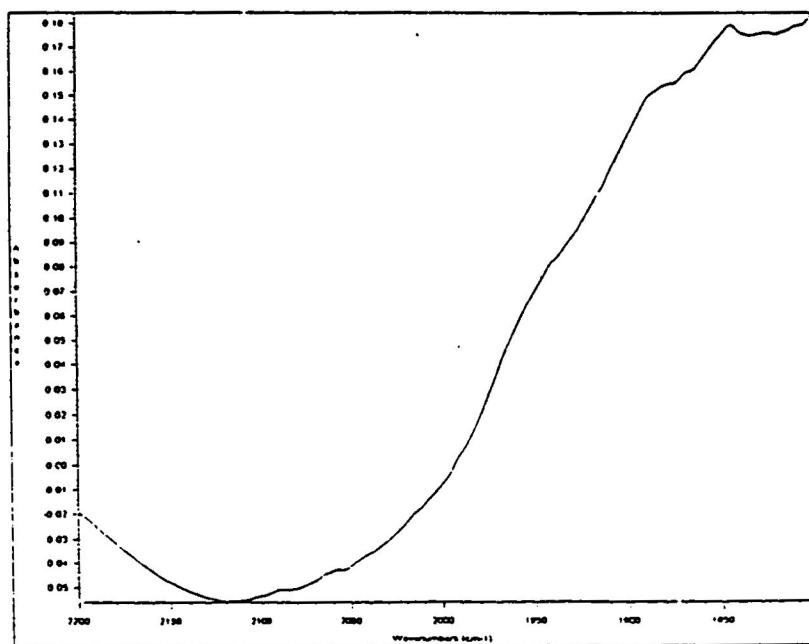


Fig. 79. DRIFTS Spectrum of (9) on γ -Alumina (4/10 coverage) at 250 °C.

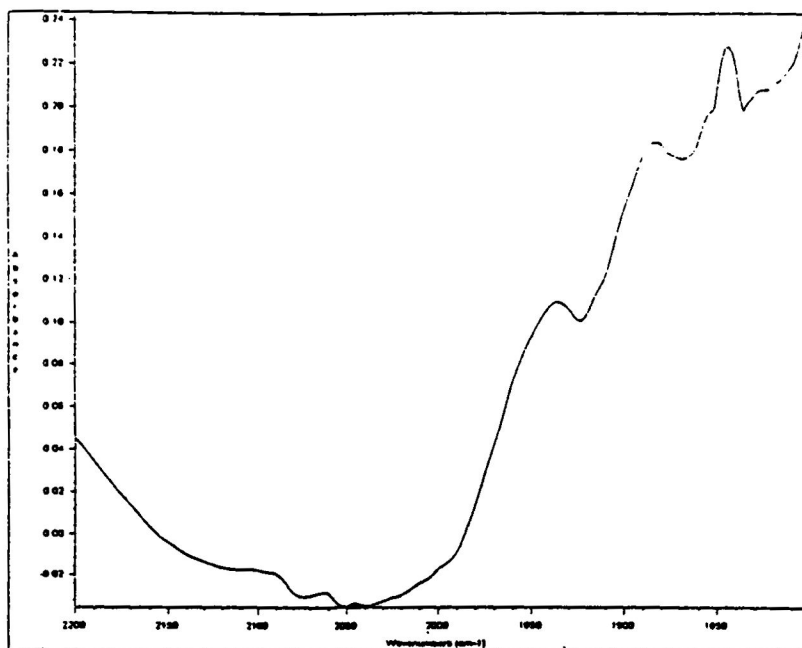


Fig. 80. DRIFTS Spectrum of (9) on γ -Alumina (4/10 coverage) at 100 °C

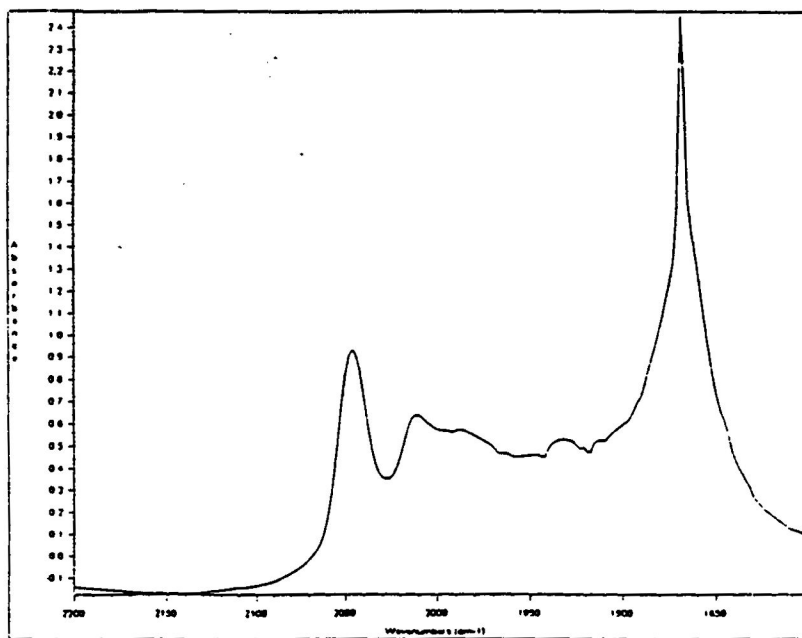


Fig. 81. DRIFTS Spectrum of (9) on γ -Alumina (3/10 coverage) at Room Temperature

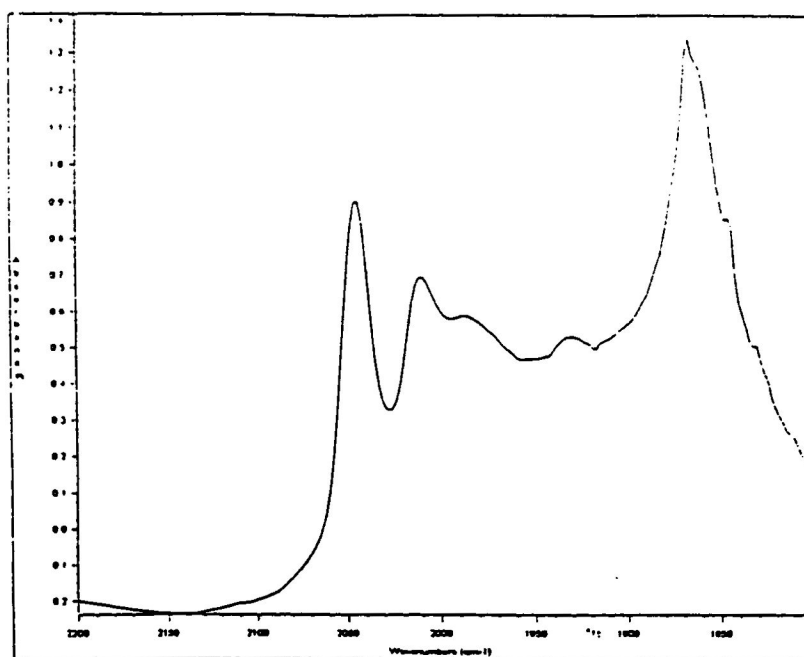


Fig. 82. DRIFTS Spectrum of (9) on γ -Alumina (3/10 coverage) at 100 °C.

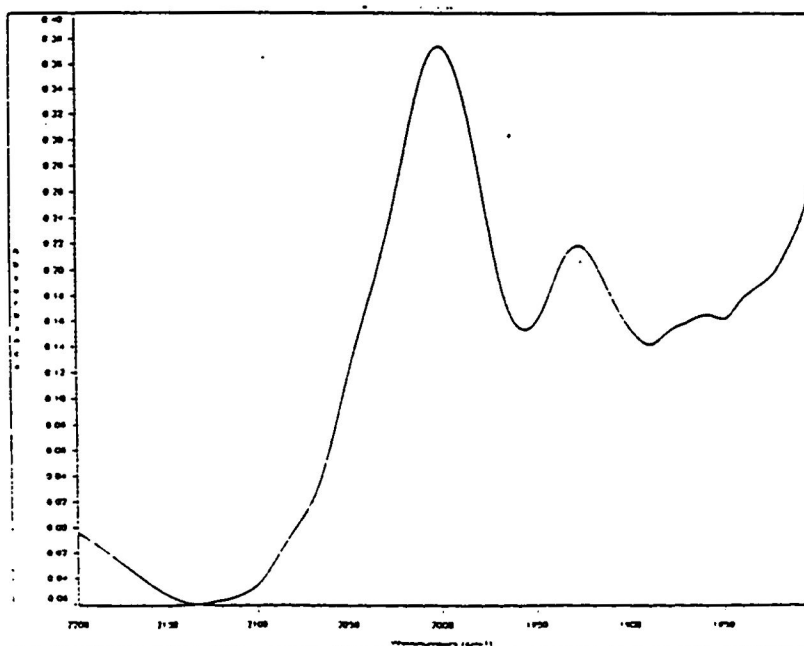


Fig. 83. DRIFTS Spectrum of (9) on γ -Alumina (3/10 coverage) at 150 °C.

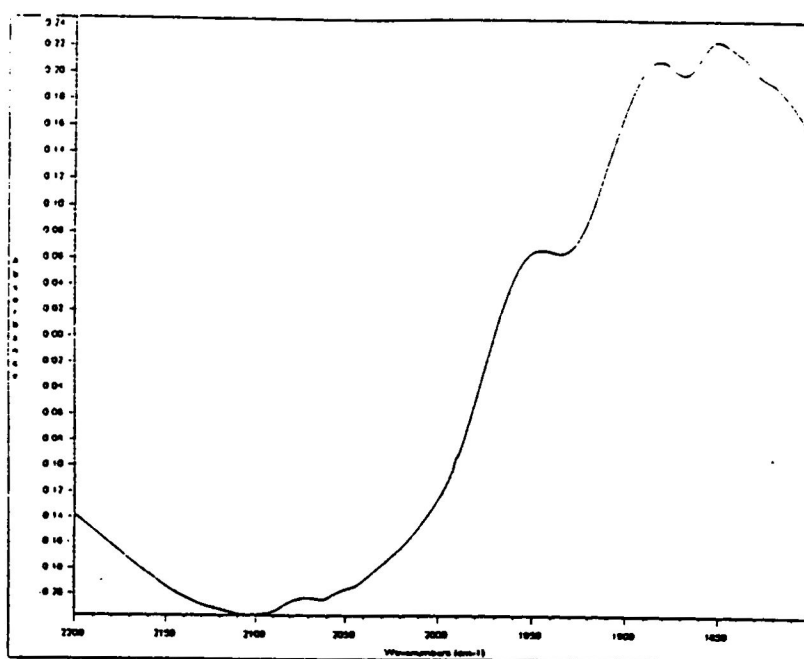


Fig. 84. DRIFTS Spectrum of (9) on γ -Alumina (3/10 coverage) at 250 °C

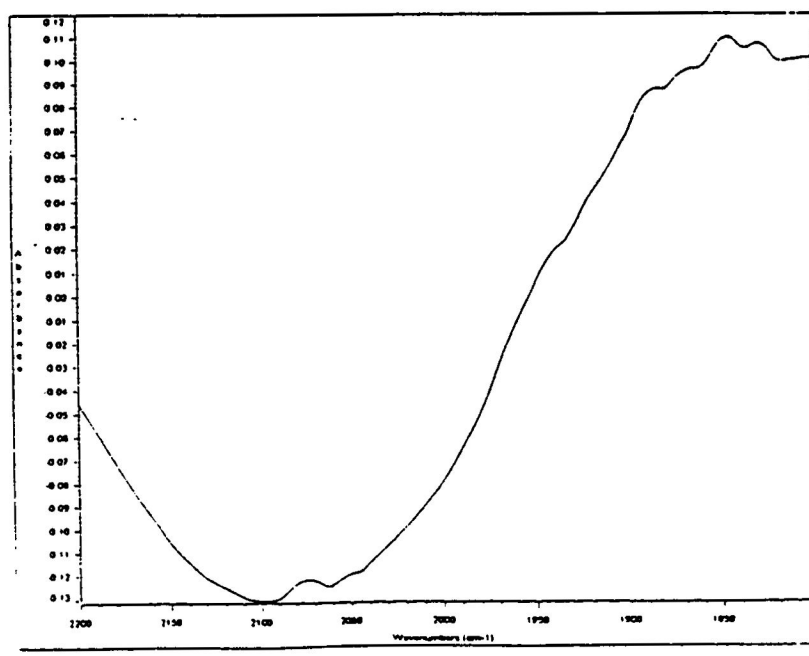


Fig. 85. DRIFTS Spectrum of (9) on γ -Alumina (3/10 coverage) at 300 °C

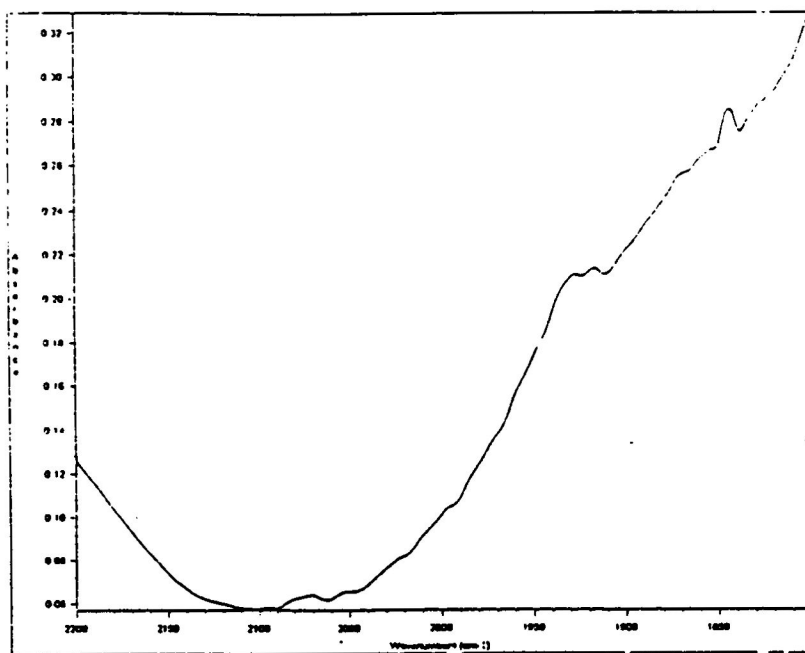


Fig. 86. DRIFTS Spectrum of (9) on γ -Alumina (3/10 coverage) at 200 °C

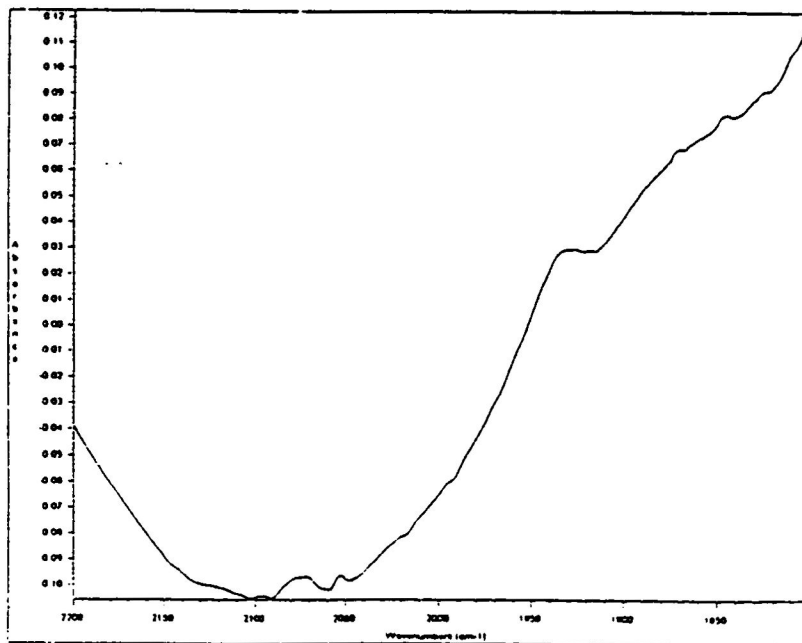


Fig. 87. DRIFTS Spectrum of (9) on γ -Alumina (3/10 coverage) at Room Temperature

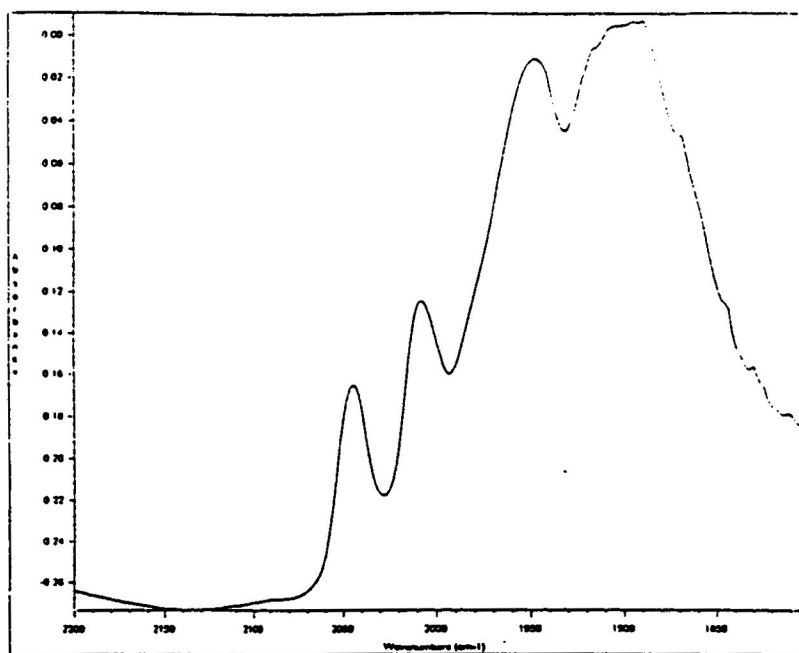


Fig. 88. DRIFTS Spectrum of (9) on γ -Alumina (2/10 coverage) at Room Temperature

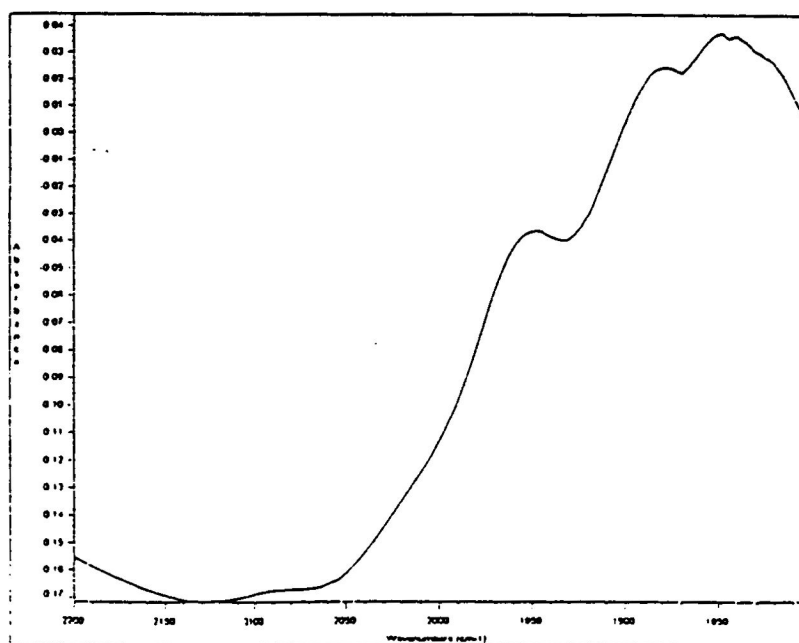


Fig. 89. DRIFTS Spectrum of (9) on γ -Alumina (2/10 coverage) at 200 °C

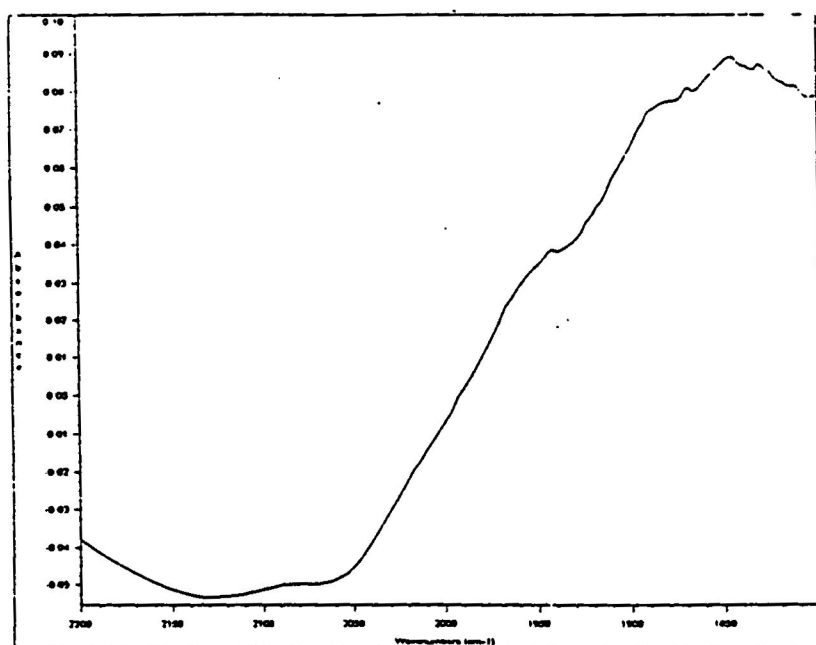


Fig. 90. DRIFTS Spectrum of (9) on γ -Alumina (2/10 coverage) at 300 °C.

Table XI. DRIFTS data for (9) as a function of temperature and coverage (in wavenumbers)

Temperature in degree Celsius	Pure compound dissolved in hexane	Pure compound	Coverage on gamma alumina		
			4/10	3/10	2/10
Room Temperature	2045.7 (m)	2047.2 (s)	2051.6	2051.6 (m)	2045.7 (w)
	2009.9 (w)	2011.3 (s)	2024.5	2024.5 (w)	2008.4 (w)
	1978.4 (s)	1975.5 (s)	1993.1	1993.1 (vs)	1949.9 (s)
	1932.3 (vs)	1926.5 (s)	1936.7	1936.7 (vw)	1899.5 (s)
	1909.7 (s)	1868.7 (m)	1842.4	1842.4 (vs)	
			1868.7		
40		2047.2	2051.6	2047.9	2045.7
		1926.5	1936.7		1899.5
		1868.7	1842.4		
60		2047.2	2051.6	2047.2	2045.7
		2011.3	2024.5	2011.3	2008.4
		1975.5	1993.1	1869.5	1949.2
		1925	1840.2		1899.5
		1868.7			
		2047.2	2051.6	2047.2	2045.7
		2011.3	2024.5	2011.3	2008.4
80		1974	1993.1	1868.7	1949.2
		1925	1830		1899.5
		1868.7			
100		2045	2045	2045 (m)	2043.5
		2009.9	2009.1	2008.4 (w)	2007.7
		1965.3		1831.4 (s)	1947.7
		1974.5			1893.6
		1921.4			
80		2045		2045	2043.5
		2009.9		2008.4	2006.9
		1965.3		1830	1947
		1974.5			1892.9
		1921.4			
60		2045			2043.5
		2009.9			2007.7
		1965.3			1947.7
		1974.5			1892.1
		1921.4			
40		2045			2043.5
		2009.9			2007.7
		1965.3			1947.7
		1974.5			1892.9
		1921.4			
Room Temperature		2045			2043.5
		2009.9			2007.7
		1965.3			1947.7
		1974.5			1892.1
		1921.4			

Table XI. (continued)

150		2042.8 (w) 2009.9 (m) 1958 (s) 1891.4 (s)	1956.5 (s) 1890.7 (s)	2000.4 (s) 1928 (w)	
100		2042.8 2009.9 1958 1891.4	1956.5 (vs) 1890.7 (s)		
200		2042.8 2010.6 1958 1891.4	1955.8 (w) 1885.6 (s) 1848.3 (s)	1996 1928	1952.8 1883.4 1845.3
100		2042.8 2010.6 1958 1891.4	1956.5 1889.9 1850.5		
250		2042.8 2010.6 1958 1891.4	1952.8 1885.6 1848.3	1956.5 (m) 1884.8 (s) 1852.7 (s)	
200		2042.8 2010.6 1958 1891.4	1955.8 1885.6 1846.1	1935.3 1831.4	
300		2042.8 2010.6 1958 1891.4	1952.1 1886.3 1846.1		
350		1951.4 (m) 1887 (s) 1847.5 (s)			
300		1951.4 1887 1847.5			
400		1951.4 (w) 1925 (m) 1887.8 (m)			
350		1951.4 1925 1887.8			
300					
200				1844.6 (s)	
100			1938.9 (w) 1885.6 (m) 1845.3 (s)	1935.3	
Final Room Temperature		1951.4 (w) 1932.4 (w) 1887.8 (m)	1939.7 1885.6 1845.3	2075.7 (vw) 2053.7 (vw) 1935.3 (m)	2043.5 2007.7 1947.7 1892.9

CHAPTER 4

CONCLUSION

DRIFTS analysis and TPDE were carried out on the following compounds: cyclopentadienyliron dicarbonyl dimer, (**1**); di- μ -carbonyl-cis- μ -(1-5- η :1'-5'- η' -dicyclopentadienyldimethylsilane)bis(carbonyldiiron)(FeFe), (**3**) ; cyclopenta- dienyliron dicarbonyl dimer and di- μ -carbonyl-cis- μ -(1-5- η :1'-5'- η' -dicyclopenta-dienyldimethylsilane)bis(carbonyldiiron)(FeFe), (**1** and **3**); cyclopenta- dienyldicarbonyliodoiron (II), (**4**); cyclopentadienyl-dicarbonyl-2,4-cyclopenta-dienyliron (**5**); and [α,α' -m-xylenebis(η^5 -cyclopentadienyl)]bis[tricarbonyl-molybdenum] (**9**); on γ -alumina as function of decarbonylation. Assuming four OH⁻ groups per binding site and 4.4×10^{20} of these sites/m², samples of approximately 1/10, 1/20, 2/10, 3/10, and 4/10 coverage were prepared and analyzed. Each of the compounds were analyzed in terms of decarbonylation as a function of temperature. Comparisons of decarbonylation were made with respect to pure compounds and compounds supported on γ -alumina and non-supported compounds. The analysis showed that based on the shifts in wavenumbers for the pure compounds, **1** formed a trimer, (**1** and **3**) formed a trinuclear species, **4** melted, and the reaction of **9** was not fully determined by this study. The data for **3** was indicative of an equilibrium reaction occurring between the bridged and unbridged species. When placed on alumina and heated **5** formed ferrocene.

Further analysis on alumina indicated that as the coverage increased so did the intensity of the bands. The site of Lewis acid binding was also identified based on the shift in wavenumbers relative to the pure compound. The data also indicated that decarbonylation occurred more readily on alumina than for the pure compound. This process of decarbonylation occurred faster on alumina due to the fact that the introduction of the Lewis acid, alumina, catalyzed the decarbonylation of the compounds. Complete decarbonylation only occurred for **5**. It was expected that if heated to a high enough temperature complete decarbonylation would occur leaving the metal cluster and cyclopentadienyl fragments as illustrated in reaction 14. The analysis indicated that all of the compounds on alumina experienced some decarbonylation. On alumina, decarbonylation occurred more readily because of a complexation with a Lewis acid site removed electron density directly or indirectly from the metal, thus decreasing backbonding, causing the carbonyl bond to metal bond to weaken.

While the analysis carried out provided information more research in this area is needed. Further studies in this field can be carried out using other supports with complexes incorporating transition metal carbonyls with non-cyclic substituents.

REFERENCES

1. Petrucci, R.H.; Harwood, W.S.; *General Chemistry; Principles & Modern Application*, 6 Edition, Macmillan Publishing Co., New York, **1993**, 791.
2. Burwell, R.L., *J. Cat.*, **1984**, 86, 301.
3. Ibid., 303.
4. Ibid., 302.
5. Ibid., 304
6. Imelik, B.; Naccache, C.; Coudrier, G.; Ben Teerit, Y.; Verdrine, J.C.; *Studies in Surface Science and Catalysis, Vol. 20: Catalysis by Acids and Bases*; Knozinger, H., Elsevier Publ. Comp., Amsterdam, Oxford, New York, Tokyo, **1985**, 114.
7. Bjorklund, R.B.; Burwell, R.L.; *J. Colloid Interface Sci.*, **1979**, 70(2), 388.
8. Ibid., 831.
9. Burwell, R.L., *J. Cat.*, **1984**, 86. 302.
10. Yermakov, Yu. I.; Kuznetsov, B.N.; Zakharov, V.A.; *Studies in Surface Science and Catalysis: Vol. 8*; Elsevier Publ. Comp., Amsterdam, Oxford, New York, **1981**, 15.
11. Ibid., 13.
12. Yermakov, Yu I.; Kuznetsov, B.N.; Zakharov, V.A.; *Catalysis by Supported Complexes*; Elsevier Publ. Comp., Amsterdam, Oxford, New York, Tokyo, **1981**, 34.

13. Iwasawa, Y.; Ichinose, H.; Ogasawara, S., *J. Chem. Soc., Faraday I*, **1981**, 77, 1763.
14. Imelik, B.; Naccache, C.; Coudrier, G.; Ben Teerit, Y.; Verdrine, J.C., "Studies in Surface Science and Catalysis, Vol. 20: Catalysis by Acids and Bases", Knozinger, H., Elsevier Publ. Comp., Amsterdam, Oxford, New York, Tokyo, **1985**, 114.
15. Yerakoov, Y.I.; Catal, *Rev. Sci, Eng.*, **1976**, 13, 77.
16. Lamiecki, M.; Burwell, R.L.; *J. Colloid Interface Sci.*, **1980**, 75, 951, .
17. Howe, R.F.; Davidson, D.E.; Whan, D.A., *J. Chem. Soc. Faraday Trans*, **1972**, 68, 2266.
18. Smith, A. K.; Hugues, F.; Theolier, A.; Basset, J.M.; Ugo, R.; Zanderighi, G.M.; Bilhou, J.L.; Bournol, V; Graydon, W.F., *J. Inorg. Chem.*, **1979**, 18, 3104.
19. Kazusaka, A.; Howe, R.F.; *J. Mol, Cat.*, **1980**, 9, 200.
20. Ibid., 204
21. Brenner, A.; Hucul, D.A.; *J.C.S. Chem. Commun.*, **1982**, 15, 831.
22. Psaro, R.; Zanderright, G.M.; Besson, B; Smith, A.K.; Basset, J.M.; *J. Organomet. Chem.* **1981**, 213, 215.
23. Brenner, A.; Burwell, R.L.; *J. Amer. Chem. Soc.*, **1975**, 97, 2565.
24. Bjorklund, R.B. Burwell Jr., R.L.; *J.Coll. & Inter. Science*, **1979**, 70(2), 386.
25. Ibid., 390.
26. Hugues, F.; Smith, A.K.; Ben Taarit, Y.; Basset, J.M. *J. Chem. Soc., Chem. Comm.*, **1980**, 68.
27. Ibid., 69.

28. Ibid., 70.
29. Ibid., 68.
30. Smith, A.K.; Besson, B.; Basset, J.M.; Psaro, R.; Fusi, A.; Ugo, R.; *J. Organomet. Chem.*, **1980**, 192, c33.
31. Watters, K.L.; Howe, R.F.; Chojnacki, T.P.; Fu, C.M.; Schneider, R.L.; Wong, N.B., *J. Cat.*, **1980**, 66, 425.
32. Ibid., 432.
33. Du, H.; Fang, L.; Wu, R.; *J. Cat.*, **1992**, 13(2), 91.
34. Du, H.; Fang, L.; Wu, R.; *J. Cat.*, **1993**, 14(5), 334.
35. Anderson, J.R.; Elmes, P.S., Howe, R.F.; Mainwaring, D.E., *J. Cat.*, **1977**, 50, 508.
36. Psaro, R.; Zanderright, G.M.; Besson, B.; Smith, A.K.; Basset, J.M.; *J. Organomet. Chem.* **1981**, 213, 216.
37. Smith, A.K.; Besson, B.; Basset, J.M.; Psaro, R.; Fusi, A.; Ugo, R.; *J. Organomet. Chem.*, **1980**, 192, c34.
38. Guczi, L.; Beck, A.; *Polyhedron*, **1988**, 7(22/23), 2389.
39. Tessier-Youngs, C; Corres, F.; Pioch, D.; Burwell, R.L; Shriver, D.F.; *Organomet.*, **1983**, 2(7), 901.
40. Kazusaka, A.; Howe, R.F.; *J. Mol. Cat.*, **1980**, 9, 187.
41. Brenner, A.; Burwell, R.L.; *J. Amer. Chem. Soc.*, **1975**, 97(9), 2566.
42. Nelson, G.O.; Wright, M.E.; *J. Organomet. Chem.*; **1982**, 239, 360.
43. Ibid., 361
44. Piper, T.S.; Wilkinson, G; *J. Inorg, Nucl. Chem.*; **1956**, 2, 107.

45. Ibid., 108
46. Wegner, P.A.; Uski, V.A.; *Inorg. Chem.*, **1979**, 18(3), 647.
47. Ibid., 648.
48. Ibid., 649
49. Ibid., 650
50. Abotsi. G.M.K.; Scaroni, A.W.; "A Review of Carbon Supported Hydrosedulfurization Catalyst", Elsevier Science Publishers B.V., Amsterdam, **1988**, 113.
51. Piper, T.S.; Wilkinson, G; *J. Inorg, Nucl. Chem.*; **1956**, 2, 117.
52. Ibid p. 115.
53. Pouchert, C.J.; "The Aldrich Library of FT-IR Spectra"; Aldrich Chemical Company, Inc. USA, **1985**,1(2) 1105.